Characterization of Unsaturated Stony Vadose Zones Using Standard Physical Methods

by

John A. Owsiany
New Mexico Institute of Mining and Technology

March 1995

Submitted in partial fulfillment of the requirements for the degree of Master of Science in Hydrology

TABLE OF CONTENTS

LIST OF TABLES

LIST OF FIGURES

ACKNOWLEDGEMENT

I wish to express my gratitude and appreciation to the Waste-Management Education and Research Consortium and the Tinker Foundation for funding this research project. I would also like to express my gratitude to the U.S. Department of the Interior: Fish and Wildlife Service for granting us permission to collect sand in the Sevilleta National Wild Life Refuge north of Socorro.

I offer special thanks to my advisor Dr. Jan M.H. Hendrickx whose trust and generous support enabled me to pursue this research with confidence in an environment free of unnecessary complications. I am also grateful to Tzung-mow "Mike" Yao for all his help in the lab and his emotional support when difficulties were encountered. Without his support I would not have been able to conquer the frustration I felt when results appeared less than prefect. I am indebted to Kelly Kriel whose personal knowledge of the behind the scenes supply network at Tech facilitated the acquisition of necessary equipment even though funding was limited.

Finally, I dedicate this work to my mother and my brother for their love and support throughout this whole endeavor.

ABSTRACT

The relationship of unsaturated hydraulic conductivity to the volume percent of stones in a soil profile was the focus of this research. An additional objective was the evaluation of two physical measurement methods utilized in determining unsaturated hydraulic properties in stony soils. These methods were the Time Domain Reflectometry (TDR) technique for water content measurement and the instantaneous profile method for determination of unsaturated hydraulic conductivity. Homogeneous and heterogeneous soil profiles were studied in a series of column experiments to determine their unsaturated hydraulic properties. Homogeneous profiles consisted of a fine uniform sand collected from a near by field area, while the heterogeneous profiles consisted of a single layer of hard composite spheres packed uniformly in a single sand layer of variable thickness. Volumetric water content and soil water tension measurements were collected and analyzed using the instantaneous profile method. The performance and accuracy of the TDR probes was also investigated to determine the suitability of this instrument for stony soils. The effectiveness of the TDR in stony soils is directly related to the representative elementary volume (REV) sampled by the instrument. The volume of soil sampled by the TDR probes used in this study was investigated empirically. Results of this research indicate that the unsaturated hydraulic conductivity of layered stony soils can be estimated accurately utilizing a simple correction for the volume of stones present in the soil profile. The instantaneous profile method, as applied to layered stony soils, must be corrected for the volume of stones present in the soil profile to avoid an overestimation of volumetric water content for the stony layers. Additionally, this method is limited in its ability to estimate hydraulic gradients in the region of impeding stone layers. Finally, when using the TDR technique

in heterogeneous soils containing stones the effective sample volume of the probes must be determined so that water content measurements may be quantified as being real matrix water contents or volumetric water contents to avoid errors in data analysis.

INTRODUCTION

The hydraulic properties of stony vadose zones are of great interest because of their wide spread occurrence in different geographic regions and manner in which they are utilized. The economic potential of stony soils is quite limited in regard to agricultural use or other land intensive developments. This means that these areas are often relegated to industrial use, landfills, or land treatment of waste water. Such practices carry a greater potential for soil and groundwater contamination than those of more economically desirable lands. As such, a better understanding of their hydraulic properties is essential to accurately predict the movement of water and dissolved contaminants in these systems.

A review of the current literature indicates a lack of information regarding the hydraulic properties of stony vadose zones. Only a limited number of studies describe, in a quantitative fashion, the effect that a given volume of stones has on unsaturated hydraulic conductivity. Mehuys et al.(1975) studied several desert soils and found that the apparent conductivities were higher for soils containing stones greater than one centimeter in diameter at volumetric water contents ranging from 5% to 20%. Bower and Rice (1985) developed an expression to estimate the bulk saturated hydraulic conductivity for stony soils using the measured value for the saturated matrix and the volume of stones present. This in turn may be used to estimate the unsaturated $K(\theta)$ or $K(\Psi)$ relationships for stony soils using a simple curve fitting procedure. The work of Brakensiek et al.(1994) provides equations for modifying soil/water physical properties in the presence of coarse rock fragments.

The reliability of the research methods used to obtain hydraulic characteristics was also evaluated to determine their effectiveness in stony soils. We focused on the use of the Time Domain Reflectometry (TDR) technique as applied to the instantaneous profile method. Reports in the literature indicate that the area of influence affecting TDR measurements is confined to a region with maximum dimensions of 60 mm x 80 mm, with an asymmetrically distributed cross sectional area of 3600 mm^2 (Baker & Lascano 1989). This is for a two wire probe with wave guides 300 mm long having a separation distance of 50 mm. A similar area of influence was found by Topp and Davis (1985). It is further stated that the "effective" cross-sectional area is approximately 1000 mm^2 with maximum dimensions of 20 mm x 65 mm (Baker & Lascano 1989). The work of Knight et al. (1994), and Zegelin et al. (1992) suggest that this area of influence should be considerably less for a three wire probe. The area of influence for the three wire probes used in this study was empirically determined to assess the accuracy of measurements made in the stony layers.

The objective of this research is to investigate the effect that a given volume of stones, as a single layer, has on the hydraulic properties of a soil and to evaluate the effectiveness of the standard physical methods used in the collection of these data.

METHODS AND MATERIALS

A series of instantaneous profile experiments were conducted using both homogeneous and heterogeneous soil profiles in a number of large scale column experiments. The data were examined for direct relationships between the volume percent of stones in a profile and corresponding changes in the unsaturated hydraulic conductivity. Data from the heterogeneous profiles was further analyzed by comparing it to results fitted to the homogeneous profile data using the program RETC, van Genuchten et al. (1992).

Field Soil

Seven column experiments were conducted: three using columns packed with homogeneous sand and four using columns packed with layers of sand and rubber spheres. The sand was collected from the Sevilleta National Wild Life Refuge along the bank of the Rio Salado, an ephemeral stream, fifteen miles north of Socorro, New Mexico. This field sand consists of ancient flood plain deposits of the Rio Salado. The size distribution of this sand, based on sieve analysis data, is presented in Table 1. A series of hard composite rubber spheres, 6.4 cm in diameter, were used to represent stones in the heterogeneous profiles. These artificial stones were chosen because unlike natural materials their size and shape are uniform. This eliminates a significant number of variables from the experiment and allows a more direct assessment of the unsaturated hydraulic conductivity. The homogeneous sand columns established baseline hydraulic parameters for the field soil that was used, and served as a reference for the examination of layered profile experiments. Column size,

Sevilleta Field sand					
Sieve	Diameter	Weight	Cumulative	Percent (%)	Percent (%)
Number	(mm)	Retained	Weight	Passed	Retained
30	0.6	1.05	1.05	0.99927	0.00073
40	0.417	8.5	9.55	0.93316	0.06684
60	0.25	56.03	65.58	0.54095	0.45905
100	0.15	53.83	119.41	0.16415	0.83585
140	0.12	16.15	135.56	0.051099	0.948901
200	0.075	3.29	138.85	0.02807	0.97193
bottom		4.01	142.86	0	1

Table 1. Sieve analysis of the Sevilleta field soil.

shape, drainage conditions, and water application rates were all kept constant throughout all of the experiments. The following describes, in detail, the experimental setup utilized and presents the procedures used in conducting the experiments.

Soil Columns

The soil columns were constructed using a series of polyvinyl-chloride(PVC) plastic rings. Each ring was thirty centimeters in diameter and ten centimeters high. A total of fifteen rings were used in the construction of each column. Rings were placed on top of one another and the joints sealed with duct tape to prevent the leakage of water. This created a single rigid piece of pipe that served as the column, (Figure 1). A length of 1.5 meters was found to be sufficient for obtaining near unit gradient conditions in the homogeneous soil profiles. Each ring was given a numbered designation starting at the top of the column, which was taken as the ground surface datum, to facilitate data collection and record keeping. Six of the rings in the upper seventy centimeters were instrumented to collect soil water tension and volumetric water content measurements, (Figure 1). These measurement stations, rings two through seven, were positioned at regular intervals throughout the top portion of the column, spaced in an equidistant fashion ten centimeters apart. The single non-instrumented ring at the very top of the column and those at the bottom were positioned solely for maintaining the uniformity of wetting during infiltration, and to eliminate unwanted drainage effects near the last measurement station.

Column Packing

After the columns were assembled they were filled completely with either a homogeneous or

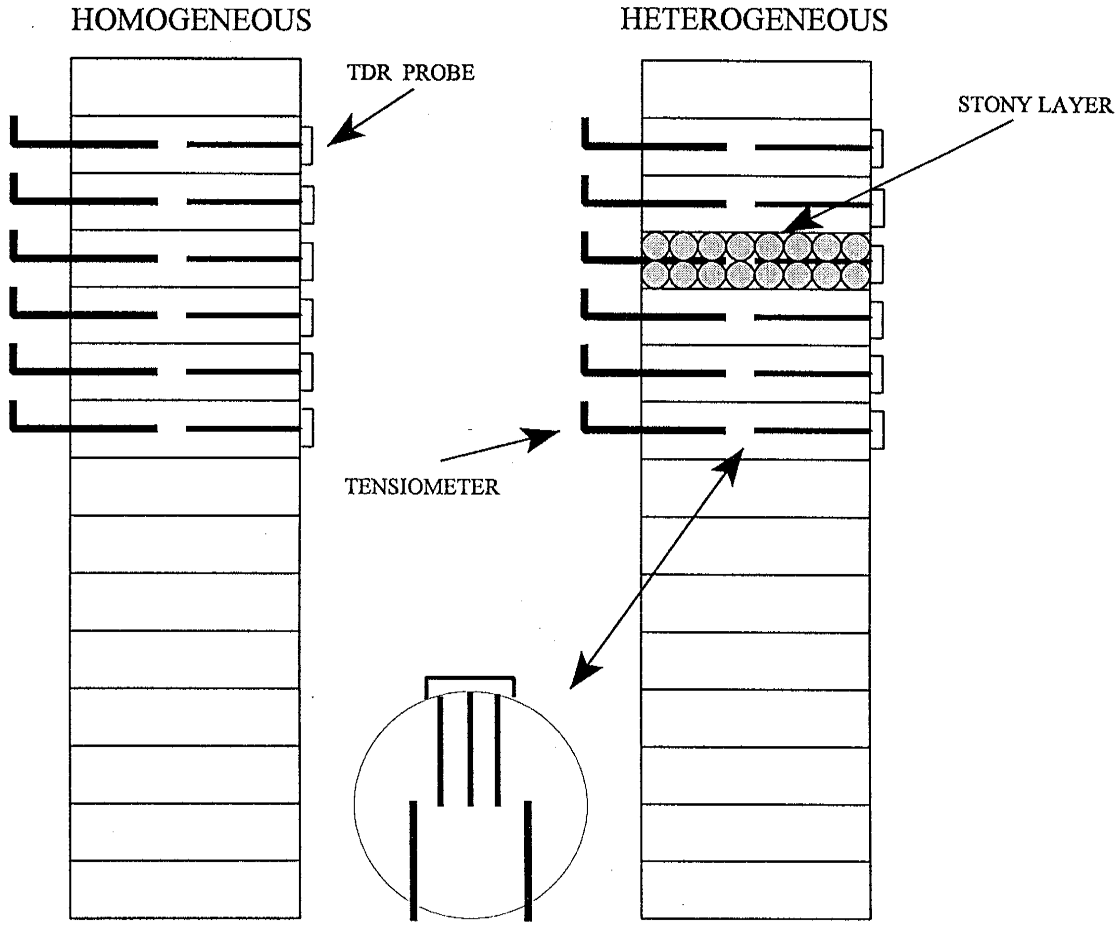

Figure 1. Schematic representation of soil columns illustrating homogeneous and heterogeneous profiles, along with instrument placement.

heterogeneous layered soil profile. Each soil profile was constructed using the following procedure. First, the field sand was placed in a bulk drying facility and air dried for a minimum of three weeks. Sand dried in this fashion typically has a residual water content of less than one tenth of one percent. The sand was then sieved to remove any foreign material that may have been introduced during the collection and drying process. The sieve was constructed from U.S. 20 size mesh, which was slightly larger than the largest particle diameter of the sand. The columns were then filled by pouring discrete quantities of the sand through a randomizer placed on top of the column. The randomizer consists of a series of screens and sieves that distribute the flow of sand uniformly over the entire area of the column. This promotes uniformity throughout the soil profile and helps to eliminate the formation of packing irregularities which may contribute to the development of preferential flow paths. Periodically during this process the sand in the column was settled by striking the top edge of the column with a rubber mallet. An equal number of strokes were administered at four points on the column edge separated by ninety degrees of arc. This helped to impart a uniform bulk density to the sand in the columns. Tensiometers were emplaced in the soil columns as they were filled with sand, at the designated elevations. This procedure was repeated until the column was completely filled.

Columns having layered profiles had an additional step included in the above procedure. When the sand reached the elevation of the base of the third measurement station, approximately 40 cm below ground surface, a layer of rubber spheres was placed in the column. These spheres were packed tightly in a uniform layer within the same horizon. A total of eighteen spheres fit in one layer and constitutes a volumetric percentage of 55% within the layer. The density of sphere packing was maintained in all of the heterogeneous experiments, only the thickness of this impeding layer was varied from experiment to experiment. When the thickness of the layer was increased the additional balls were placed in the open macropore spaces between the balls of the layer immediately below in such a way as to maintain the density of packing and volumetric percentage. Sand was added concurrently with the spheres and settled as described above. Sand, when poured from a constant height, will tend to settle to a consistent bulk density. This is the basis of the sand-funnel technique used to determine the bulk density of soils insitu, (Klute 1986). This was the only additional step used in preparing the heterogeneous columns that differed from that of the homogeneous case.

TDR probes were inserted into the columns at each of the measurement stations after the profiles had been fully wetted. Approximately one hour before water application to the columns ceased, probes were inserted into the columns through access ports in the column walls. This was done so that the presence of the probes in the soil profile would not adversely effect the flow of water during the wetting phase of the experiment.

Applied Flux Conditions

A flux was induced in the soil columns by the application of water using a rain simulator. This device simulated rainfall by applying water through a series of small diameter needles, (Becton&Dickinson 20G1), producing droplets of water. These needles are attached to the bottom of a reservoir that has dimensions of 55 cm x 55 cm x 3 cm which is fed by a Master Flex peristaltic pump. The reservoir is constructed in such a way so that there is no change in storage during the experiment, so the metered pump reading is in fact the outflow rate over the application area of the reservoir. The reservoir is mounted in a steel frame that is actuated by two electric motors to move in two horizontal directions simultaneously. This helps to create a random pattern of water droplet application.

After preliminary experiments demonstrated the feasibility of this approach, a pumping rate of 0.13 cm/min was deemed the most appropriate for studying unsaturated flow in the field soil utilizing this experimental approach. Higher pumping rates induced saturated conditions in and near the last measurement station unnecessarily complicating the study. The period of water application lasted for approximately eight hours, typically overnight. Soil water tension was then checked at all of the measurement stations to ensure that a steady state condition had been achieved.

Instrumentation of Measurement Stations

Instrumentation of the soil columns consisted of six measurement stations being positioned at ten centimeter intervals starting at the second ring segment of the column. Each station consisted of two tensiometers and one TDR probe. All three devices were positioned in the center of the ten centimeter ring segments, coplanar with each other, (Figure 1). The TDR probe occupied a position between each of the two tensiometers extending into the column 15 cm. Tensiometers were placed on either side of the TDR probe, also extending into the column approximately 15 cm. Two tensiometers were used due to the size of the column, and the necessity of determining if the wetting of the column was uniform across its width. Tensiometers were constructed using materials that would not interfere with the functioning of the TDR. The materials consisted of nonconductive plastics and ceramic cups. As an added precaution they were placed outside of the volume of soil sampled by the TDR probe.

TDR Calibration

Three wire TDR probes were used in conjunction with a Tektronix 1502B cable tester to collect measurements of volumetric water content. The probes consisted of three stainless steel wave guides 15 cm long with a separation distance of 3 cm. Data used in calibrating the TDR was plotted as measured apparent probe length verses volumetric water content for the field soil, and a linear regression fitted to the data. The equation of the line fitted to this data provided the calibration curve for the TDR in this field soil, where the x- coordinate is the measured apparent length of the TDR probe and the returned y intercept is the calculated volumetric water content.

TDR Sensitivity in Stony Soils

A crucial element in the study of unsaturated hydraulic conductivity is the accurate measurement of soil water content. When analyzing data using the instantaneous profile method the accuracy of this measurement is extremely critical because the timed rate of change of water content in the soil profile is an essential parameter of the analysis method. As such, how well the TDR performs in a soil with a high content of stones is of great interest. Drungil et al. (1989), state that the TDR can be used to determine water content in soils containing up to 50% coarse stone fragments, 0.5-1.25 cm in diameter, without a significant loss in accuracy. The effect of different soil types on TDR measurements was the focus of research conducted by Richardson et al. (1992), who stated that variable physical properties such as bulk density had no apparent effect on estimates of soil water content using the TDR technique. However, the work of Knight et al. (1994), Knight (1992), Baker & Lascano (1989) suggest that the TDR technique may susceptible to perturbations occurring in the sample volume of the TDR probe. Due to this apparent conflict in the literature it was necessary to determine if the soil water content measurements collected during the instantaneous profile experiments were valid for the study of the heterogeneous profiles. The critical question as it pertains to the heterogeneous profiles in this study is what is actually being measured in the stony layer by the TDR. Is the measurement a point measurement, i.e. the real matrix water content , or is it a larger volume averaged measurement including portions of the stones which are, in fact, dry in their interior? In order to properly address this question the sample volume of the three wire TDR probe used in this study was experimentally determined.

Experimental Determination of TDR Sample Volume

A series of known water content samples were created using the Sevilleta field soil by adding a known volume of water to a known volume of sand. The wetted sample, in sealed plastic bags, was then placed into an oven and warmed to a constant temperature of 38C° over a period of 24 hours. During this time the samples were mixed and rotated frequently in the sealed plastic bags. This process helped to distribute the water uniformly throughout the soil. The soil was then removed from the oven and allowed to cool to room temperature while it was again mixed and rotated in the plastic bag. Condensation on the bag surface was kept in contact with the soil to help minimize water loss and accurately reproduce the calculated water content. This uniformly wet soil was utilized in two experimental procedures to empirically determine the range of influence for the three wire TDR probe.

The first experimental procedure consisted of placing a mass of wet soil between two acrylic plates and recording the TDR measurements while the separation distance between the two plates was decreased in discrete intervals. The TDR probe was placed in the center of the soil mass bisecting the distance separating the two plates. Initial readings were taken at a separation distance of six centimeters, which is beyond the range of influence of the probe, (Baker & Lascano 1989, and

Topp and Davis 1985). This separation distance of six centimeters has been experimentally determined for a two wire probe arrangement to be the area of maximum dimension using 10% relative sensitivity as a threshold value, (Baker & Lascano 1989). Three wire probes have a significantly decreased spread of energy in the far field, (Knight et al. 1994), so this upper limit of six centimeters was chosen with confidence for the evaluation of the three wire probe. The separation distance was decreased until the layer of soil between the two acrylic plates was approximately ten to fifteen millimeters thick, which was significantly less than the thickness of the soil envelope placed around the probes in the stony profiles.

The second approach used in determining the field of influence around the probe wave guides was one focused on discerning the relative contribution of the outer two wave guides as compared to that of the central conductor. The three wire probe with one central conductor and two outer wave guides emulates a coaxial line and reduces the impedance mismatch between the wave guides and the coaxial transmission line. This results in a different spatial sensitivity function as well as a different energy distribution around the probe, as compared to a two wire probe. Most of the energy and most of the measurement weight is concentrated around the central wave guide of the three wire probe, (Zegelin et al. 1992). A series of small columns were packed with field soil prepared as discussed above. Each of the columns had a slightly smaller inner diameter than the one preceding it. The distribution of size ranges was 10 cm, 6.4 cm, and 3.1 cm. Initially this permits the probe to be completely inserted into the soil with the wave guides entirely surrounded by the medium. At the end point of column size only the central conductor is in the medium. In this way the relative sensitivity of the central conductor, as compared to the outer conductors, was determined for the three wire probe.

Using this approach the specific volume of soil being sampled by the TDR probe was experimentally determined for the instrument configuration used in this research. This empirical approach provided a quick and direct method of evaluating the volume of soil sampled by the TDR. Additionally, these methods may be extrapolated to any field soil or laboratory situation independent of scale without requiring a mathematically rigorous approach to estimate electromagnetic field distributions. If one chooses to estimate electric field densities or spatial weighting functions utilizing the theoretical approach, sufficient information regarding theory and examples be can found in Zegelin et al. (1992), Knight (1992) and Knight et al. (1994).

Soil Water Content

Volumetric water content was calculated for each of the column experiments from TDR readings using the above calibration curve. In the homogeneous soil profiles the calculated water content represents a volumetric water content due to the uniformity of the soil medium and distribution of soil moisture in it. Where volumetric water content is defined as

$$\theta_v = (\rho_b \theta_g) \div \rho_w \qquad (1)$$

having ρ_b and ρ_w as the bulk density of dry soil and water respectively, and θ_g as gravimetric water content. Water content measurements made in stony layers represented only the matrix between the stones, based on the sample volume experiments, and had to be converted to volumetric water contents. This was done by multiplying the matrix water content by the volumetric percentage of stones in that layer. This volume averages the matrix water content converting it to a volumetric measurement. The equation used in this conversion is defined as

$$\theta_v = \theta_m \times (1 - V_{stones}) \qquad (2)$$

having θ_m as the matrix water content and V_{stones} as the volume of stones in the layer one is working with.

Water Tension Measurements

Soil water tension measurements were collected using tensiometers. Tensiometers were constructed using small diameter ceramic cups and rigid plastic tubing. Ceramic cups were 1 inch long and 3/8 inch wide with a bubbling pressure of 800 mbars. The assembled tensiometers were L-shaped with each piece being approximately 15 cm long. Rubber septa were seated in the tubing opposite the cups using vacuum grease to prevent leakage. All tension measurements were corrected for the height of the water filled plastic tubing above the cup.

Instantaneous Profile Analysis

Data collected during the drainage phase of the column experiments consisted of soil water tension and soil water content. These data were analyzed using the instantaneous profile method developed by Hillel et al. (1972), which was derived from the work of Watson (1966). The method which Hillel derived is more properly suited to field situations where the water table is absent or to deep to effect soil moisture flow. This approach is more commonly applied to field situations and is considered a standard method in the field of soil physics. This was the method of analysis employed to analyze the raw data. The only variation from Hillel's method was the use of the TDR to measure soil water content instead of a neutron moisture probe. The following analytical procedure was employed in handling the raw data.

Soil water tension and soil water content measurements were collected simultaneously starting immediately after water application to the column ceased. During the first two hours of the post wetting time period readings were taken every fifteen minutes. Readings were then taken every thirty minutes for two more hours, at which point measurements were taken at intervals based on the rate of change in the observed data. The soil water content data were then plotted against time for each depth. The soil moisture flux for a given depth interval was calculated by fitting a function to the above curves using the mathematical curve fitting program Jandel Scientific Table Curve. This allowed the slope of the curve to be determined at any given point, which was then multiplied by its representative layer thickness to obtain the flux through each layer. Hydraulic head profiles were calculated and plotted for each measurement station as hydraulic head with depth through time. The hydraulic gradient was then determined for each station based on these plots. Hydraulic conductivity as a function of water content was then calculated by dividing the known flux through each layer, at the specific time intervals, by the corresponding hydraulic gradient values. These data were then plotted as hydraulic conductivity against volumetric water content and tension for analysis.

RESULTS AND DISCUSSION

Water Content Measurements

TDR Calibration

The results of calibrating the TDR to the field soil are presented as Figure 2. It shows data from one of three calibration experiments that were performed, it also shows the linear regression curve fitted to the experimental data.

A comparison of this calibration curve with the one developed by Topp et al. (1980) shows a high degree of correlation between the two when compared as dielectric constant verses volumetric water content. This comparison, presented as Figure 3, validates the method of calibration used, and suggests that this approach is a relatively easy way to calibrate the TDR to a particular field soil one is studying. The laboratory calibration curve specific to the Sevilleta field soil was used to determine water content in all of the column experiments.

Determination of TDR Sample Volume

Results of three parallel plate experiments are presented as Figures 4 through 6. Each of the experiments were conducted in identical fashion with the exception that the initial known water content varied from approximately 18% to 7%. The results suggest that the minimum thickness of soil, above and below the plane containing the wave guides, should be limited to 15 mm to maintain maximum confidence in water content measurements.

Figure 4 illustrates the effect on TDR measurements when the total soil layer thickness is

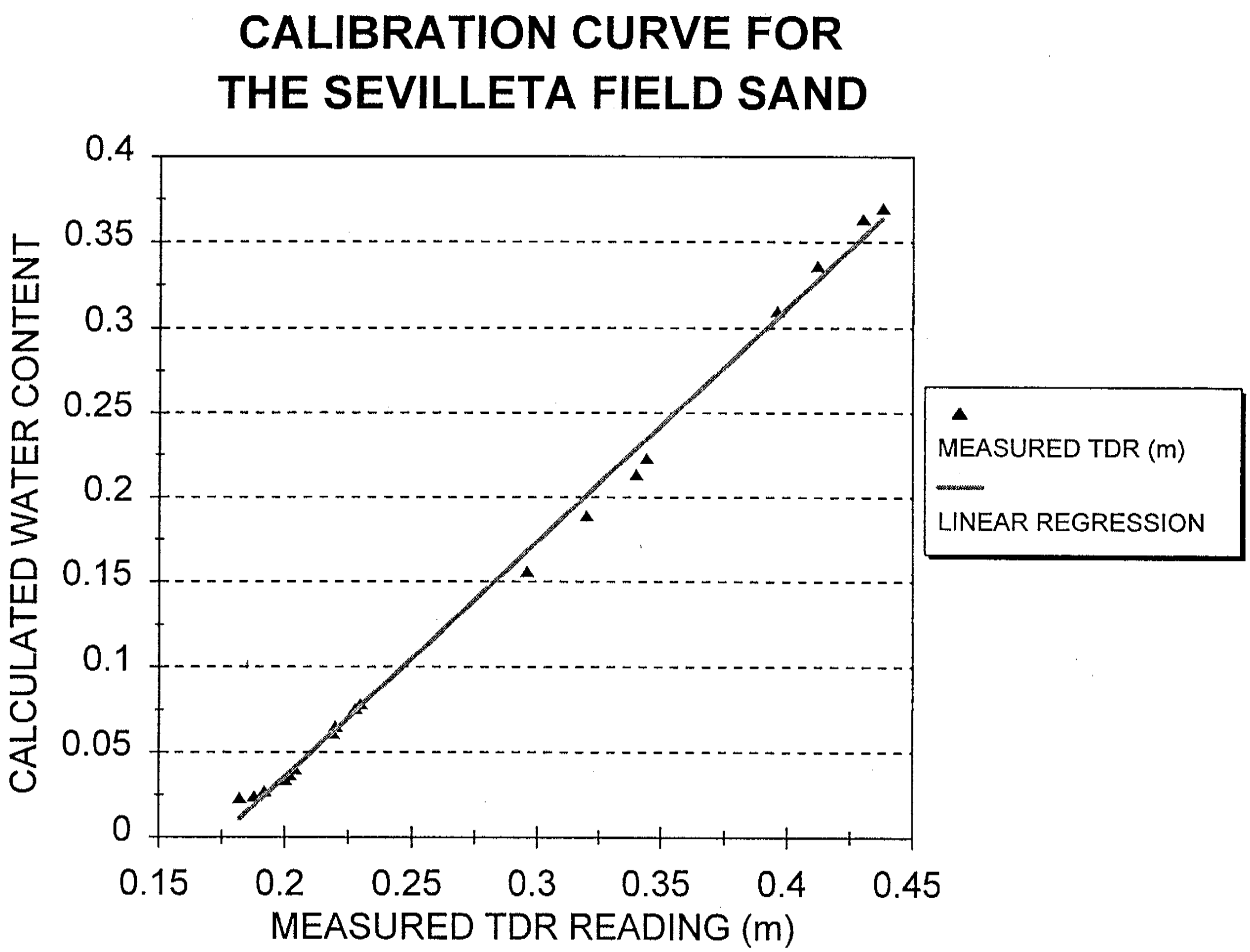

Figure 2. TDR calibration curve for the Sevilleta field sand.

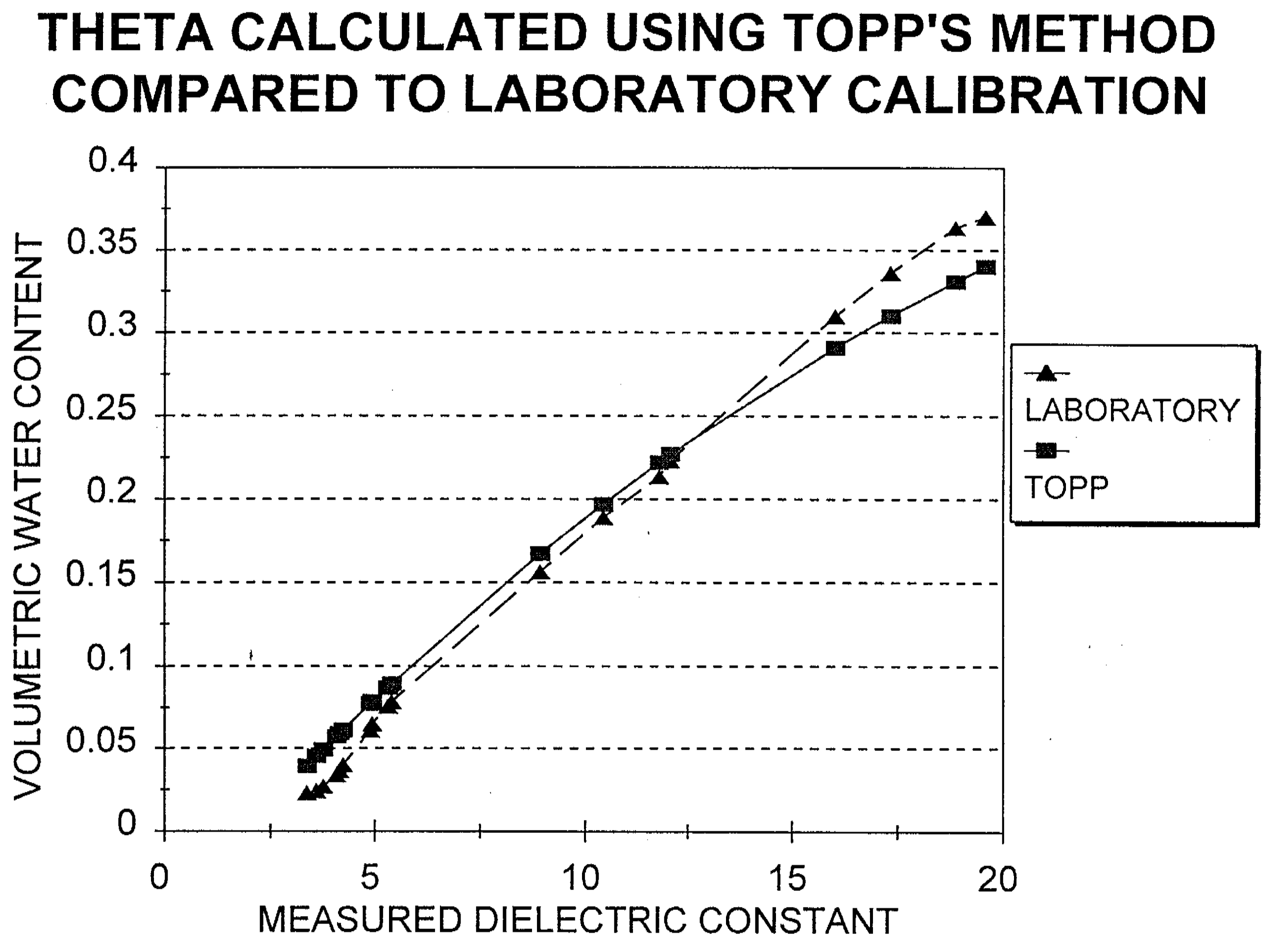

Figure 3. Comparison of estimated volumetric water content using the equation of Topp et al. (1980) as compared to that calculated using the laboratory calibration curve determined in this study.

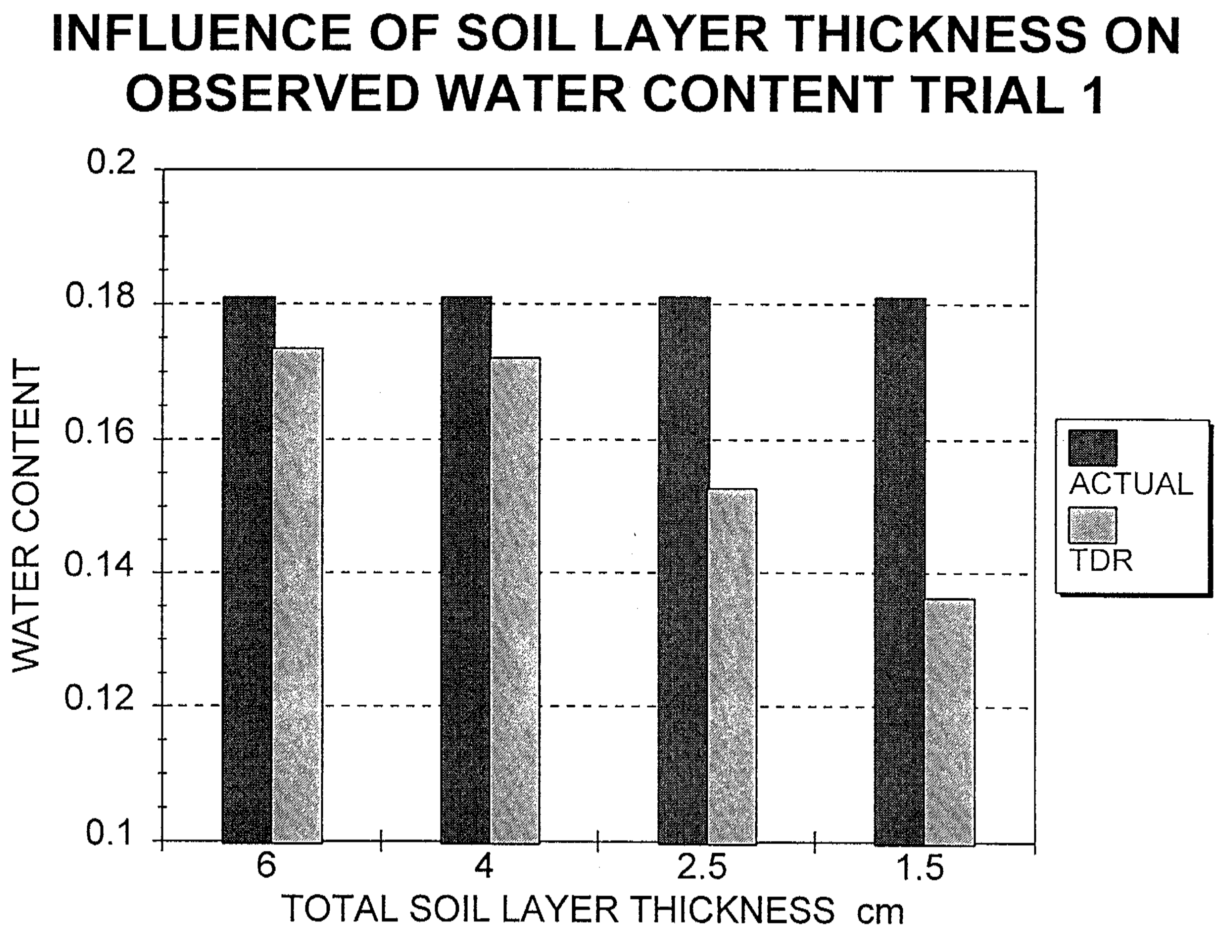

Figure 4. Influence of soil layer thickness on Time Domain Reflectometry measurement of soil water content. Trial 1, approximately eighteen percent water content.

decreased from 60 mm to 15 mm. For thicknesses of 60 mm and 40 mm the TDR readings were unaffected. At these distances the readings are within one percent of the calculated value of the soil as it was constructed. This is typical of nonautomated measurements made in the field or lab, and is near the resolution limit of the instrument in this configuration. Additionally, it should be noted that it is very difficult to prevent zero water loss during sample preparation and experimental manipulation. Decreasing the separation distance further to 25 mm and 15 mm the difference in measured water content as compared to the unaffected readings is an underestimation of approximately two and four percent. The presence of the dry acrylic plates within the sample volume of the TDR probe leads to an underestimation of the actual water content for the soil even though its physical properties were unchanged. With a volumetric water content of 18% this soil is moderately wet considering that the maximum field saturation ranges from 32% to 34%.

Figure 5 also illustrates the effect of decreasing soil layer thickness TDR measurements for a less wet soil. Again good agreement is observed between actual and measured water contents for separation distances of 60 mm and 40 mm, while significant measurement error begins to occur at a distance of 25 mm.

The soil in Figure 6 was the least wet of the soils tested in this fashion. It exhibits a similar trend of decreasing measurement accuracy with deceasing separation distance. Through a comparison of the three experiments it is clear that a homogeneous distribution of soil material within the field of influence surrounding the probe is essential to the accurate measurement of water content. Figure 7 is a plot of the error in volumetric water content between actual and measured values for each of the experiments at various separation distances. All of the measured readings in the range of 60 mm and 40 mm are within 1% of the actual values. At distances less than this the error in measured water

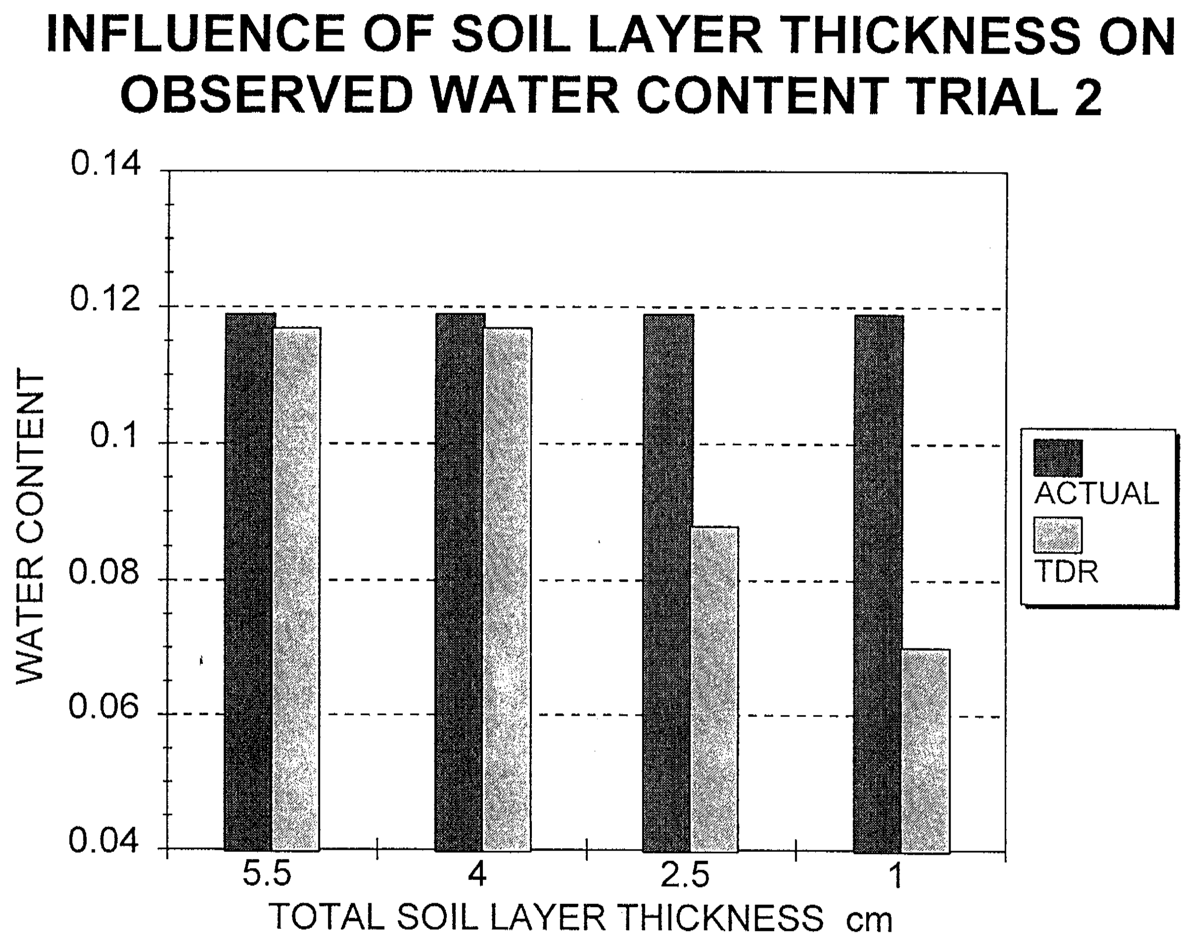

Figure 5. Influence of soil layer thickness on Time Domain Reflectometry measurement of soil water content. Trial 2, approximately twelve percent water content.

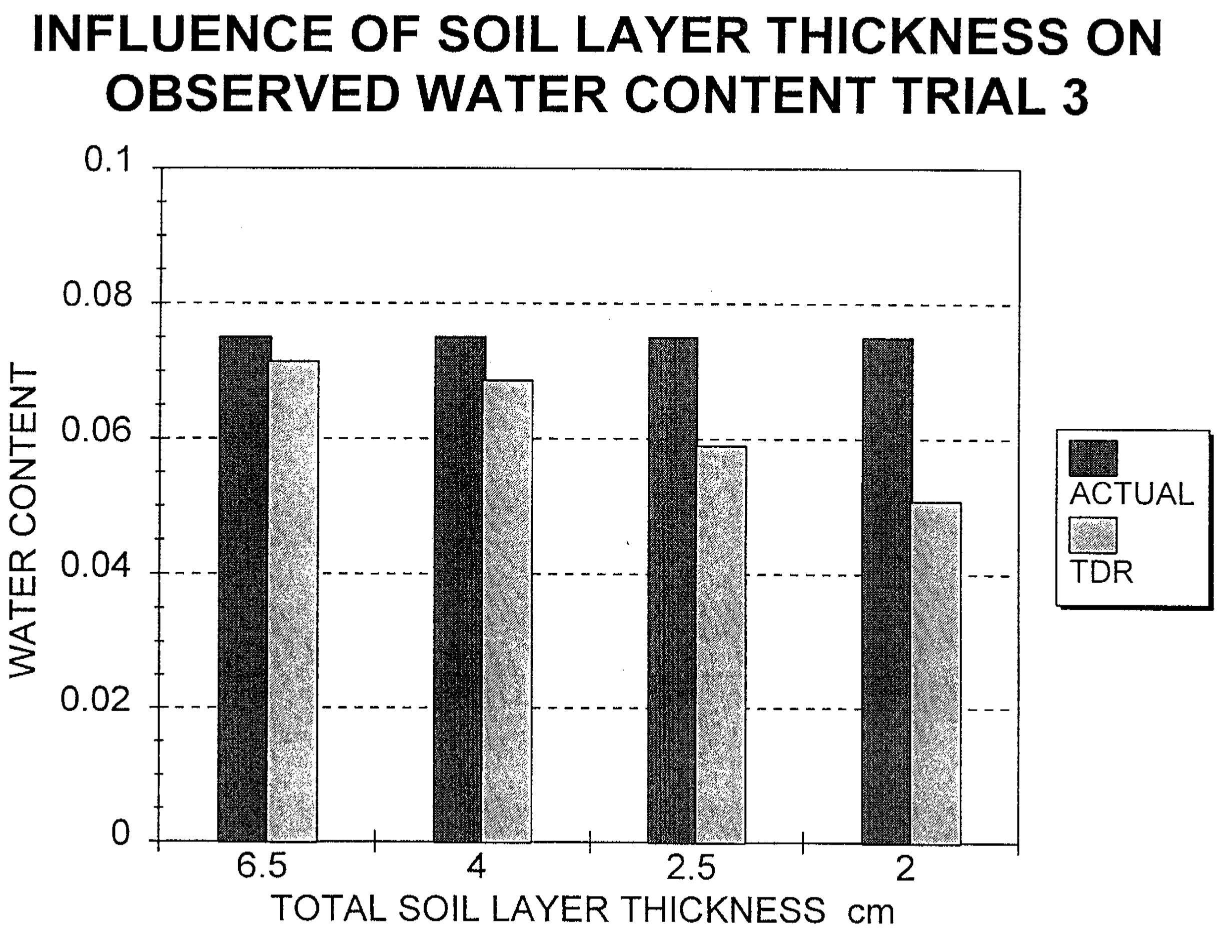

Figure 6. Influence of soil layer thickness on Time Domain Reflectometry measurement of soil water content. Trial 3, approximately eight percent water content.

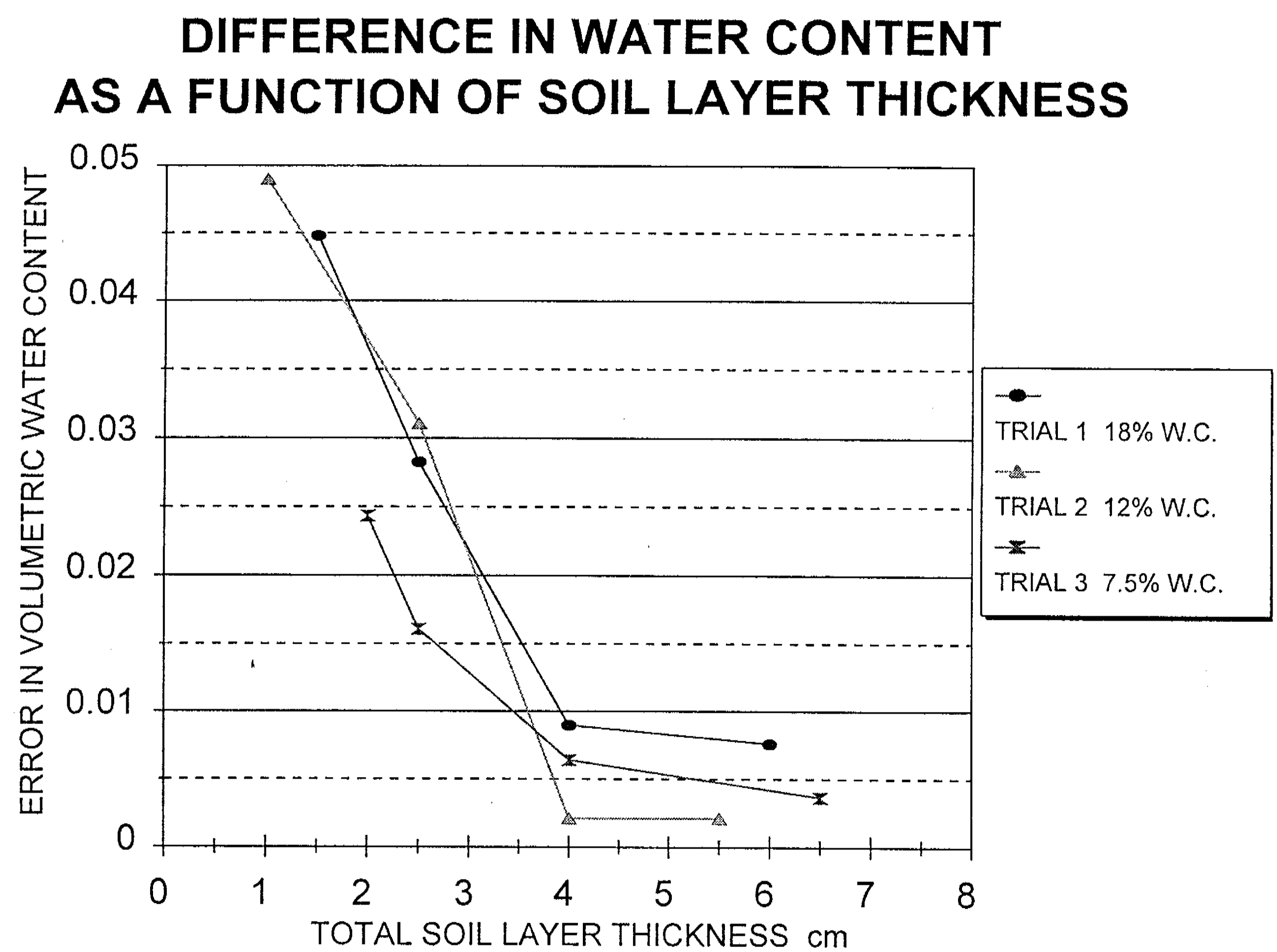

Figure 7. The observed error in volumetric water content between calculated and measured water content, as a function of soil layer thickness, for three soils having different initial water contents.

content increases and approaches a maximum of 5%. If the soil has a volumetric water content of 20% an error in the water content measurement of just 4% constitutes a relative error of 20% which is unacceptable for either field or laboratory work. This demonstrates that the maximum area of influence for the three pronged probe is relatively small, approximately 15 mm above and below the plane containing the wave guides of the probe. This result differs somewhat from that of Baker & Lascano (1989) where they describe an effective cross-sectional area containing most of the measurement sensitivity as 1000 mm^2 with dimensions of 20 mm x 65 mm, i.e. a 20 mm thick soil layer, for a probe having two wave guides 300 mm long separated by 50 mm. Some of the observed difference in sensitivity is due to the type of probe used, three wire verses two wire, while some difference may be attributed to the use of a soil matrix instead of water filled tubes oriented in an air matrix. In the absence of experimental data if one only examined the literature one would expect the area of influence to be significantly less then that measured in our tests.

Influence and Weighting of Wave Guides

The three wire probe, which emulates a coaxial conductor, strongly weights measurements as a function of position relative to the central conductor. These results are presented in Figures 8 and 9. Figure 8 shows a slightly higher observed water content than the actual value for the two cases in which the entire probe was surrounded by soil, still a difference of less than 1%. This is most likely the result of the way in which the columns were packed. The case where only the central conductor was in the soil the reading was 3% less than when the entire probe was is in the soil. A comparison of measured water content values indicates that the central conductor is responsible for approximately 65% of the total water content measurement. A measurement of 8.3% volumetric

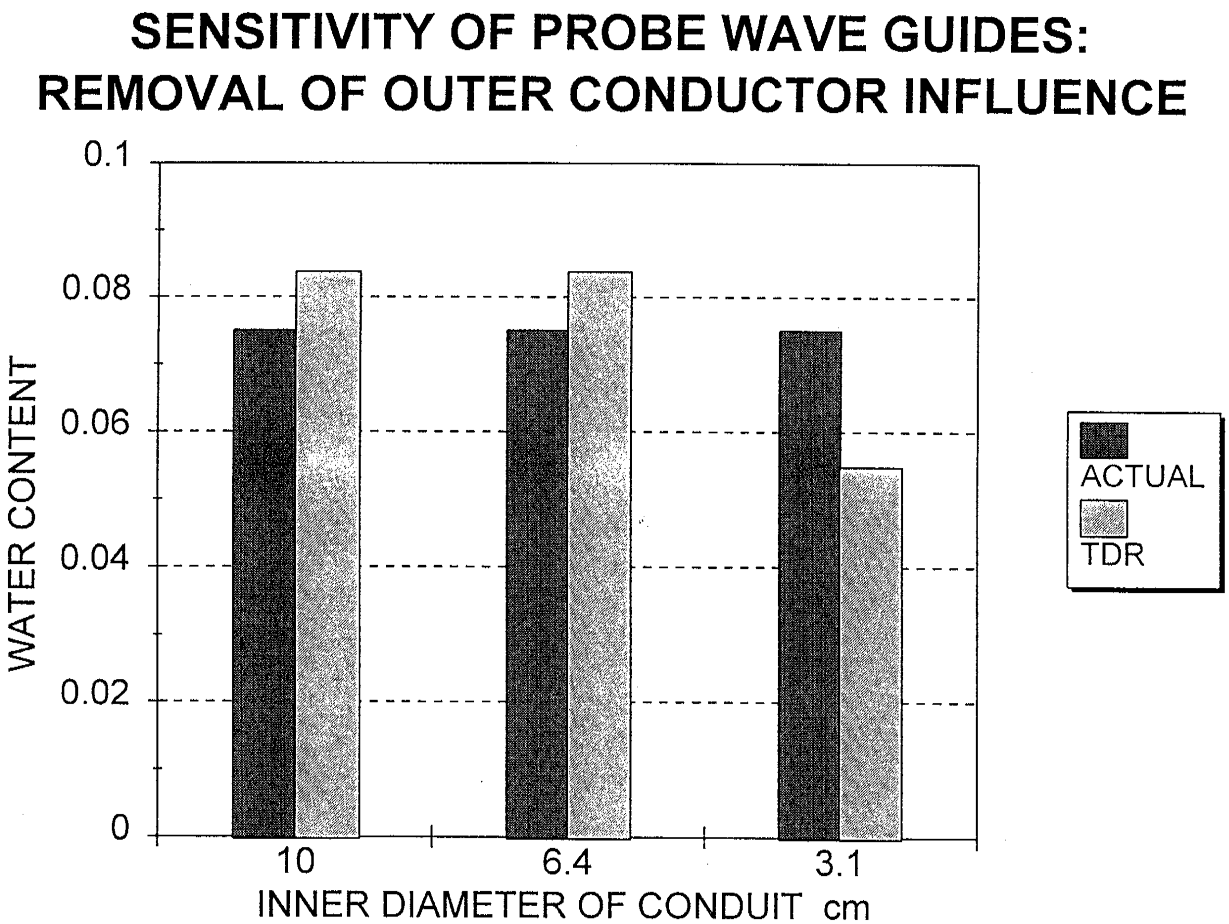

Figure 8. Sensitivity of Time Domain Reflectometry measurements to the removal of outer wave guide contribution.

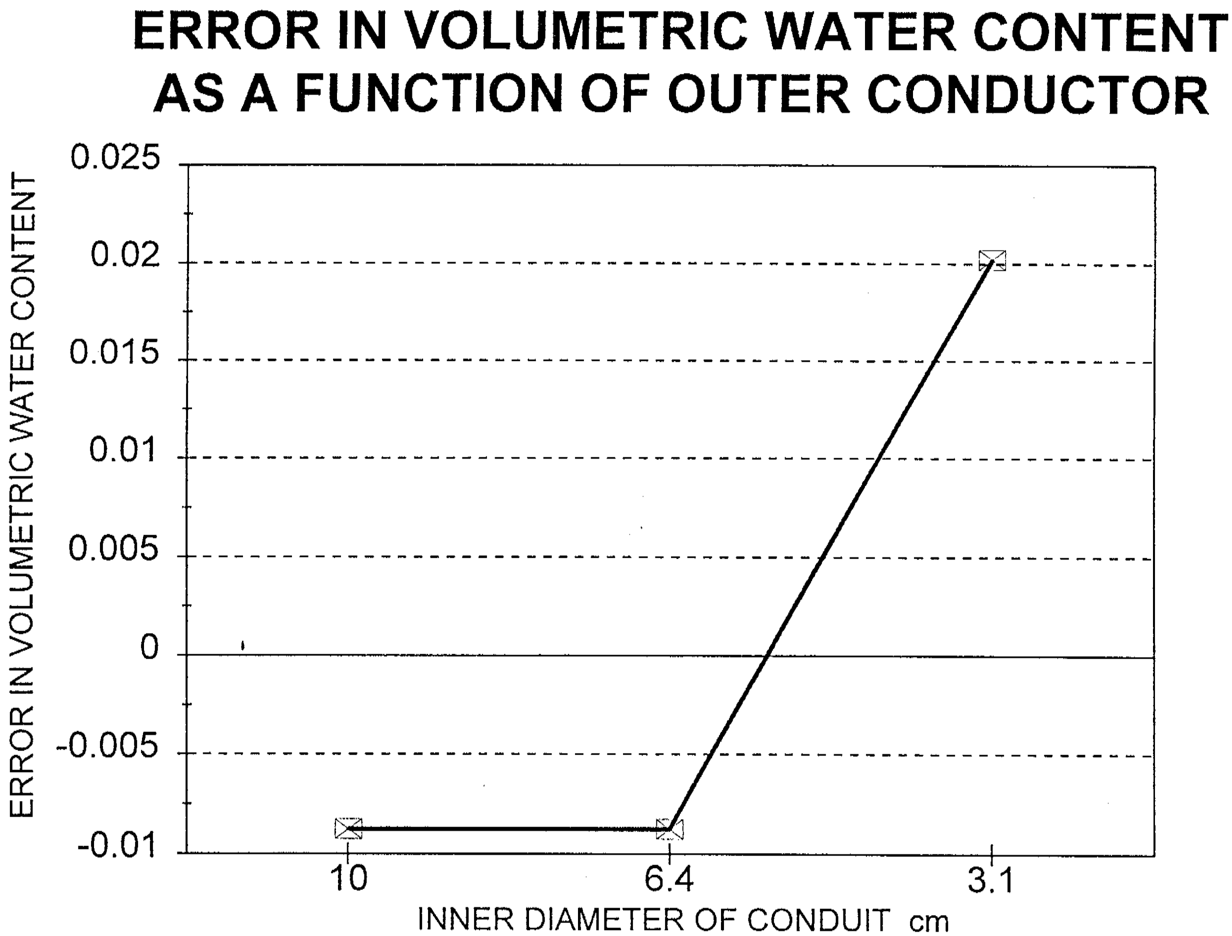

Figure 9. Error in the Time Domain Reflectometry measurement of a moist soil, removal of outer conductor contribution to the reading.

water content when the entire probe is in the soil and 5.4% when only the central conductor is in the soil. Zegelin et al. (1992) present several plots of electric field distributions for probes of various configurations. A comparison of these plots indicates that the electric field distribution lines are centered about the central conductor of the three wire probe with a greater density than in the two wire case. The above experimental finding is in agreement with this work and that performed by Knight (1992) which states that there is strong weighting of the TDR measurement of water content close to the central conductor of multiwire probes. This indicates that mutiwire probes are better suited to measuring water content in stony soils, a result of the sample volume being confined to a smaller area about the central conductor.

Smaller "miniprobes" similar to those described by Sobczuk et al. (1992) would be close to ideal. Probes of this type sample a much smaller volume of soil so they are less likely to produce errors associated with the inclusion of dry stones in water content measurements. This reduction in sample volume returns a value more representative of a point than a larger volume averaged area, a distinct advantage when working in stony soils.

Correction for the Volume of Stones Present

Based on the experimental findings of the two approaches used to determine TDR sensitivity, and the available literature, its reasonable to state that the TDR technique, when applied to stony soils, should be used with caution. It can not be used with impunity in all stony soil types. The design of the probe and its associated sample volume determine the type of water content being measured. Probes having large sample volumes, when used in stony soils, will return a measurement that is influenced by the matrix and the stones present in the soil profile. This measurement may or may not be representative of the volumetric water content for the stony layer, a potential error when using the TDR technique in stony soils. However, probes of small design and associated small sample volume will typically return values that are more representative of the matrix water content alone. These "real" matrix water contents must then be converted to volumetric water contents for use in analyzing data. The probes used in this study have such a small sample volume that the water content measurements collected were representative of the matrix between the stones. As a result of this the matrix water contents had to be converted to volumetric water contents in order to properly analyze the data.

The true volumetric water content for the heterogeneous profiles was calculated using equation two. This converts the real matrix water content to a volumetric water content, through volume averaging, for the stony layer. The spatial distribution of stones in the profile and the volumetric percentage of stones present are critical factors used for correcting water content measurements in stony soils. One must know if the water content values collected using the TDR are volumetric water contents, representing an entire horizon or true matrix water contents representing only that portion of the horizon filled with matrix. An inability to determine type of water content measurement being recorded, and not correcting for the volume of stones present in the layer, can lead to significant error in the calculation of unsaturated hydraulic conductivity, due to its exponential nature.

The construction of the heterogeneous soil profiles allowed an envelope of soil matrix to be placed around the TDR probes and tensiometers so that stones were not in direct contact with the instruments. This combined with the above empirical findings dictates that the soil water tension and water content readings represent true or "real" matrix values. When referring to water content measurements in the remainder of the paper it will be clearly stated as being the real matrix water content or volumetric water content.

Hydraulic Properties

Soil Water Retention

The observed and fitted soil water retention curve for the homogeneous profile is presented as Figure 10. It should be recognized that these results are for a transient system. Unlike soil water retention relationships obtained by hanging column methods, which by there very nature are static equilibrium measurements, the data presented in this figure document a dynamic relation between soil water tension and volumetric water content. True equilibrium conditions may not have been achieved during the experiment due to the transient nature of the analysis method. The fitted curve was developed by inputting $\Psi(\theta)$ and $K(\theta)$ data into the unsaturated soils model RETC, utilizing a simultaneous fit along with the *van Genuchten - Mualem* models for analysis. This fitted curve was then used as a baseline condition for the purpose of comparing the heterogeneous and homogeneous soil profiles.

Figure 11 presents the results for a single impeding layer 6.5 cm thick with a volume percent of stones of 55% within the layer. A bifurcation in the previously observed data trend results. The bifurcation seen in the data is explained as being the result of differential water contents existing in the soil profile at the beginning of the experiment due to the impeding layer. This differentiation of water content is responsible for initiating a unique scanning curve for each layer as desorption takes place within that layer. Scanning behavior and hysteresis effects have been observed in field soils in numerous studies, Sobczuk et al. (1992), Dane and Wierenga (1975), Poulovassilis and Tzimas

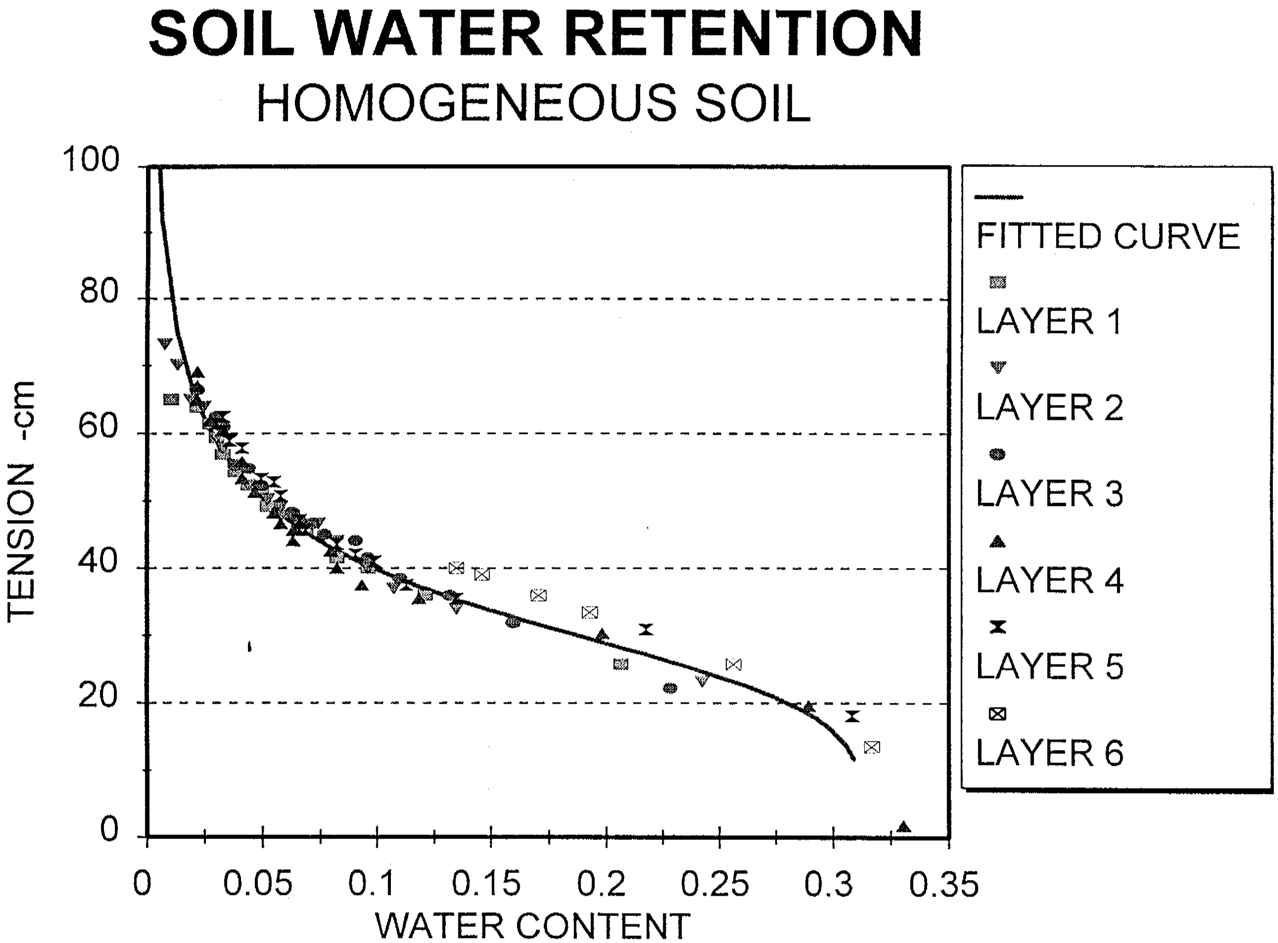

Figure 10. Soil water retention curve for the Sevilleta field soil, homogeneous soil profile. RETC curve fit utilizing the models of *van Genuchten* and *Mualem.*

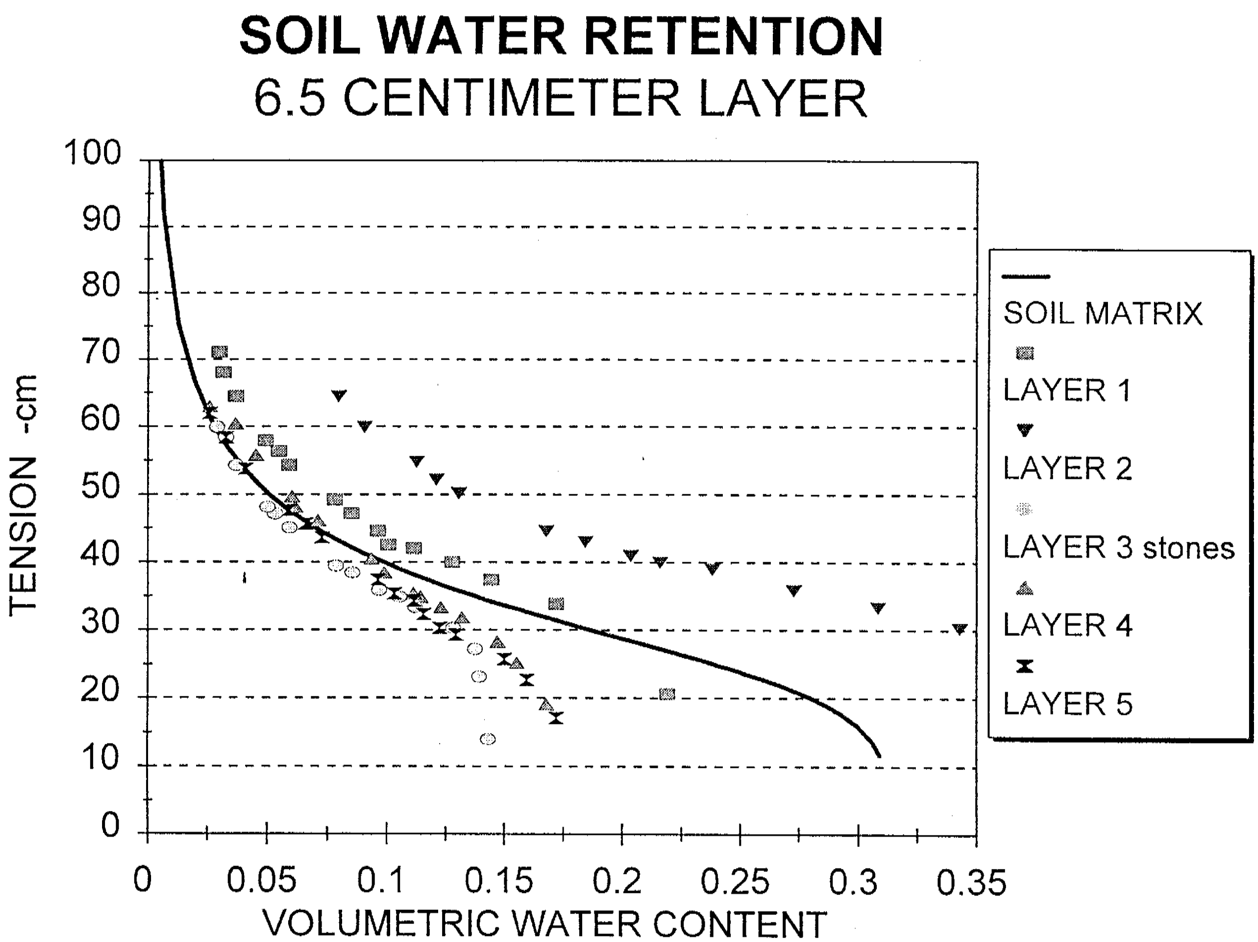

Figure 11. Soil water retention curve for the Sevilleta field soil, heterogeneous soil profile. Impeding stone layer 6.5 centimeters thick in layer three. Volumetric water content, (θ_V), corrected for the volume of stones present.

(1974).

The water content of the stone layer was corrected for the volume of stones present using equation 2. Layer 2 demonstrates a markedly different scanning behavior due to the inclusion of stones in the soil profile. This is the result of that layer experiencing, to a greater extent than the other layers, the effects of drainage for a water content near saturation. It naturally more closely approximates the true drainage scanning curve, with the associated higher tensions, for the field soil than the less wet layers above and below it. Layers 4 & 5 behave similarly, a result of their initial water contents being nearly identical. As such, they both follow scanning curves that closely approximate one another. It is interesting to note that even though both of these matrix layers are below the stony layer their soil water retention character is effected by its presence.

The results of the 10 centimeter impeding stone layer are presented as Figure 12. The data is again bifurcated as compared to the homogeneous case. All layers approximate a similar trend with the exception of layer 2, which is immediately above the stone layer. Layer 2 is again distinctly offset from the layers above or below it. It is clear that the impeding stone layer, i.e. layer 3, is exerting an influence on the soil horizon ten centimeters above it, affecting the unsaturated flow of water in this region. Again layers 4 & 5 follow nearly identical scanning curves as desorption occurs in the profile while layer 3 behaves distinctly different than the matrix layers.

Figure 13 presents data for the 16 centimeter thick stone layer. The data presented in this plot again shows bifurcated trends in the soil water retention curve similar to the previous two heterogeneous soil profiles. The soil water retention character of the soil is so effected by the presence of the impeding stone layer that the layers composed only of matrix no longer approximate the soil water characteristic of the homogeneous profile. This is well evidenced by the fact that

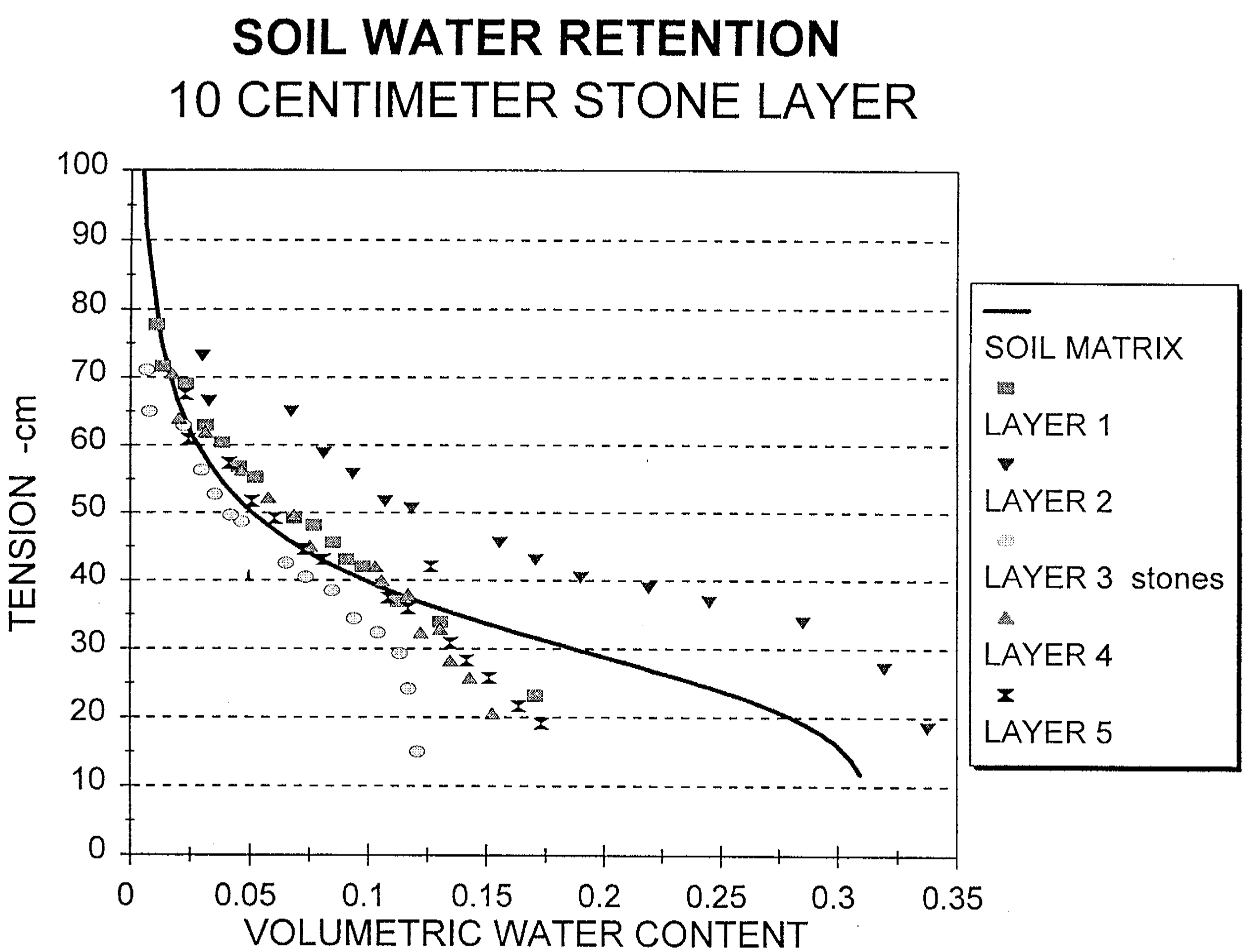

Figure 12. Soil water retention curve for the Sevilleta filed soil, heterogeneous soil profile. Impeding stone layer 10 centimeters thick in layer 3. Volumetric water content, (θ_V), corrected for the volume of stones present.

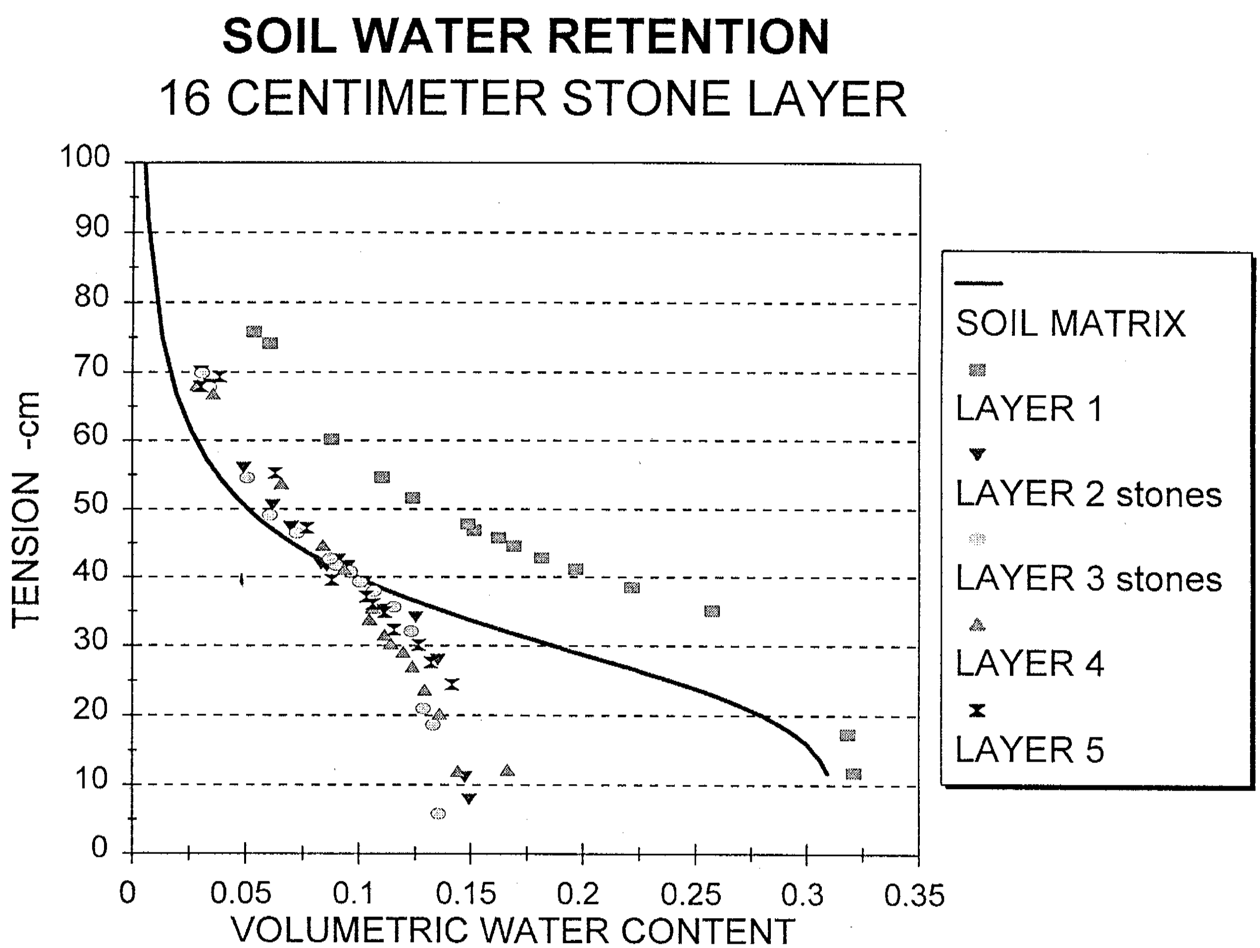

Figure 13. Soil water retention curve for the Sevilleta field soil, heterogeneous soil profile. Impeding stone layer 16 centimeters thick in layers two and three. Volumetric water content, (θ_V), corrected for the volume of stones present.

layers 4 & 5 now behave different from one another and no longer approximate the fitted curve for the soil matrix. The presence of such hysteric behavior in a layered soil with varying water contents is quite reasonable, if not somewhat unexpected.

Conductivity and Tension Relationships

In an effort to further quantify changes in the unsaturated properties of layered stony soils the unsaturated hydraulic conductivity was plotted against tension for both the homogeneous and heterogeneous cases. The graphs illustrate how the conductivity-tension relationship is influenced by the scanning behavior first observed in the soil water retention plots. Trends observed in the K(h) data correspond to increases and decreases in the soil water tension due to hysteresis. These data are presented as Figures 14 through 17. Figure 14 illustrates the relation between hydraulic conductivity and tension for the homogeneous soil profile. The fitted curve was the result of using RETC to fit the data as described above.

Figure 15 presents the relationship between conductivity and soil water tension for an impeding stone layer of 6.5 centimeters. Data from layers 1, 3, 5 are used to assess the behavior of the soil profile. Layers 3 and 4 are not presented for reasons of clarity, while the layers shown correspond to positions above, within, and below the impeding stone layer. The behavior of each of these layers is distinctly different from those in the heterogeneous profile. Layer 1 indicates that at low water contents, and similar conductivities, tensions are higher when the stony layer is present. At higher volumetric water contents the observed tensions are lower when the stone layer is present. Measured tensions in the stone layer and layer below it are consistently lower than for the homogeneous case.

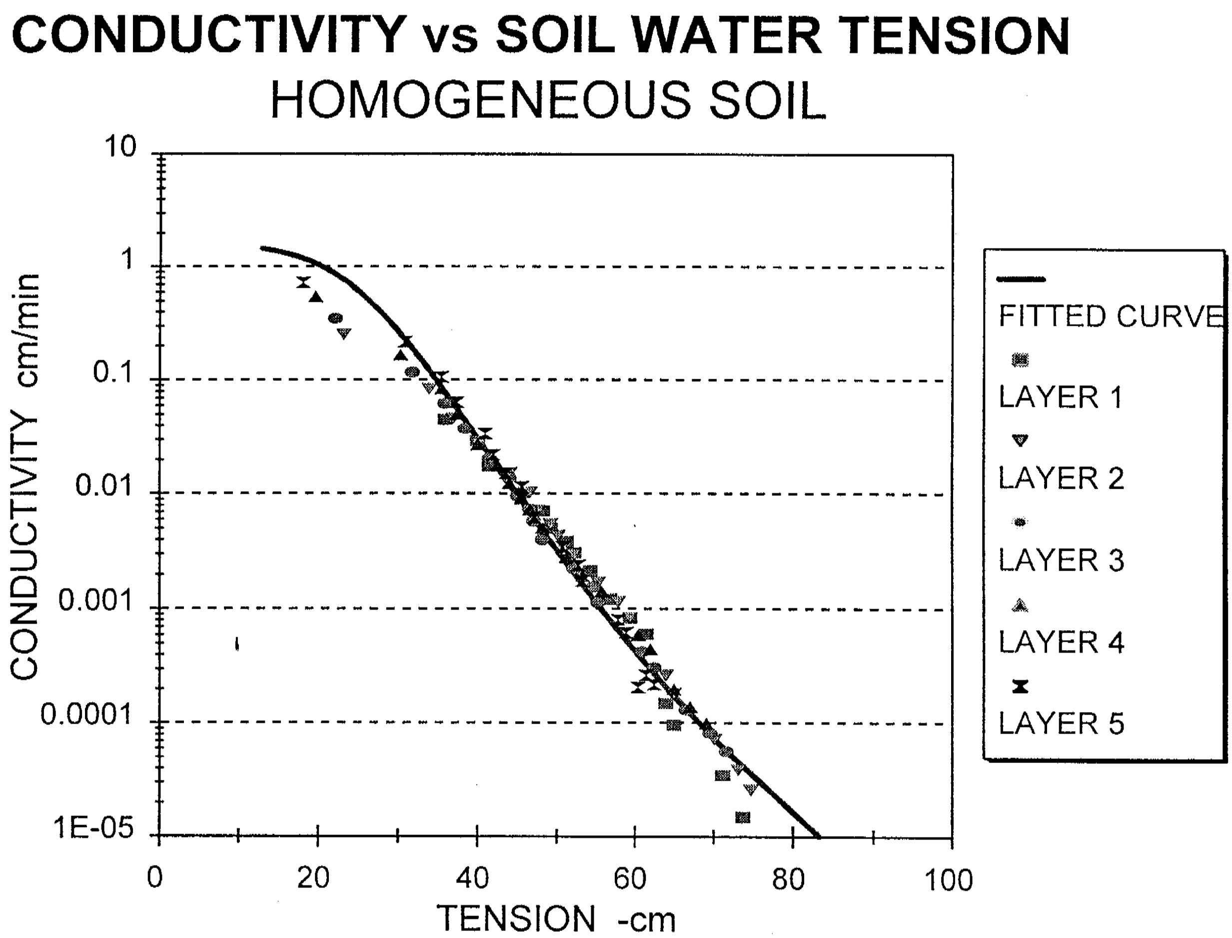

Figure 14. Unsaturated hydraulic conductivity verses tension, homogeneous soil profile. RETC fitted curve utilizing the models of *van Genuchten* and *Mualem*.

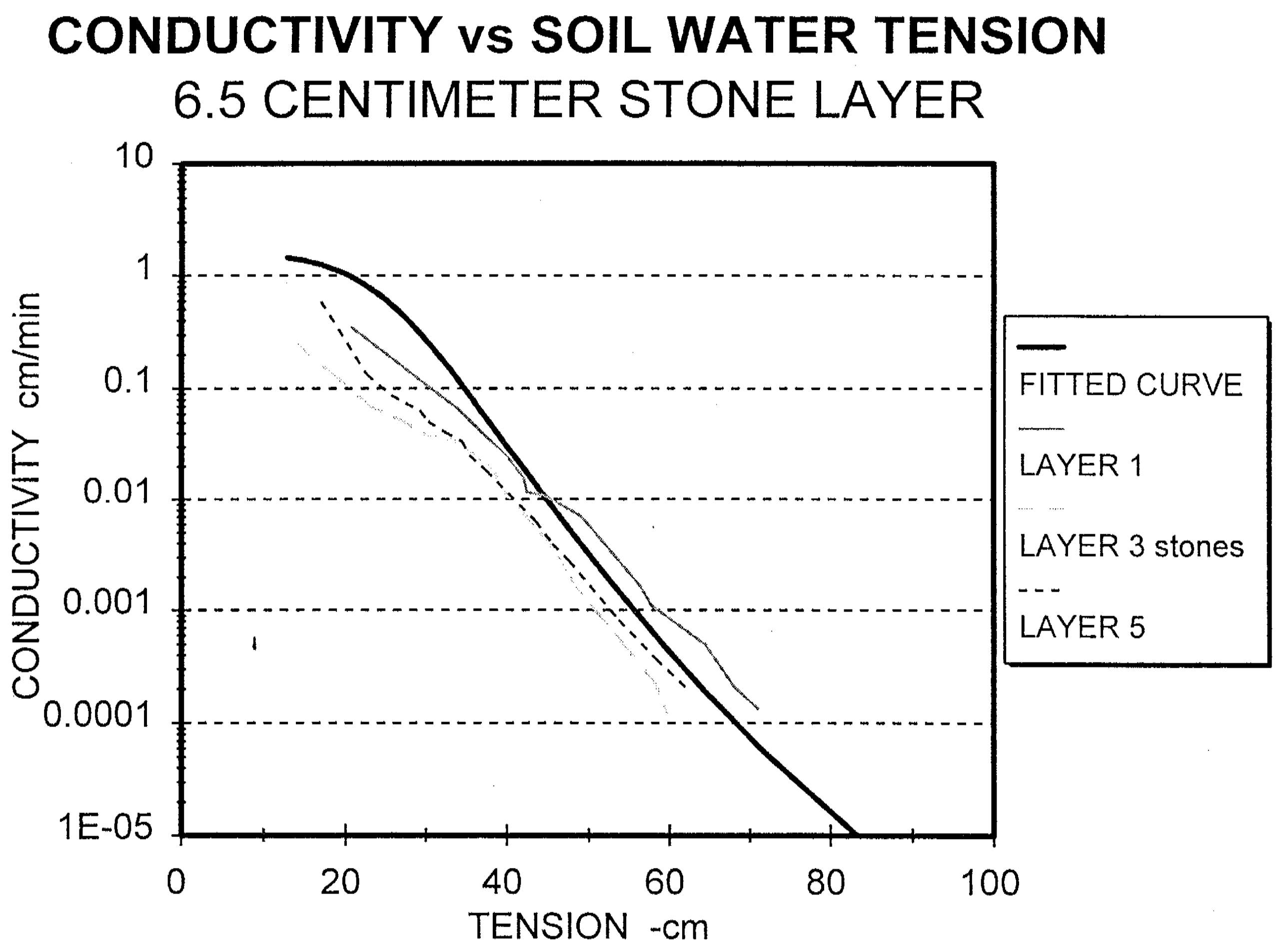

Figure 15. Unsaturated hydraulic conductivity verses tension. Heterogeneous soil profile, 6.5 centimeter stone layer.

When examined in conjunction with the data in Figure 11 this behavior can be explained as resulting from the different scanning curves initiated in each of the layers due to different initial water contents. Therefore, one would expect to see similar or identical hydraulic conductivity values at different soil water tensions, depending on the specific scanning curve followed during desorption. And this is, in fact, what is observed in the data.

Figure 16 is for the 10 centimeter impeding stone layer. Again all three layers behave differently than in the homogeneous case. Tensions for low volumetric water contents are higher than predicted for layers 1&3, while tensions at high water contents are lower than predicted for all layers. When compared to the soil water retention data for this soil profile the behavior is similar for each of the layers, (Figure 12). In each case, i.e. for each layer, the values of tension begin at values below the fitted curve, cross it at some critical threshold value, and end up at values higher than predicted. Clearly similar conductivities are occurring at different tensions due to hysteresis effects.

Data for the 16 centimeter stone layer, Figure 17, also exhibits similar hysteric behavior based on the observed tensions. Increasing the thickness of the impeding layer has more strongly effected the upper most layer than either the stone layer or the layer below it. This is the result of the top layer having a significantly higher initial volumetric water content than either of the other layers. This strongly influences the starting point of the scanning curve for this layer, and its desorption character during the remainder of the experiment. As in the previous heterogeneous profiles the K(h) curve for the stony layer is below the matrix layer immediately above it in the soil profile, and tends to run parallel to it. This experimental result was observed in each of the heterogeneous profiles, and is consistent with behavior predicted by Bower and Rice (1984) for stony soils using a theoretical approached based on stone geometry and the matrix $K(\Psi)$ characteristic. The observed experimental

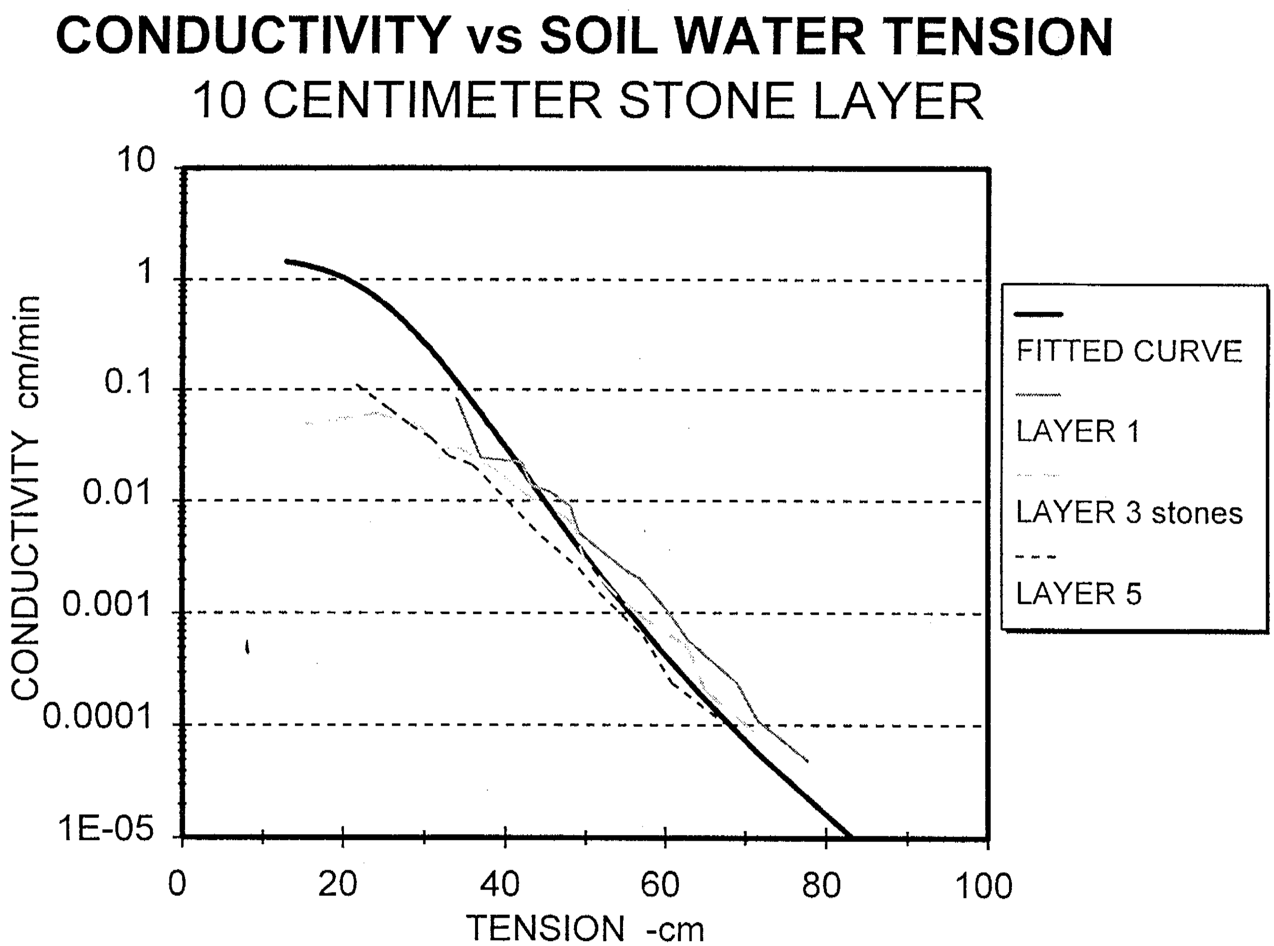

Figure 16. Unsaturated hydraulic conductivity verses tension. Heterogeneous soil profile, 10 centimeter stone layer.

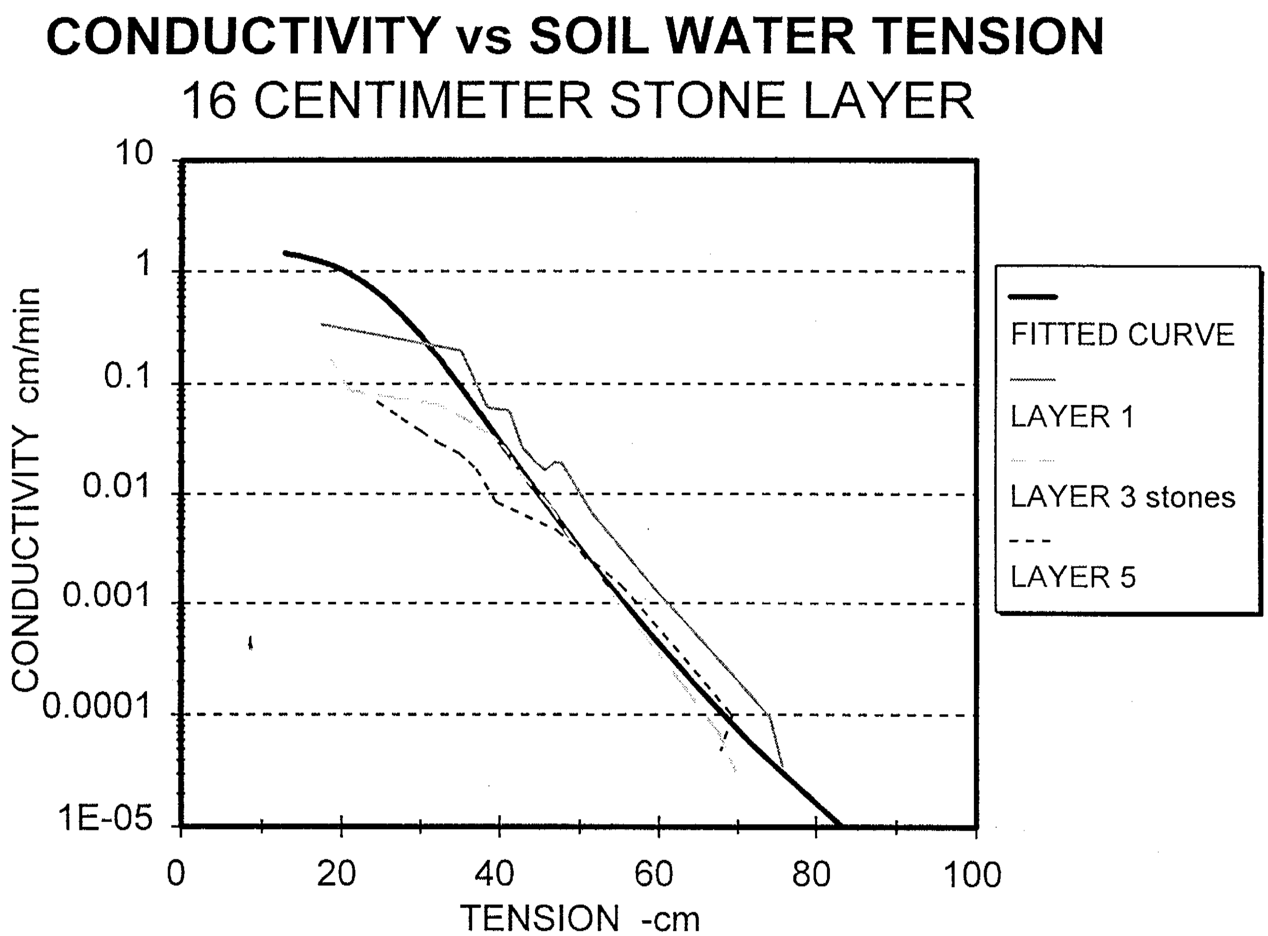

Figure 17. Unsaturated hydraulic conductivity verses tension. Heterogeneous soil profile, 16 centimeter stone layer.

data validates the theoretical approach of Bower and Rice (1984) as well as the results obtained in the laboratory experiments. Further strengthening the argument for hysteresis effects in stony layered soils.

Hysteresis effects on the relationship between hydraulic conductivity and suction have been observed in nonlayered soil profiles by Sobczuk et al. (1992), Poulovassilis and Tzimas (1974), Vachaud and Thony (1971), and in layered profiles by Dane and Wierenga (1975). The observed results indicate that the presence of an impeding stone layer increases the likelihood of such hysteric behavior occurring.

Hydraulic Conductivity Water Content Relationships

Hydraulic conductivity as a function of volumetric water content is presented in Figures 18 through 22. Figure 18 shows the relationship between unsaturated conductivity and volumetric water content for the homogeneous soil profile.

Figure 19 presents data for an impeding stone layer of 6.5 centimeters. All layers approximate the trend of the homogeneous soil profile with the exception of layer 2, the layer immediately above the stone layer. The stone layer shows a trend toward a slightly higher conductivity at a similar volumetric water content. Soil water retention data for layer three with a 6.5 centimeter impeding stone layer shows that at low volumetric water contents measured tensions approximate the fitted curve for the homogeneous profile, while at higher volumetric water contents the tension is somewhat less than the fitted values. This trend is also observed in the hydraulic conductivity data where at lower volumetric water contents the data approximates the fitted curve and at higher volumetric water contents the conductivity is slightly greater than the fitted values. This is the result

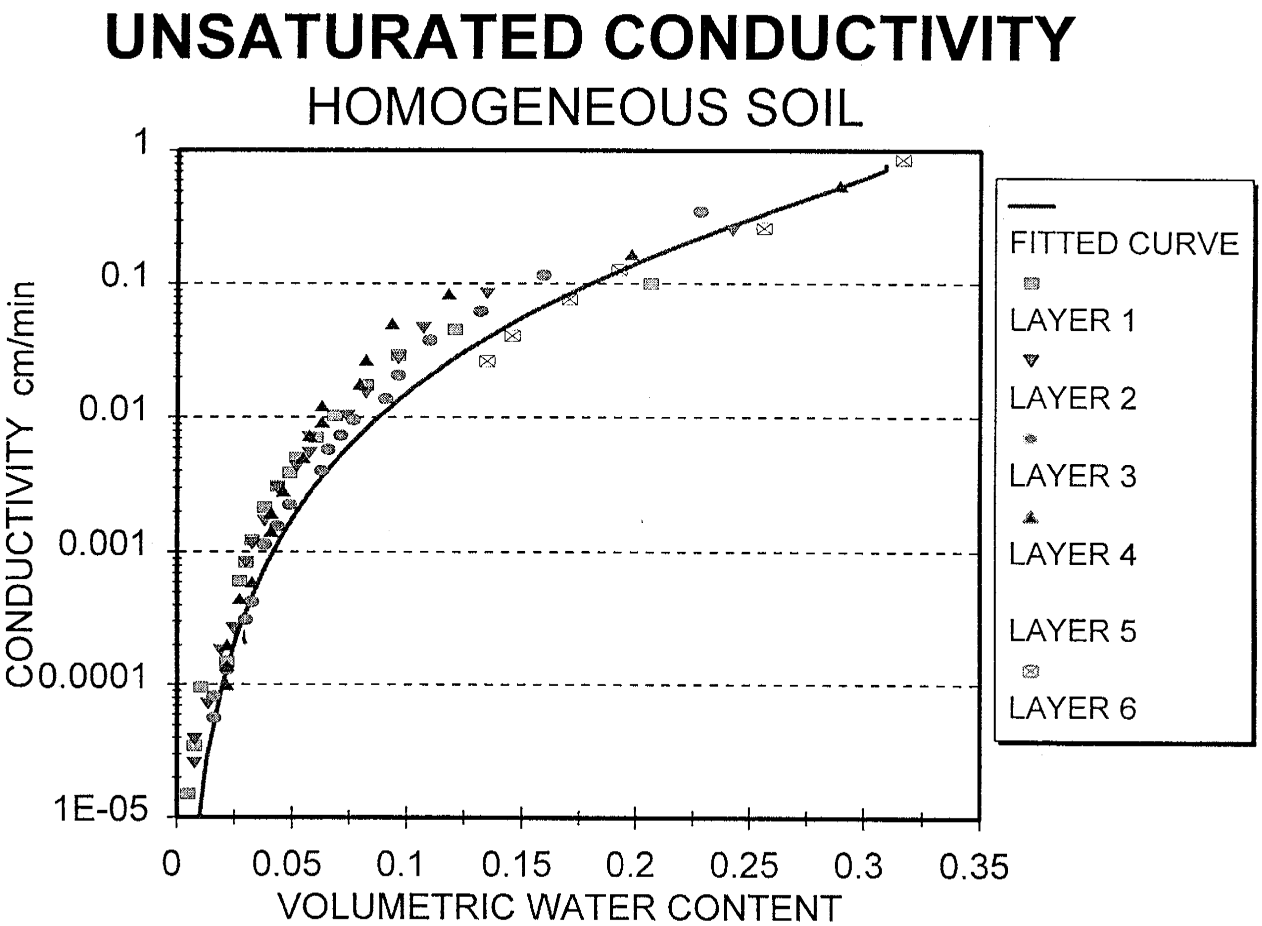

Figure 18. Unsaturated hydraulic conductivity verses volumetric water content, homogeneous soil profile. RETC curve fit utilizing the models of *van Genuchten* and *Mualem.*

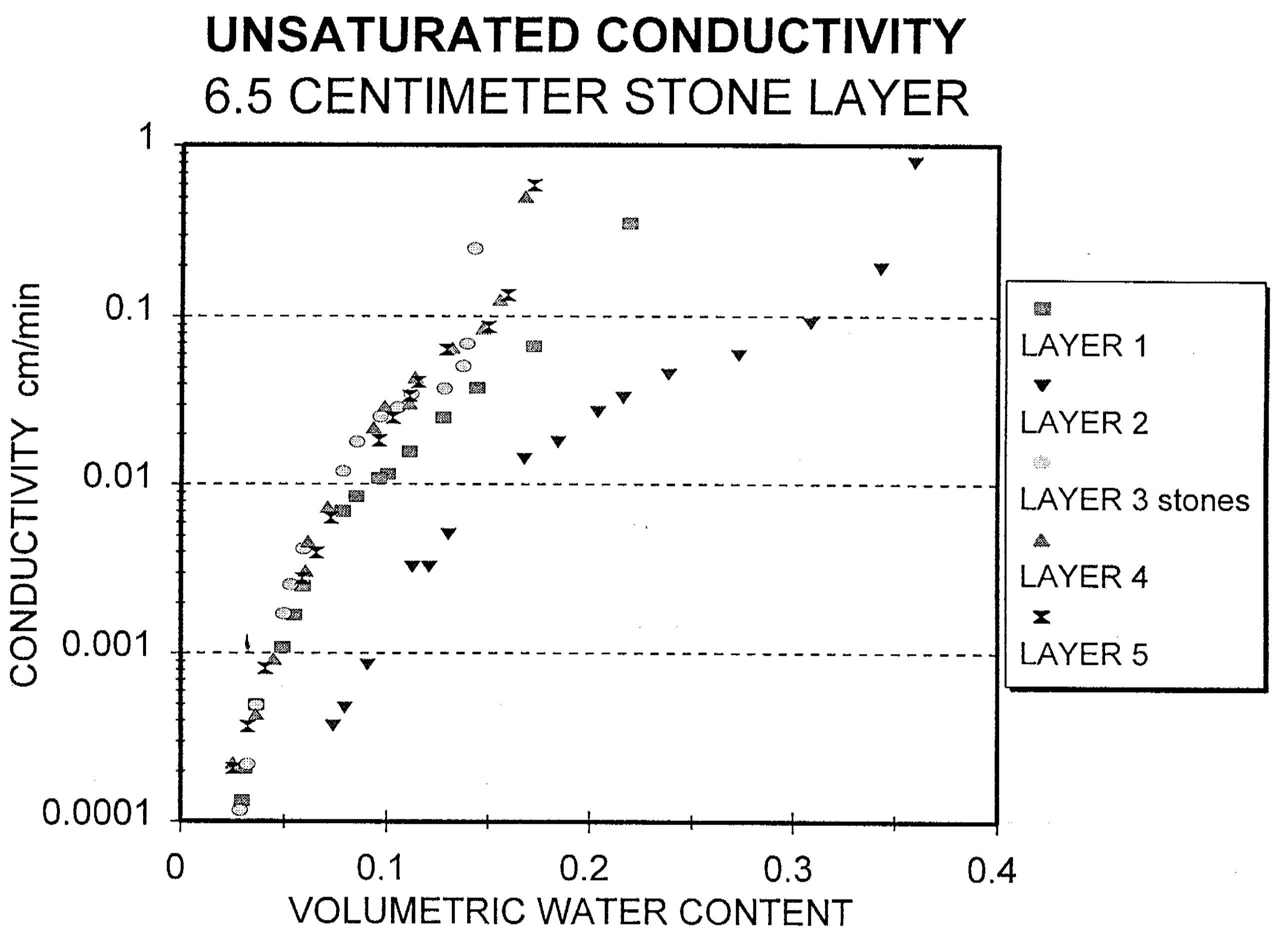

Figure 19. Unsaturated hydraulic conductivity verses volumetric water content, (θ_V), heterogeneous soil profile. Water content corrected for the volume of stones present.

of a hysteresis effect where lower tensions are occurring at similar water contents permitting higher conductivity values to exist in the soil. The behavior of layer 2 is interesting because it suggests that a low conductivity layer is present in the soil when, in fact, none exists. An examination of the data provided an explanation for this behavior. A comparison of the calculated flux and gradient for both the homogeneous and heterogeneous profiles revealed that the heterogeneous profiles had lower fluxes at higher water contents, along with gradients that were overestimated. This produces conductivities that are unreasonably low for such high water contents. A lower flux value divided by an overestimated gradient value yields a lower unsaturated hydraulic conductivity value for a given water content. This result when examined in conjunction with the lower fluxes that are occurring at substantially higher water contents explains the behavior of layer 2. The observed fluxes are unreasonable given the high volumetric water content for the layer, a result of the stone layer impeding the flow of water out of the profile. The high gradient values are a result of the analysis method being unable to properly estimate the gradient in the region immediately above the stone layer. The linear approximation of the hydraulic gradient between two measurement depths in the instantaneous profile method is not capable of accurately predicting the nonlinear gradients occurring in the profile, even though the data points are only 10 cm apart. The improper estimation of the hydraulic gradient in the region of the stone layer combined with the reduced flux at high water content suggests that a low conductivity layer is present at a location in the soil where none exists. This "pseudo" layer appears on each of the remaining two heterogeneous conductivity plots. A simulation was run for the heterogeneous profiles using Chain _ 2D, an unsaturated flow model, to examine hydraulic gradients in the region of the stone layer. The result illustrates the nonlinear nature of the gradient in the region of the stone layer, and is presented as Figure 20.

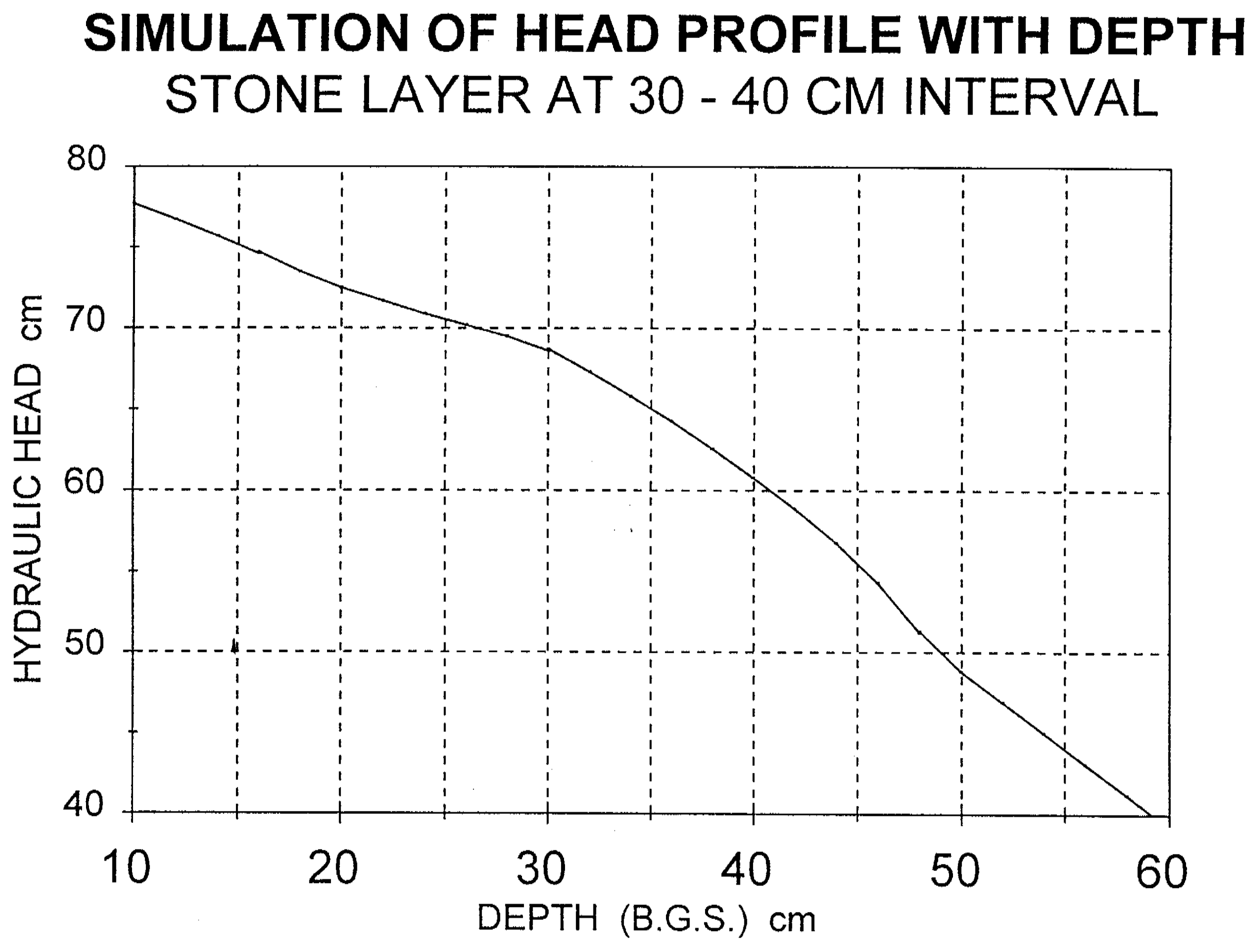

Figure 20. Computer simulation of the head with depth profile for a heterogeneous soil column using Chain _2D.

Figure 21 presents the data for an impeding stone layer of 10 centimeters. The initial trends observed in the 6.5 centimeter stone layer are again present, but they are more distinct as the thickness of the layer increases. Again layers 2 and 3 do not approximate the fitted curve or the surrounding matrix. The stony layer has higher conductivity values at similar water contents while layer 2 behaves similar to the "pseudo" low conductivity layer described above. The observed behavior is the result of processes occurring that are similar to those described for the 6.5 centimeter profile, hysteresis effects combined with errors in estimating the hydraulic gradient.

Figure 22 presents the data for an impeding layer of 16 centimeters. In this profile the thickness of the stone layer was increased to a maximum of 16 centimeters, being positioned in layers two and three. The clarity of the previously observed trends has been degraded somewhat by this change. Layers 2&3 exhibit higher conductivities at similar water contents than the fitted curve, while layer 1, now the layer immediately above the stone layer, exhibits lower conductivities at higher volumetric water contents. The observed effects are consistent throughout all of the heterogeneous profile experiments, with the degree of the hysteresis effect being related to the thickness of the stone layer and the proportion of differential wetting.

Estimation of Conductivity in Stony Soils

A comparison of several methods used to estimate the hydraulic conductivity of stony soils was performed in order to test there validity under unsaturated conditions. The equations used to accomplish this are those of Peck and Watson (1979), Bower and Rice (1984), and a simple correction, presented here as a possible new approach, based on the volume of stones present in the soil profile as a single layer. The specific equations are as follows:

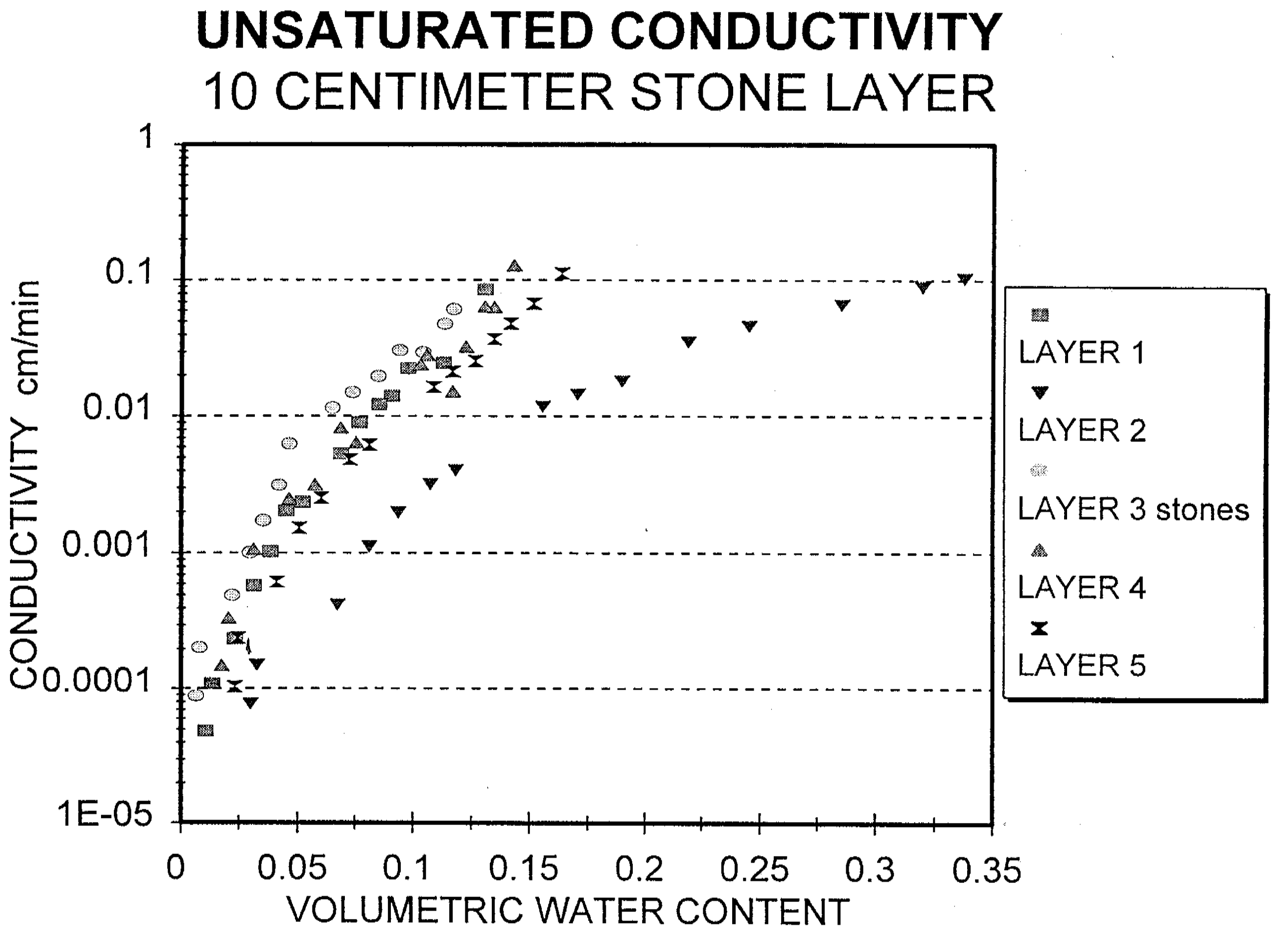

Figure 21. Unsaturated hydraulic conductivity verses volumetric water content, (θ_V), heterogeneous soil profile. Water content corrected for the volume of stones present.

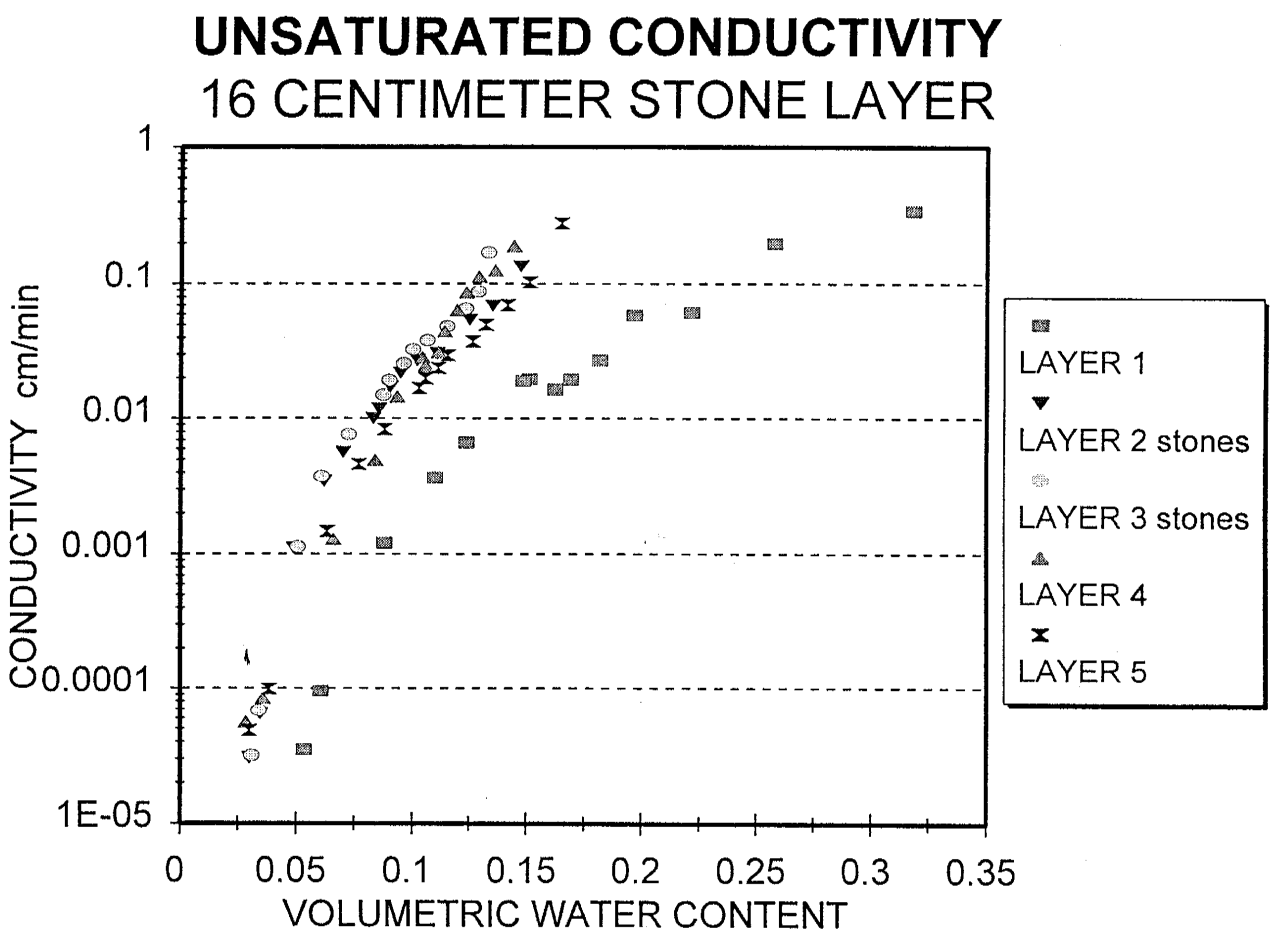

Figure 22. Unsaturated hydraulic conductivity verses volumetric water content, (θ_V), heterogeneous soil profile. Water content corrected for the volume of stones present.

$$K_b = K_s \frac{2(1-V_{st})}{2+V_{st}} \qquad (3)$$

after Peck and Watson (1979) where:

K_b = bulk hydraulic conductivity of stony soil,

K_s = hydraulic conductivity of the soil alone, and

V_{st} = volume fraction of stones.

$$K_b = K_s \frac{e_b}{e_s} \qquad (4)$$

after Bower and Rice (1984) where:

K_b = bulk hydraulic conductivity of the sand and gravel mixture,

K_s = hydraulic conductivity of the sand fraction alone,

e_b = bulk void ratio (volume of the voids divided by the volume of the solids) of the sand and stone mixture, and

e_s = void ratio of the sand.

$$K_b = K_s \times (1-V_{st}) \qquad (5)$$

and a simple volume correction where:

K_b = bulk unsaturated hydraulic conductivity of the stony soil

K_s = unsaturated hydraulic conductivity of the matrix, and

V_{st} = volume of stones in the soil as a single layer.

The heterogeneous profile containing the ten centimeter stone layer was selected for comparing the various methods, a result of it being the heterogeneous soil profile of intermediate thickness. Tables 2 & 3 present values of unsaturated hydraulic conductivity for the homogeneous soil profile at a series of tensions and volumetric water contents, and the resulting values calculated for the heterogeneous profiles using the above mentioned equations. These conductivity estimates are presented in Figures 23 & 24 as plots of the K(Ψ) and K(θ) functions.

Figure 23 shows that the relationship of unsaturated hydraulic conductivity to tension in the stony soil is only roughly approximated by each of the methods. Each of the methods fail to accurately predict the observed data at high soil water tensions. All of the methods underestimate the unsaturated hydraulic conductivity at high tensions, although all of the estimates are within an order of magnitude of the observed data. The simple volumetric correction being applied to the conductivity of the homogeneous soil is unable to accurately predict the effects of hysteresis in the soil profile. This is best illustrated by the consistent increase in the ratio of the heterogeneous conductivity to that of homogeneous conductivity, Table 2. This ratio increases with increasing soil water tension, while the volumetric correction is constant throughout all changes in tension.

Figure 24 shows the relationship of unsaturated conductivity to water content for the same soil profile. Similar to the K(Ψ) plot each of the methods behave distinctly different from one another. However, unlike the K(Ψ) plot, estimates of conductivity as a function of water content underestimate the unsaturated conductivity at high water contents, i.e. low tension. The method of Peck & Watson and Bower & Rice behave in a similar fashion, under estimating the hydraulic conductivity for the stony profile by nearly identical amounts. It is very interesting to note that by simply multiplying the homogeneous conductivity values by the simple correction for the

Tension cm H_20	K_{hmo} cm/min	K_{st} cm/min	K_{st}/K_{hmo} cm/min	K_{hmo}* (1-V_{ST}) cm/min	Peck&Watson cm/min	Bower&Rice cm/min
20	0.50	0.18	0.36	0.225	0.167	0.152
30	0.17	0.07	0.41	0.0765	0.0569	0.0517
40	0.03	0.017	0.56	0.0135	0.01004	0.0091
50	0.003	0.003	1.0	0.00135	0.001	9.1E -04
60	4.5E -04	7.0E -04	1.55	2.03E -04	1.5E -04	1.4E -04
70	7.5E -05	1.0E -04	1.33	3.37E -05	2.5E -05	2.3E -05

K_{hmo} : Unsaturated hydraulic conductivity homogeneous profile.

K_{st} : Unsaturated hydraulic conductivity heterogeneous profile.

Table 2. Calculation of unsaturated hydraulic conductivity for various tensions using the equations of Peck and Watson (1975), Bower and Rice (1984) and a simple correction for the volume of stones present in the soil profile.

Theta %	K_{hmo} cm/min	K_{st} cm/min	K_{st}/K_{hmo} cm/min	K_{hmo} * (1-V_{ST}) cm/min	Peck&Watson cm/min	Bower&Rice cm/min
2.5	0.0004	0.00018	0.45	0.00018	0.00013	0.00012
5	0.0035	0.0017	0.48	0.00158	0.00117	0.00106
7.5	0.01	0.0065	0.65	0.0045	0.00335	0.00304
10	0.03	0.015	0.50	0.0135	0.01004	0.00912
12.5	0.06	0.031	0.52	0.0270	0.02008	0.01824
15	0.09	0.055	0.61	0.0405	0.03012	0.02736
17.5	0.15	0.09	0.60	0.0675	0.05019	0.0456
20	0.18	0.14	0.77	0.081	0.06023	0.05472
22.5	0.24	0.17	0.71	0.108	0.08031	0.07295
25	0.32	0.25	0.78	0.144	0.10708	0.09727

K_{hmo} : Unsaturated hydraulic conductivity homogeneous profile.

K_{st} : Unsaturated hydraulic conductivity heterogeneous profile.

Table 3. Calculation of unsaturated hydraulic conductivity for various volumetric water contents using the equations of Peck and Watson (1975), Bower and Rice (1984) and a simple correction for the volume of stones present in the soil profile.

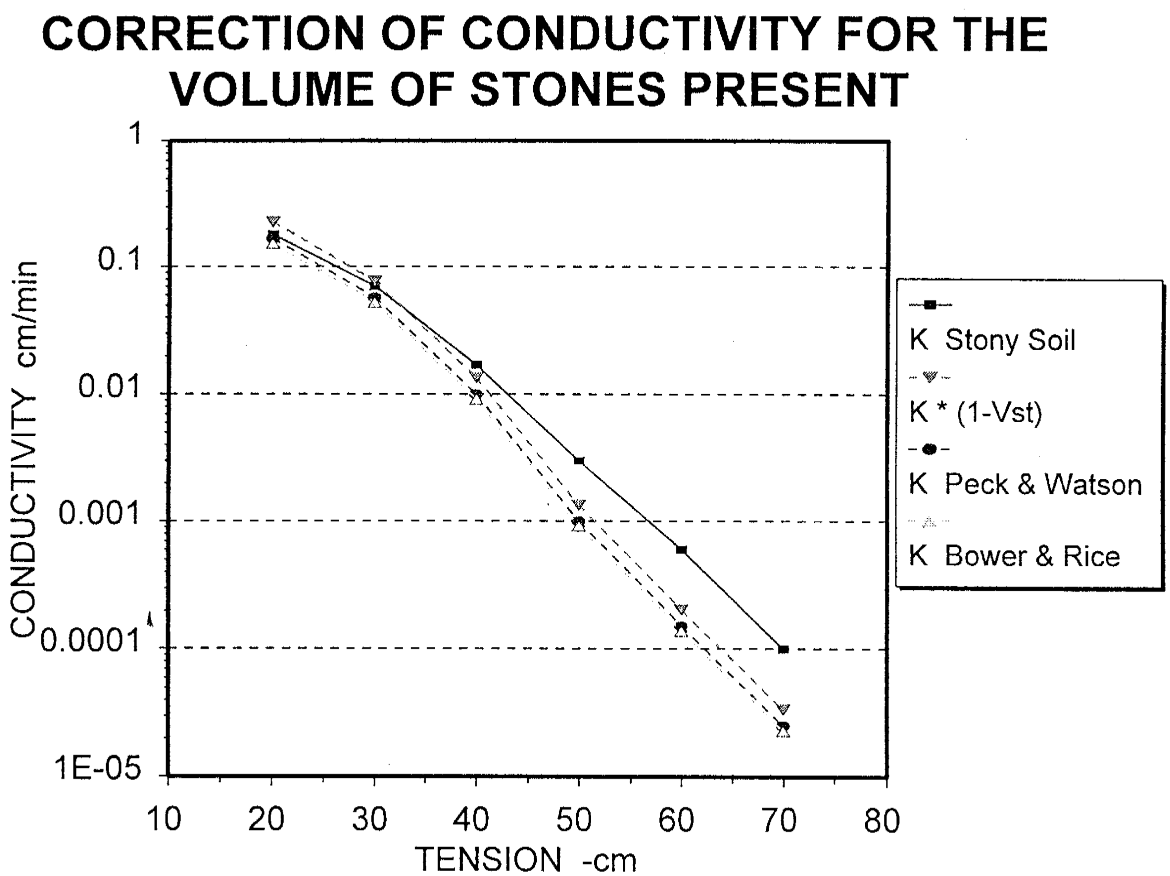

Figure 23. Correction of conductivity for the volume of stones present in the soil profile, conductivity verses tension for the 10 centimeter stone layer. A comparison of various methods.

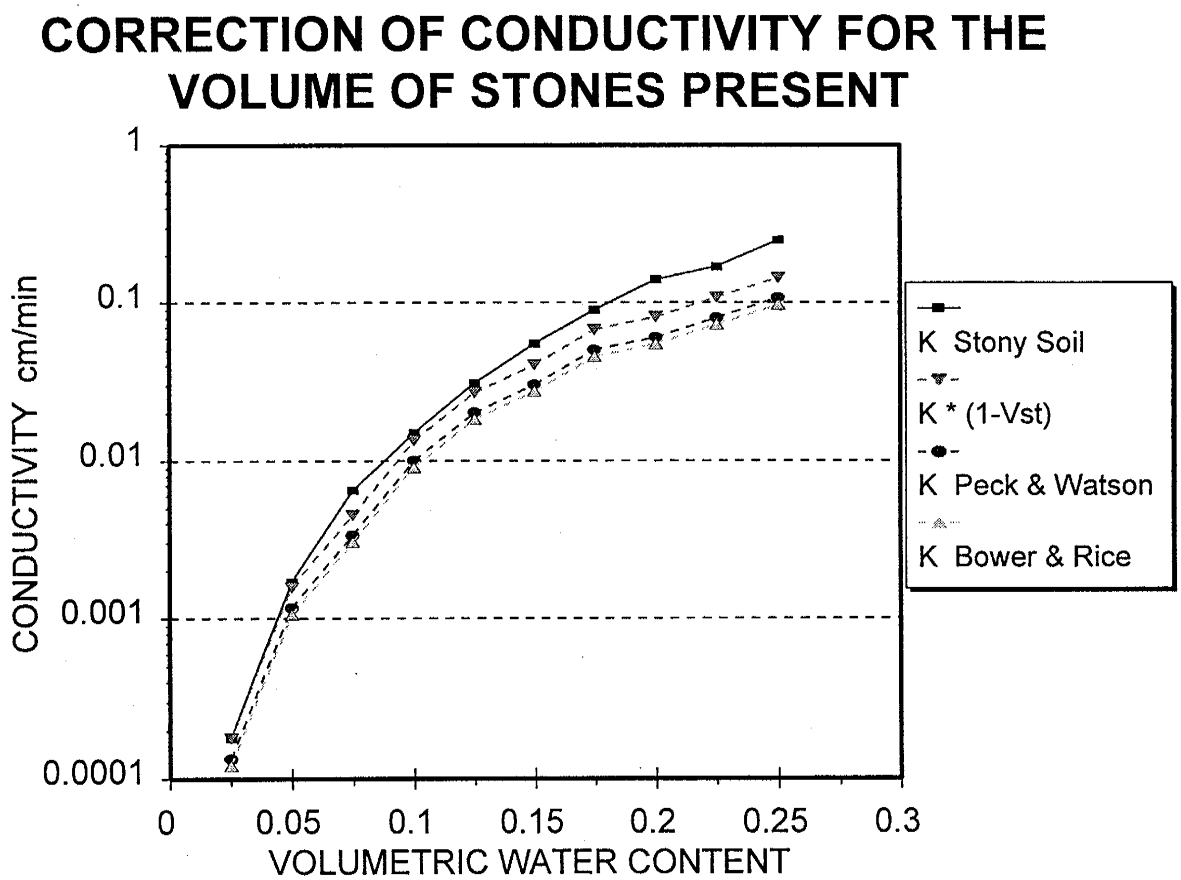

Figure 24. Correction of conductivity for the volume of stones present in the soil profile, conductivity verses volumetric water content for the 10 centimeter stone layer. A comparison of various methods.

volume of stones present in the soil profile a better prediction of the observed data is obtained. It is clear that when dealing with layered stony soils this simple volumetric correction provides an excellent estimate of the bulk unsaturated hydraulic conductivity of the soil profile.

CONCLUSION

The use of the TDR technique, tensiometry, and the instantaneous profile method proved to be valid for studying the effects of stone volume on unsaturated hydraulic conductivity in a layered stony soil. Significant findings resulting from an evaluation of the experimental approach and the heterogeneous soil profiles are as follows. First, although some studies suggest that the TDR technique may be used in stony soil with little or no loss in accuracy, [Drungil et al. (1989), Richardson et. al (1992)], the presence of stones in a soil profile may result in an improper estimation of soil water content. The presence of stones with less wet interior portions occurring in the TDR sample volume may impart significant error to the collected readings by creating a heterogeneous water distribution within the sample volume. Second, the presence of stones in a soil profile necessitate that their volume as a percentage of the soil profile be determined as well as there spacial distribution. Soils with a high volume of stones would best be studied using the TDR technique if the probes were smaller "mini-probes" similar to the ones described by Sobczuk et. al. (1992), or smaller probes constructed using the guidelines of Zegelin et al. (1992), Knight et al. (1994).Third, when utilizing the instantaneous profile method to evaluate the hydraulic character of a soil profile the analysis must be corrected for the volume of stones present in the soil profile to avoid an over estimation of the volumetric water content for the stone layer, and related underestimation of unsaturated hydraulic conductivity for this layer. Fourth, the use of the instantaneous profile method in stony layered soils requires that the lithology of the soil profile be determined during the investigation to avoid the improper identification of the low conductivity "pseudo" layer, immediately above stony layers, as a distinct lithologic horizons. The presented data strongly suggests that unique hysteric effects occur in layered stony soils when analyzed using the instantaneous profile method which have not been addressed in previous studies. Additionally, the limitations of the instantaneous profile method, with respect to the estimation of hydraulic gradients, should be considered when using the method. Finally, a comparison of the methods used to estimate unsaturated hydraulic conductivity in stony soils indicates that a simple correction for the volume of stones present in the profile is a direct and effective method to estimate bulk unsaturated hydraulic conductivity.

References

Baker, J.M., R.J. Lascano. 1989. The spatial sensitivity of time domain reflectometry. Soil Sci. 147: 378 - 383.

Bouwer, H.B., and R.C. Rice. 1984. Hydraulic properties of stony vadose zones. Ground Water. Vol. 22, no.6: 696 - 705.

Brakensiek, D.L., W.J. Rawls. 1994. Soil containing rock fragments: effects of infiltration. Catena. no. 23: 99 - 110.

Cassel, D.K., R.G. Kachanoski, G.C. Topp. 1994. Practical considerations for using a TDR cable tester. Soil Tech. 7: 113 - 126.

Dane, J.H., and P.J. Wierenga. 1975. Effect of hysteresis on the prediction of infiltration, redistribution and drainage of water in a layered soil. J. Hydrol., 25: 229 - 242.

Drungil, C.E.C., K.Abt., and T.J. Gish. 1989. Soil moisture determination in gravelly soils with time domain reflectometry. Transactions of the Am. Soc. Arg. Eng. Vol. 32, no. 1:, pp. 177 - 180.

Haines, W.B. 1930. Studies in the physical properties of soils. V. The hysteresis effect in capillary properties and the modes of moisture distribution associated therewith. Journal Agr. Sci., 20: 97 - 116.

Hillel, D.I. 1980. Fundamentals of soil physics : San Diego, Academic Press, Inc., 413 p.

Hillel, D.I., V.D. Krentos, and Y. Stylianou. 1972. Procedure and test of an internal drainage method for measuring soil hydraulic characteristics in situ. Soil Sci., 114: 395-400.

Jury, W.A., W.R. Gardner, W.H. Gardner. 1991. Soil physics: New York, John Wiley & Sons, Inc., 328 p

Klute, A. 1986. *Editor*: Methods of Soil Analysis, Part 1- Physical and Mineralogical Methods, Second Edition., Madison Wisconsin, Am. Soc. Agr. Inc. & Soil Sci. Soc. Am. Inc., 1188 p.

Knight, J.H. 1991. Discussion of "The spatial sensitivity of time domain reflectometry" by J.M. Baker and R.L. Lascano. Soil Sci., 151:254 - 255.

Knight, J.H. 1992. Sensitivity of time domain reflectometry measurements to lateral variations in soil water content. Water Resour. Res., 28: 2345 - 2352.

Knight, J.H., I. White, and S.J. Zegelin. 1994. Sample volume of TDR probes used for water content monitoring. p. 93 - 104. *In* Symposium and Workshop on Time Domain Reflectometry in

Environmental, Infrastructure, and Mining Applications: United States Department of the Interior Bureau of Mines, Special Publication: SP 19 - 94.

Mehuys, G.R., L.H. Stolzy, J. Letey, and L.V. Weeks. 1975. Effect of stones on the hydraulic conductivity of relatively dry desert soils. Soil Science Soc. Am. Proc., 39: 37 - 42.

Peck, A.J., J.D. Watson. 1979. Hydraulic conductivity and flow in non-uniform soil. In Workshop on Soil Physics and Field Heterogeneity. CSIRO Division of Environmental Mechanics, Canberra, Australia, February 12 - 14, 1979.

Poulovassilis, A., and E. Tzimas. 1974. The hysteresis in the relationship between hydraulic conductivity and suction. Soil Sci. 117: 250 - 256.

Richardson, M.D., C.A. Miesner, C.S. Hoveland, and K.J. Karnok. 1992. Time domain reflectometry in closed container studies. Agronomy Journal. Vol. 84, no. 6: 1061 - 1063.

Sobczuk, H.A., R. Plagge, R.T. Walczak, and C.H. Roth. 1992. Laboratory equipment and calculation procedure to rapidly determine hysteresis of some soil hydrophysical properties under nonsteady flow conditions. Z. Pflanzenernähr. Bodenk., 155: 157 - 163.

Spaans, E.J.A., J.M. Baker. 1993. Simple baluns in parallel probes for time domain reflectometry. Soil Sci. Soc. Am. J., 57: 668 - 673.

Topp, G.C. 1969. Soil water hysteresis measured in a sandy loam and compared with the hysteresis domain model. Soil Sci. Soc. Am. Proc., 33: 645 - 651.

Topp, G.C., and J.L. Davis. 1985. Time-domain reflectometry (TDR) and its application to irrigation scheduling. *In*: Advances in irrigation, vol. 3. D. Hillel (ed.). Academic, New York, pp. 107 - 127.

Topp, G.C., J.L. Davis, and A.P. Annan. 1980. Electromagnetic determination of soil water content: measurements in coaxial transmission lines. Water Resour. Res., 16: 574 - 582.

Topp, G.C., and E.E. Miller. 1966. Hysteresis moisture characteristics and hydraulic conductivities for glass bead media. Soil Sci. Soc. Am. Proc., 30: 156 - 162.

Vachaud, G., and J. Thony. 1971. Hysteresis during infiltration and redistribution in a soil column at different initial water contents. Water Resour. Res. 7: 111 - 127.

van Genuchten, M.Th., S.R. Yates, A.W. Warrick, and F.J. Leij. 1992. Analysis of measured, predicted, and estimated hydraulic conductivity using the RETC computer program. Soil Sci. Soc. Am. J., 56: 347 - 354.

Watson, K.K. 1966. An instantaneous profile method for determining the hydraulic conductivity of unsaturated porous materials. Water Resour. Res., 2: 709 - 715.

Wierenga, P.J. 1993. Personal communication: Informal technological exchange meeting at the University of Arizona, September 1993

Zegelin, S.J., I. White, and D.R. Jenkins. 1989. Improved field probes for soil water content and electrical conductivity measurement using time domain reflectometry. Water Resour. Res., 25: 2367 - 2376.

Zegelin, S.J., I. White, and G.F. Russel. 1992. A critique of the time domain reflectometry technique for determining field soil water content., p. 187 - 208. *In:* G.C. Topp, W.D. Reynolds, and R.E. Green (Editors), Advances in Measurement of Soil Physical Properties: Bringing Theory into Practice. Soil Sci. Soc Am., Madison WI, USA., SSSA Special Publication Number 30: 187 - 208.

APPENDIX A

CALIBRATION OF THE TDR PROBES TO THE SEVILLETA FIELD SAND

EXPERIMENTAL PROCEDURE

APPENDIX A

EXPERIMENTAL PROCEDURE

In order to collect accurate measurements of volumetric water content it was necessary to calibrate the TDR to the field soil used for this study. This required that a series of TDR measurements be made on the soil at a number of varying, but known, water contents. The procedure used was adapted from one developed Wierenga (1993) The actual calibration was performed using the following procedure and the Sevilleta field sand.

Dry field soil was placed in a small acrylic column with a free draining base. The weights of the sand, column, base, and TDR probe were measured to determine the mass of the experimental apparatus and the dry bulk density of the sand. The column was then saturated from the bottom up by placing it in a tray of water. A TDR probe was then inserted into the column and the all components reweighed. The column was then allowed to drain over a period of days while TDR readings and sample weights were recorded. The experiment was concluded when the column has again attained its original presaturation weight. This data was then used to calculate the volumetric water content for the soil when TDR measurements were recorded.

The results were then plotted as measured TDR reading verses volumetric water content, and a linear regression fitted to the data. The equation of the line fitted to this curve provided the calibration curve for the TDR in the Sevilleta field soil, where the x-coordinate is the measured TDR reading and the returned y-intercept is the calculated volumetric water content. This equation was then used to calculate volumetric water content in all of the column experiments. Figure A-1 shows the data from one of three calibration experiments, it also shows the linear regression curve fitted to the experimental data.

A comparison of this calibration curve with the one developed by Topp et al. (1980) shows a high degree of correlation between the two when compared as dielectric constant verses volumetric water content. This comparison, presented as Figure A-2, validates the method of calibration used, and suggests that this approach is a relatively easy way to calibrate the TDR to a particular field soil one is studying.

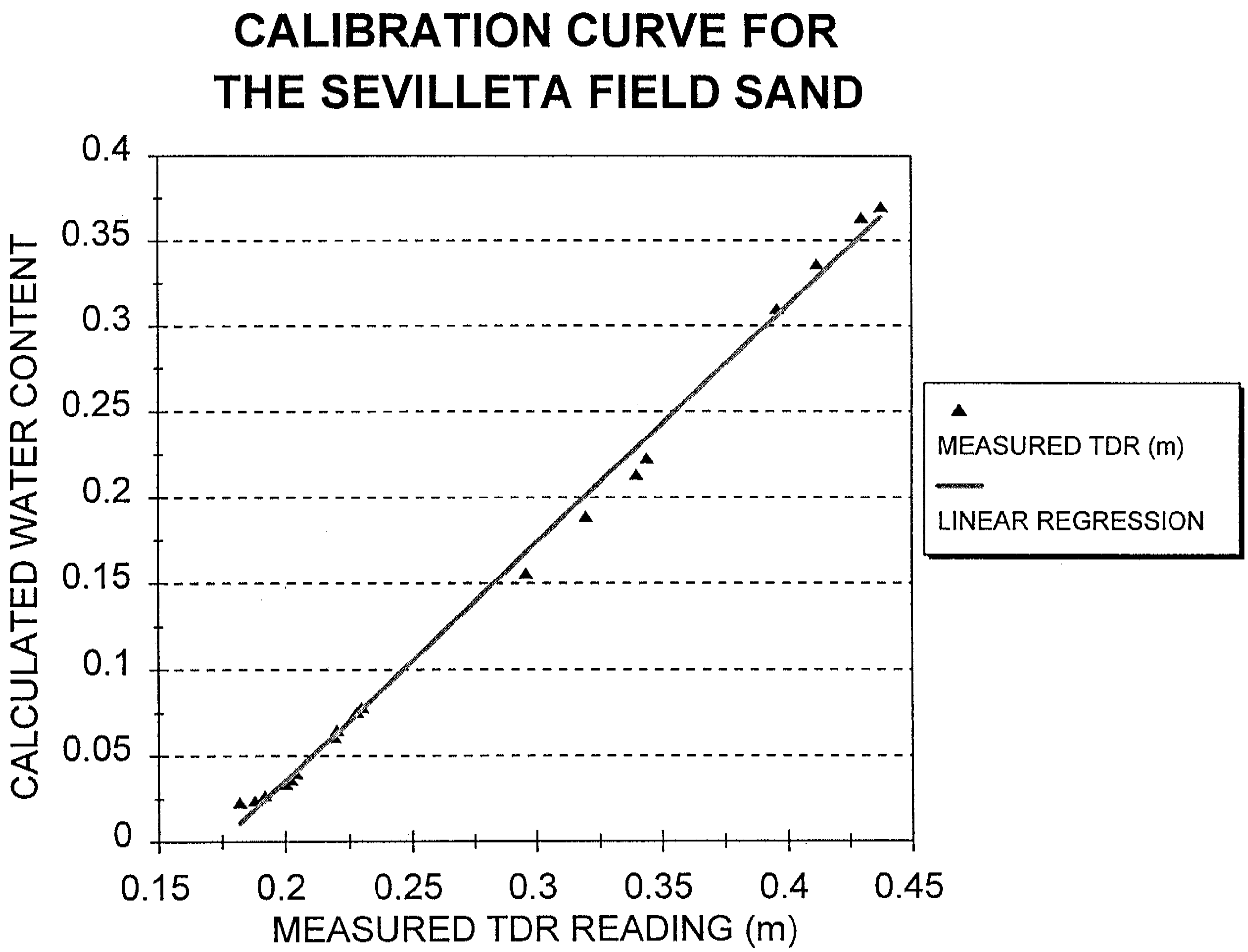

Figure A-1. TDR calibration curve for the Sevilleta field sand.

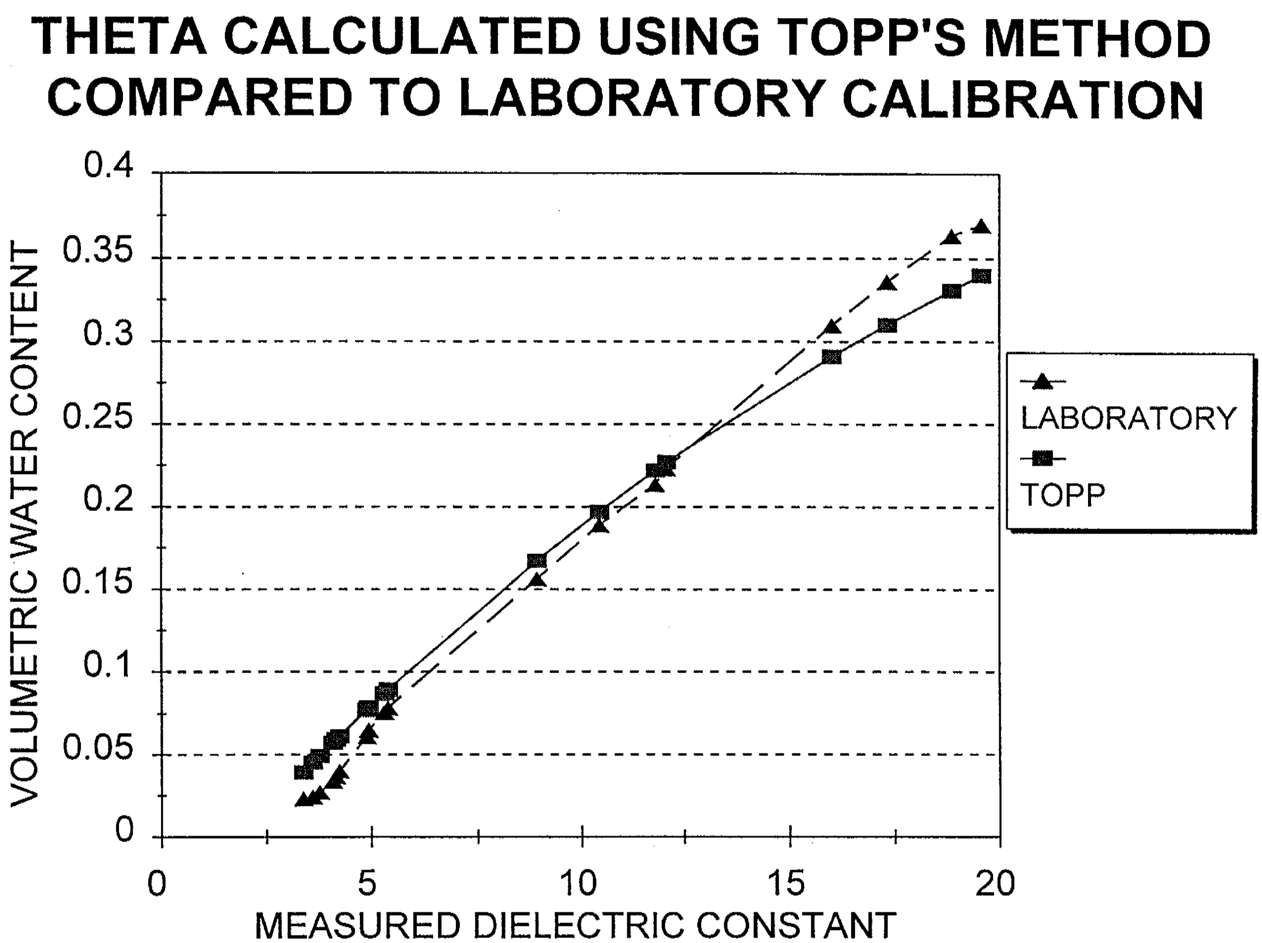

Figure A-2. Comparison of estimated volumetric water content using the equation of Topp et al. (1980) as compared to that calculated using the laboratory calibration curve determined in this study.

APPENDIX B

REVIEW OF TDR THEORY AND PRINCIPLES

APPENDIX B

TDR THEORY REVIEW

A detailed explanation of the theory and principles involved in time domain reflectometry has been presented by Topp et al. (1980), Topp & Davis (1985), while the historical development of the TDR in soil physics and its practical use is discussed by Cassel et al. (1994). Stated in the most succinct manner the TDR technique measures the velocity of propagation of a high frequency electrical signal in a dielectric medium, i.e. a moist soil, and records the amount by which this electrical pulse is attenuated in the medium. The TDR unit or cable tester, in this case the Tektronix model 1502B, initiates a step voltage pulse via its signal generator. This voltage pulse travels along the transmission line, i.e. coaxial cable, which terminates in an ordered arrangement of wave guides. The transmission line used in constructing the probes is of the same impedance as the output signal of the TDR, 50Ω, so the signal pulse travels unhindered through it. Wherever the impedance of the transmission line changes a mismatch occurs causing a portion of the signal energy to be reflected back to the cable tester unit. This pulse of reflected signal energy manifests itself as a discontinuity on the oscilloscope display. The observed discontinuity is related to the magnitude of the impedance mismatch and the dielectric property of the medium in which it occurs. The characteristic wave form seen on the display screen is due to the signal pulse encountering the impedance mismatch as it enters the wave guides of the probe, initial reflection point, and the total reflection of the signal pulse at the end of the wave guides where all of the energy is subsequently returned, final reflection point. Through a process of internal conversion the reflected voltage pulse is displayed on the oscilloscope as length on the abscissa and returned voltage on the ordinate. The apparent length of the wave guides in the soil is obtained by measuring the distance between the initial and final reflection points of the displayed wave form. This apparent length is a function of the dielectric properties of the medium. The high dielectric constant of water , approximately 80, as compared to that of soil, approximately 3 to 7, Cassel et al. (1994), illustrates why the TDR technique is effective in determining soil water content. A medium having a relatively high dielectric constant , for example a moist soil, will return an apparent length for the probe significantly greater than its true length. This apparent length is then used to calculate the dielectric constant for the soil which can then be calculated as a function of volumetric water content. A detailed description relating the measured apparent probe length, calculated dielectric constant of the medium, and calculated volumetric water content can be found elsewhere in the literature Topp (1980), Topp & Davis (1985), Spaans & Baker (1993).

The accuracy of TDR measurements in the heterogeneous profiles depend to a great extent on what volume of soil is sampled by the TDR in the stone layer. As stated above, is this measurement representative of the real matrix water content or is it a larger volume averaged measurement including portions of the stones which are dry? The volume of soil sampled is dependent upon the electric field distribution generated around the probe and what spatial weighting function is associated with the specific probe type. Several articles have appeared in the literature that address this issue from two very different approaches. One is a theoretical approach that deals primarily with transmission line theory, while the other is an empirical approach. The work of Zegelin et al. (1989), Zegelin et al. (1992), Knight (1991), Knight (1992) and Knight et al. (1994) present detailed accounts of the principles involved in estimating the sample volume and spatial weighting functions for probes of various configurations. This information would permit one to develop the necessary equations to estimate the electric field distributions and spatial weighting functions for two or three wire probes given idealized conditions of probe construction and instrument performance. However, a specific sample volume or range of influence for three wire probes similar to the ones used is not provided. This approach did not provide a readily discernable solution to the problem relating to the experimental procedure used. Empirical approaches were examined to determine if an acceptable experimental procedure could be adapted to the laboratory setup. Empirical approaches used by Topp & Davis (1985), Baker & Lascano (1989), and Richardson et al. (1992) provided a frame work for the experimental procedures detailed in the text of the paper.

APPENDIX C

EXPERIMENTAL DATA: HOMOGENEOUS SOIL PROFILE

SEVILLETA SAND - NO STONES

	COLUMN EXPERIMENT #6 HOMOGENEOUS SEVILLETTA SAND						
		TENSIOMETER READINGS mbar					
MINUTES	T1	T2	T3	T4	T5	T6	
1	-20.5	-18	-16	-15	-13	-11	
15	-38.5	-36	-35	-32.5	-31	-26.5	
30	-48.5	-46.5	-44.5	-43	-43.5	-38.5	
45	-52.5	-49.5	-48.5	-48	-48	-46	
60	-54	-52.5	-51	-50	-50	-48.5	
90	-58	-56.5	-54	-52.5	-53.5	-51.5	
120	-60.5	-59	-56.5	-55	-54.5	-52.5	
150	-61.5	-60	-57.5	-56.5	-56	-54.5	
180	-63.5	-61.5	-59	-58	-58	-55.5	
210	-64.5	-62.5	-59.5	-59	-58	-57	
270	-66.5	-64.5	-60.5	-60.5	-59.5	-58	
390	-69	-67.5	-64.5	-63.5	-63	-60	
510	-71.5	-70	-67	-65.5	-65	-61	
630	-73.5	-71.5	-67.5	-68	-65.5	-62.5	
1200	-76	-76	-73	-72.5	-70	-64	
1500	-77	-77	-74.5	-74	-71	-64	
2880	-83	-82	-78.5	-77	-73.5	-65	
4380	-85.5	-85	-81.5	-79	-72.5	-64	
5610	-87	-86.5	-83.5	-81	-74.5	-65	
		TENSIOMETER READINGS cm H2O					
MINUTES	T1	T2	T3	T4	T5	T6	
1	-20.9039	-18.3546	-16.3152	-15.2955	-13.2561	-11.2167	
15	-39.2585	-36.7092	-35.6895	-33.1403	-31.6107	-27.0221	
30	-49.4555	-47.4161	-45.3767	-43.8471	-44.357	-39.2585	
45	-53.5343	-50.4752	-49.4555	-48.9456	-48.9456	-46.9062	
60	-55.0638	-53.5343	-52.0047	-50.985	-50.985	-49.4555	
90	-59.1426	-57.6131	-55.0638	-53.5343	-54.554	-52.5146	
120	-61.6919	-60.1623	-57.6131	-56.0835	-55.5737	-53.5343	
150	-62.7116	-61.182	-58.6328	-57.6131	-57.1032	-55.5737	
180	-64.751	-62.7116	-60.1623	-59.1426	-59.1426	-56.5934	
210	-65.7707	-63.7313	-60.6722	-60.1623	-59.1426	-58.1229	
270	-67.8101	-65.7707	-61.6919	-61.6919	-60.6722	-59.1426	
390	-70.3593	-68.8298	-65.7707	-64.751	-64.2411	-61.182	
510	-72.9086	-71.379	-68.3199	-66.7904	-66.2805	-62.2017	
630	-74.948	-72.9086	-68.8298	-69.3396	-66.7904	-63.7313	
1200	-77.4972	-77.4972	-74.4381	-73.9283	-71.379	-65.2608	
1500	-78.5169	-78.5169	-75.9677	-75.4578	-72.3987	-65.2608	
2880	-84.6351	-83.6154	-80.0465	-78.5169	-74.948	-66.2805	
4380	-87.1844	-86.6745	-83.1056	-80.5563	-73.9283	-65.2608	
5610	-88.7139	-88.2041	-85.145	-82.5957	-75.9677	-66.2805	

	CORRECTED TENSIOMETER READINGS AT CUPS					
MINUTES	T1	T2	T3	T4	T5	T6
1	-7.40385	-4.8546	-2.8152	-1.7955	0.2439	2.2833
15	-25.7585	-23.2092	-22.1895	-19.6403	-18.1107	-13.5221
30	-35.9555	-33.9161	-31.8767	-30.3471	-30.857	-25.7585
45	-40.0343	-36.9752	-35.9555	-35.4456	-35.4456	-33.4062
60	-41.5638	-40.0343	-38.5047	-37.485	-37.485	-35.9555
90	-45.6426	-44.1131	-41.5638	-40.0343	-41.054	-39.0146
120	-48.1919	-46.6623	-44.1131	-42.5835	-42.0737	-40.0343
150	-49.2116	-47.682	-45.1328	-44.1131	-43.6032	-42.0737
180	-51.251	-49.2116	-46.6623	-45.6426	-45.6426	-43.0934
210	-52.2707	-50.2313	-47.1722	-46.6623	-45.6426	-44.6229
270	-54.3101	-52.2707	-48.1919	-48.1919	-47.1722	-45.6426
390	-56.8593	-55.3298	-52.2707	-51.251	-50.7411	-47.682
510	-59.4086	-57.879	-54.8199	-53.2904	-52.7805	-48.7017
630	-61.448	-59.4086	-55.3298	-55.8396	-53.2904	-50.2313
1200	-63.9972	-63.9972	-60.9381	-60.4283	-57.879	-51.7608
1500	-65.0169	-65.0169	-62.4677	-61.9578	-58.8987	-51.7608
2880	-71.1351	-70.1154	-66.5465	-65.0169	-61.448	-52.7805
4380	-73.6844	-73.1745	-69.6056	-67.0563	-60.4283	-51.7608
5610	-75.2139	-74.7041	-71.645	-69.0957	-62.4677	-52.7805

	HYDRAULIC HEAD AT THE TENSIOMETER CUPS H					
MINUTES	T1	T2	T3	T4	T5	T6
1	-18.6539	-26.1046	-34.8152	-43.0455	-51.7561	-59.7167
15	-37.0085	-44.4592	-54.1895	-60.8903	-70.1107	-75.5221
30	-47.2055	-55.1661	-63.8767	-71.5971	-82.857	-87.7585
45	-51.2843	-58.2252	-67.9555	-76.6956	-87.4456	-95.4062
60	-52.8138	-61.2843	-70.5047	-78.735	-89.485	-97.9555
90	-56.8926	-65.3631	-73.5638	-81.2843	-93.054	-101.015
120	-59.4419	-67.9123	-76.1131	-83.8335	-94.0737	-102.034
150	-60.4616	-68.932	-77.1328	-85.3631	-95.6032	-104.074
180	-62.501	-70.4616	-78.6623	-86.8926	-97.6426	-105.093
210	-63.5207	-71.4813	-79.1722	-87.9123	-97.6426	-106.623
270	-65.5601	-73.5207	-80.1919	-89.4419	-99.1722	-107.643
390	-68.1093	-76.5798	-84.2707	-92.501	-102.741	-109.682
510	-70.6586	-79.129	-86.8199	-94.5404	-104.781	-110.702
630	-72.698	-80.6586	-87.3298	-97.0896	-105.29	-112.231
1200	-75.2472	-85.2472	-92.9381	-101.678	-109.879	-113.761
1500	-76.2669	-86.2669	-94.4677	-103.208	-110.899	-113.761
2880	-82.3851	-91.3654	-98.5465	-106.267	-113.448	-114.781
4380	-84.9344	-94.4245	-101.606	-108.306	-112.428	-113.761
5610	-86.4639	-95.9541	-103.645	-110.346	-114.468	-114.781

		WATER CONTENTS via TDR					
MINUTES	TDR #1	THETA 1	TDR #2	THETA 2	TDR#3	THETA 3	
1	0.364	0.261682	0.384	0.289267	0.364	0.261682	
15	0.324	0.206514	0.35	0.242374	0.34	0.228581	
30	0.262	0.121003	0.272	0.134795	0.29	0.159621	
45	0.244	0.096177	0.252	0.107211	0.27	0.132037	
60	0.234	0.082385	0.244	0.096177	0.254	0.109969	
90	0.224	0.068593	0.234	0.082385	0.244	0.096177	
120	0.218	0.060318	0.228	0.07411	0.24	0.09066	
150	0.212	0.052043	0.216	0.057559	0.23	0.076868	
180	0.21	0.049284	0.216	0.057559	0.226	0.071351	
210	0.206	0.043767	0.212	0.052043	0.222	0.065835	
270	0.202	0.03825	0.206	0.043767	0.22	0.063076	
390	0.198	0.032734	0.202	0.03825	0.21	0.049284	
510	0.196	0.029975	0.198	0.032734	0.206	0.043767	
630	0.194	0.027217	0.196	0.029975	0.202	0.03825	
1200	0.19	0.0217	0.192	0.024458	0.198	0.032734	
1500	0.182	0.010666	0.188	0.018941	0.196	0.029975	
2880	0.18	0.007908	0.184	0.013425	0.19	0.0217	
4380	0.178	0.005149	0.18	0.007908	0.186	0.016183	
5610	0.178	0.005149	0.18	0.007908	0.186	0.016183	
MINUTES	TDR #4	THETA 4	TDR #5	THETA 5	TDR #6	THETA 6	
1	0.414	0.330643	0.422	0.341677	0.426	0.347193	
15	0.384	0.289267	0.398	0.308576	0.404	0.316851	
30	0.318	0.198239	0.332	0.217548	0.36	0.256166	
45	0.26	0.118245	0.272	0.134795	0.314	0.192722	
60	0.242	0.093419	0.256	0.112728	0.298	0.170655	
90	0.234	0.082385	0.246	0.098936	0.28	0.145829	
120	0.232	0.079627	0.24	0.09066	0.272	0.134795	
150	0.22	0.063076	0.234	0.082385	0.264	0.123761	
180	0.22	0.063076	0.224	0.068593	0.258	0.115486	
210	0.216	0.057559	0.222	0.065835	0.252	0.107211	
270	0.214	0.054801	0.222	0.065835	0.25	0.104453	
390	0.208	0.046526	0.216	0.057559	0.242	0.093419	
510	0.204	0.041009	0.214	0.054801	0.242	0.093419	
630	0.204	0.041009	0.21	0.049284	0.24	0.09066	
1200	0.198	0.032734	0.204	0.041009	0.24	0.09066	
1500	0.194	0.027217	0.2	0.035492	0.236	0.085144	
2880	0.19	0.0217	0.196	0.029975	0.232	0.079627	
4380	0.19	0.0217	0.198	0.032734	0.23	0.076868	
5610	0.19	0.0217	0.198	0.032734	0.23	0.076868	

		SLOPE OF WETTNESS CURVES dTH/dt					
MINUTES	dTH/dt 1	dTH/dt 2	dTH/dt 3	dTH/dt 4	dTH/dt 5	dTH/dt 6	
1	0.017587	-0.21604	-0.1189	-0.25823	-0.22126	-2293.9	
15	0.003901	0.011903	0.007469	0.015332	0.013611	0.010979	
30	0.001852	0.003259	0.002714	0.004087	0.004132	0.003706	
45	0.0013	0.001534	0.001431	0.001899	0.002014	0.001905	
60	0.000778	0.00091	0.000904	0.001117	0.001215	0.001177	
90	0.000448	0.000444	0.000473	0.00054	0.000604	0.000591	
120	0.000298	0.00027	0.0003	0.000327	0.000371	0.000361	
150	0.000215	0.000185	0.000211	0.000224	0.000252	0.000245	
180	0.000165	0.000137	0.000159	0.000165	0.00019	0.000179	
210	0.000131	0.000106	0.000125	0.000127	0.000148	0.000137	
270	8.93E-05	7.07E-05	8.48E-05	8.45E-05	9.88E-05	8.82E-05	
390	5.07E-05	3.94E-05	4.48E-05	4.69E-05	5.53E-05	4.64E-05	
510	3.34E-05	2.59E-05	3.24E-05	3.08E-05	3.65E-05	2.90E-05	
630	2.40E-05	1.87E-05	2.37E-05	2.22E-05	2.65E-05	2.01E-05	
1200	8.64E-06	7.12E-06	9.25E-06	8.40E-06	1.01E-05	6.57E-06	
1500	6.05E-06	5.13E-06	6.71E-06	6.04E-06	7.28E-06	4.47E-06	
2880	2.13E-06	2.00E-06	2.67E-06	2.35E-06	1.58E-06	1.48E-06	
4380	1.08E-06	1.11E-06	1.49E-06	1.30E-06	1.12E-06	7.38E-07	
5610	7.28E-07	7.84E-07	1.06E-06	9.18E-07	2.85E-06	4.93E-07	
	WATER CONTENT dTH/dt TIMES THE THICKNESS OF THE LAYER						
MINUTES	H2O 1	H2O 2	H2O 3	H2O 4	H2O 5	H2O 6	
1	0.351742	-2.16039	-1.18903	-2.58235	-2.21259	-22939	
15	0.078028	0.119025	0.074693	0.153319	0.136109	0.109792	
30	0.037038	0.03259	0.027144	0.04087	0.041318	0.03706	
45	0.026	0.015344	0.014313	0.018991	0.020139	0.019048	
60	0.015566	0.009098	0.009037	0.011172	0.012153	0.011769	
90	0.00896	0.004438	0.004728	0.0054	0.006037	0.005911	
120	0.005958	0.002704	0.002995	0.003272	0.003713	0.003606	
150	0.004308	0.001854	0.002108	0.002235	0.002521	0.002453	
180	0.00329	0.001369	0.001586	0.001646	0.001899	0.001788	
210	0.002612	0.001062	0.001249	0.001274	0.001479	0.001367	
270	0.001786	0.000707	0.000848	0.000845	0.000988	0.000882	
390	0.001015	0.000394	0.000448	0.000469	0.000553	0.000464	
510	0.000668	0.000259	0.000324	0.000308	0.000365	0.00029	
630	0.00048	0.000187	0.000237	0.000222	0.000265	0.000201	
1200	0.000173	7.12E-05	9.25E-05	8.4E-05	0.000101	6.57E-05	
1500	0.000121	5.13E-05	6.71E-05	6.04E-05	7.28E-05	4.47E-05	
2880	4.25E-05	2E-05	2.67E-05	2.35E-05	1.58E-05	1.48E-05	
4380	2.17E-05	1.11E-05	1.49E-05	1.3E-05	1.12E-05	7.38E-06	
5610	1.46E-05	7.84E-06	1.06E-05	9.18E-06	2.85E-05	4.93E-06	

	SLOPE OF HEAD WITH DEPTH CURVE dH/dz						
MINUTES							
1	0.824041	0.824041	0.824041	0.824041	0.824041	0.824041	
15	0.78321	0.78321	0.78321	0.78321	0.78321	0.78321	
30	0.83237	0.83237	0.83237	0.83237	0.83237	0.83237	
45	0.899241	0.899241	0.899241	0.899241	0.899241	0.899241	
60	0.903621	0.903621	0.903621	0.903621	0.903621	0.903621	
90	0.883421	0.883421	0.883421	0.883421	0.883421	0.883421	
120	0.848669	0.848669	0.848669	0.848669	0.848669	0.848669	
150	0.868965	0.868965	0.868965	0.868965	0.868965	0.868965	
180	0.858745	0.858745	0.858745	0.858745	0.858745	0.858745	
210	0.858937	0.858937	0.858937	0.858937	0.858937	0.858937	
270	0.841561	0.841561	0.841561	0.841561	0.841561	0.841561	
390	0.83553	0.83553	0.83553	0.83553	0.83553	0.83553	
510	0.807934	0.807934	0.807934	0.807934	0.807934	0.807934	
630	0.797906	0.797906	0.797906	0.797906	0.797906	0.797906	
1200	1.166719	0.926453	0.797029	0.712655	0.651894	0.603309	
1500	1.275822	0.949546	0.783085	0.67852	0.605326	0.548153	
2880	1.231703	0.871951	0.685473	0.569634	0.489955	0.428911	
4380	1.457801	0.848679	0.585443	0.440171	0.34885	0.283948	
5610	1.483246	0.874968	0.587874	0.426936	0.326467	0.256221	
		FLUX TROUGH EACH LAYER					
MINUTES	Q1	Q2	Q3	Q4	Q5	Q6	
1	0.351742	-1.80865	-2.99768	-5.58003	-7.79262	-22946.8	
15	0.078028	0.197053	0.271747	0.425066	0.561174	0.670966	
30	0.037038	0.069628	0.096773	0.137642	0.178961	0.216021	
45	0.026	0.041344	0.055657	0.074648	0.094787	0.113835	
60	0.015566	0.024664	0.033701	0.044873	0.057026	0.068794	
90	0.00896	0.013398	0.018127	0.023527	0.029564	0.035475	
120	0.005958	0.008662	0.011657	0.014928	0.018641	0.022248	
150	0.004308	0.006162	0.00827	0.010506	0.013027	0.015479	
180	0.00329	0.004659	0.006245	0.007891	0.00979	0.011577	
210	0.002612	0.003674	0.004923	0.006197	0.007676	0.009043	
270	0.001786	0.002493	0.003341	0.004186	0.005174	0.006056	
390	0.001015	0.001409	0.001857	0.002326	0.002879	0.003343	
510	0.000668	0.000928	0.001252	0.00156	0.001925	0.002216	
630	0.00048	0.000667	0.000904	0.001126	0.001391	0.001592	
1200	0.000173	0.000244	0.000336	0.00042	0.000521	0.000587	
1500	0.000121	0.000172	0.000239	0.0003	0.000373	0.000417	
2880	4.25E-05	6.26E-05	8.93E-05	0.000113	0.000129	0.000143	
4380	2.17E-05	3.28E-05	4.77E-05	6.07E-05	7.18E-05	7.92E-05	
5610	1.46E-05	2.24E-05	3.3E-05	4.22E-05	7.07E-05	7.56E-05	

	CONDUCTIVITY AS A FUNCTION OF WATER CONTENT						
MINUTES	K1	K2	K3	K4	K5	K6	
1	0.42685	-2.19485	-3.63778	-6.77154	-9.45659	-27846.7	
15	0.099626	0.251597	0.346965	0.542723	0.716505	0.856688	
30	0.044497	0.083651	0.116261	0.165362	0.215001	0.259525	
45	0.028913	0.045977	0.061893	0.083012	0.105408	0.12659	
60	0.017226	0.027294	0.037295	0.049659	0.063108	0.076132	
90	0.010142	0.015166	0.020519	0.026632	0.033465	0.040156	
120	0.00702	0.010206	0.013735	0.01759	0.021965	0.026215	
150	0.004958	0.007091	0.009517	0.01209	0.014991	0.017813	
180	0.003831	0.005425	0.007272	0.009188	0.0114	0.013482	
210	0.003041	0.004278	0.005731	0.007215	0.008936	0.010528	
270	0.002123	0.002962	0.00397	0.004974	0.006148	0.007196	
390	0.001215	0.001686	0.002222	0.002784	0.003446	0.004002	
510	0.000827	0.001148	0.001549	0.001931	0.002383	0.002743	
630	0.000601	0.000836	0.001133	0.001411	0.001743	0.001995	
1200	0.000148	0.000263	0.000422	0.00059	0.0008	0.000973	
1500	9.48E-05	0.000181	0.000306	0.000442	0.000616	0.000761	
2880	3.45E-05	7.17E-05	0.00013	0.000198	0.000262	0.000334	
4380	1.49E-05	3.86E-05	8.14E-05	0.000138	0.000206	0.000279	
5610	9.82E-06	2.56E-05	5.62E-05	9.89E-05	0.000217	0.000295	

	SOIL WATER RETENTION DATA HOMOGENEOUS PROFILE							
	FITTED CURVE					LAYER 1		
THETA		TENSION			THETA		TENSION	
0.0016		136.8			0.206514		25.75845	
0.0033		112.2			0.121003		35.95545	
0.0065		91.96			0.096177		40.03425	
0.013		75.28			0.082385		41.5638	
0.0195		66.87			0.068593		45.6426	
0.026		61.41			0.060318		48.19185	
0.0326		57.44			0.052043		49.21155	
0.0391		54.34			0.049284		51.25095	
0.0456		51.81			0.043767		52.27065	
0.0521		49.68			0.03825		54.31005	
0.0586		47.84			0.032734		56.8593	
0.0651		46.22			0.029975		59.40855	
0.0716		44.78			0.027217		61.44795	
0.0781		43.48			0.0217		63.9972	
0.0846		42.28			0.010666		65.0169	
0.0977		40.17						
0.1042		39.21				LAYER 2		
0.1107		38.31			THETA		TENSION	
0.1172		37.46			0.242374		23.2092	
0.1237		36.65			0.134795		33.91605	
0.1302		35.88			0.107211		36.97515	
0.1367		35.13			0.096177		40.03425	
0.1432		34.41			0.082385		44.11305	
0.1498		33.72			0.07411		46.6623	
0.1563		33.04			0.057559		47.682	
0.1628		32.39			0.057559		49.21155	
0.1693		31.74			0.052043		50.23125	
0.1758		31.11			0.043767		52.27065	
0.1823		30.48			0.03825		55.32975	
0.1888		29.86			0.032734		57.879	
0.1953		29.25			0.029975		59.40855	
0.2018		28.63			0.024458		63.9972	
0.2084		28.02			0.018941		65.0169	
0.2149		27.4			0.013425		70.1154	
0.2214		26.78			0.007908		73.1745	
0.2279		26.14						
0.2344		25.5						
0.2409		24.83						
0.2474		24.15						
0.2539		23.43						
0.2604		22.68						
0.267		21.88						
0.2735		21.01						
0.28		20.05						
0.2865		18.97						

0.293		17.7					
0.2995		16.08					
0.306		13.71					
0.3093		11.72					
	LAYER 3					LAYER 5	
THETA		TENSION			THETA		TENSION
0.228581		22.1895			0.308576		18.1107
0.159621		31.87665			0.217548		30.85695
0.132037		35.95545			0.134795		35.4456
0.109969		38.5047			0.112728		37.485
0.096177		41.5638			0.098936		41.05395
0.09066		44.11305			0.09066		42.07365
0.076868		45.13275			0.082385		43.6032
0.071351		46.6623			0.068593		45.6426
0.065835		47.17215			0.065835		45.6426
0.063076		48.19185			0.065835		47.17215
0.049284		52.27065			0.057559		50.7411
0.043767		54.8199			0.054801		52.7805
0.03825		55.32975			0.049284		53.29035
0.032734		60.9381			0.041009		57.879
0.029975		62.46765			0.035492		58.8987
0.0217		66.54645			0.029975		61.44795
					0.032734		60.42825
					0.032734		62.46765
	LAYER 4					LAYER 6	
THETA		TENSION			THETA		TENSION
0.330643		1.7955			0.316851		13.52205
0.289267		19.64025			0.256166		25.75845
0.198239		30.3471			0.192722		33.4062
0.118245		35.4456			0.170655		35.95545
0.093419		37.485			0.145829		39.01455
0.082385		40.03425			0.134795		40.03425
0.079627		42.5835					
0.063076		44.11305					
0.063076		45.6426					
0.057559		46.6623					
0.054801		48.19185					
0.046526		51.25095					
0.041009		53.29035					
0.041009		55.8396					
0.032734		60.42825					
0.027217		61.9578					
0.0217		65.0169					
0.0217		67.0563					
0.0217		69.0957					

	HYDRAULIC CONDUCTIVITY TENSION DATA HOMOGENEOUS PROFILE						
	FITTED CURVE					LAYER 1	
TENSION		K			TENSION		K
123.6		9.47E-08			35.95545		0.044497
103.1		7.97E-07			40.03425		0.028913
86.02		6.7E-06			41.5638		0.017226
71.64		5.65E-05			45.6426		0.010142
64.29		0.000197			48.19185		0.00702
59.47		0.000477			49.21155		0.004958
55.94		0.00095			51.25095		0.003831
53.17		0.001668			52.27065		0.003041
50.9		0.002687			54.31005		0.002123
48.97		0.004064			56.8593		0.001215
47.31		0.005857			59.40855		0.000827
45.84		0.008127			61.44795		0.000601
44.52		0.01093			63.9972		0.000148
43.33		0.01435			65.0169		9.48E-05
42.24		0.01842			71.1351		3.45E-05
41.23		0.02324			73.68435		1.49E-05
40.28		0.02886			75.2139		9.82E-06
39.4		0.03536					
38.57		0.04281				LAYER 2	
37.78		0.0513			TENSION		K
37.03		0.06089			23.2092		0.251597
36.3		0.07168			33.91605		0.083651
35.61		0.08375			36.97515		0.045977
34.94		0.09719			40.03425		0.027294
34.29		0.1121			44.11305		0.015166
33.65		0.1286			46.6623		0.010206
33.03		0.1467			47.682		0.007091
32.42		0.1667			49.21155		0.005425
31.82		0.1885			50.23125		0.004278
31.23		0.2123			52.27065		0.002962
30.64		0.2383			55.32975		0.001686
30.06		0.2666			57.879		0.001148
29.47		0.2973			59.40855		0.000836
28.89		0.3307			63.9972		0.000263
28.3		0.3668			65.0169		0.000181
27.7		0.4059			70.1154		7.17E-05
27.09		0.4482			73.1745		3.86E-05
26.47		0.4939			74.70405		2.56E-05
25.83		0.5433					
25.17		0.5967					
24.47		0.6545					
23.74		0.7171					
22.96		0.7849					
22.12		0.8588					
21.18		0.9394					

20.12		1.028					
18.85		1.126					
17.25		1.237					
14.87		1.366					
12.85		1.444					
	LAYER 3					LAYER 5	
TENSION		K			TENSION		K
22.1895		0.346965			18.1107		0.716505
31.87665		0.116261			30.85695		0.215001
35.95545		0.061893			35.4456		0.105408
38.5047		0.037295			37.485		0.063108
41.5638		0.020519			41.05395		0.033465
44.11305		0.013735			42.07365		0.021965
45.13275		0.009517			43.6032		0.014991
46.6623		0.007272			45.6426		0.0114
47.17215		0.005731			45.6426		0.008936
48.19185		0.00397			47.17215		0.006148
52.27065		0.002222			50.7411		0.003446
54.8199		0.001549			52.7805		0.002383
55.32975		0.001133			53.29035		0.001743
60.9381		0.000422			57.879		0.0008
62.46765		0.000306			58.8987		0.000616
66.54645		0.00013			61.44795		0.000262
69.60555		8.14E-05			60.42825		0.000206
71.64495		5.62E-05			62.46765		0.000217
	LAYER 4						
TENSION		K					
19.64025		0.542723					
30.3471		0.165362					
35.4456		0.083012					
37.485		0.049659					
40.03425		0.026632					
42.5835		0.01759					
44.11305		0.01209					
45.6426		0.009188					
46.6623		0.007215					
48.19185		0.004974					
51.25095		0.002784					
53.29035		0.001931					
55.8396		0.001411					
60.42825		0.00059					
61.9578		0.000442					
65.0169		0.000198					
67.0563		0.000138					
69.0957		9.89E-05					

	HYDRAULIC CONDUCTIVITY DATA HOMOGENEOUS PROFILE						
	FITTED CURVE					LAYER 1	
THETA		K			THETA		K
0.0016		4.58E-08			0.206514		0.099626
0.0033		3.86E-07			0.121003		0.044497
0.0065		3.24E-06			0.096177		0.028913
0.013		2.73E-05			0.082385		0.017226
0.0195		9.52E-05			0.068593		0.010142
0.026		0.000231			0.060318		0.00702
0.0326		0.00046			0.052043		0.004958
0.0391		0.000807			0.049284		0.003831
0.0456		0.001301			0.043767		0.003041
0.0521		0.001968			0.03825		0.002123
0.0586		0.002836			0.032734		0.001215
0.0651		0.003936			0.029975		0.000827
0.0716		0.005297			0.027217		0.000601
0.0781		0.006951			0.0217		0.000148
0.0846		0.008929			0.010666		9.48E-05
0.0912		0.01127			0.007908		3.45E-05
0.0977		0.01399			0.005149		1.49E-05
0.1042		0.01715			0.005149		9.82E-06
0.1107		0.02077					
0.1172		0.0249				LAYER 2	
0.1237		0.02956			THETA		K
0.1302		0.03482			0.242374		0.251597
0.1367		0.04069			0.134795		0.083651
0.1432		0.04725			0.107211		0.045977
0.1498		0.05452			0.096177		0.027294
0.1563		0.06256			0.082385		0.015166
0.1628		0.07142			0.07411		0.010206
0.1693		0.08116			0.057559		0.007091
0.1758		0.09184			0.057559		0.005425
0.1823		0.1035			0.052043		0.004278
0.1888		0.1163			0.043767		0.002962
0.1953		0.1301			0.03825		0.001686
0.2018		0.1452			0.032734		0.001148
0.2084		0.1616			0.029975		0.000836
0.2149		0.1794			0.024458		0.000263
0.2214		0.1987			0.018941		0.000181
0.2279		0.2195			0.013425		7.17E-05
0.2344		0.2421			0.007908		3.86E-05
0.2409		0.2666			0.007908		2.56E-05
0.2474		0.2931					
0.2539		0.3218					
0.2604		0.353					
0.267		0.3869					
0.2735		0.4239					
0.28		0.4644					

0.2865		0.5091					
0.293		0.559					
0.2995		0.6155					
0.306		0.6824					
0.3093		0.7227					
0.3093		0.78					
	LAYER 3					LAYER 5	
THETA		K			THETA		K
0.228581		0.346965			0.308576		0.716505
0.159621		0.116261			0.217548		0.215001
0.132037		0.061893			0.134795		0.105408
0.109969		0.037295			0.112728		0.063108
0.096177		0.020519			0.098936		0.033465
0.09066		0.013735			0.09066		0.021965
0.076868		0.009517			0.082385		0.014991
0.071351		0.007272			0.068593		0.0114
0.065835		0.005731			0.065835		0.008936
0.063076		0.00397			0.065835		0.006148
0.049284		0.002222			0.057559		0.003446
0.043767		0.001549			0.054801		0.002383
0.03825		0.001133			0.049284		0.001743
0.032734		0.000422			0.041009		0.0008
0.029975		0.000306			0.035492		0.000616
0.0217		0.00013			0.029975		0.000262
0.016183		8.14E-05			0.032734		0.000206
0.016183		5.62E-05			0.032734		0.000217
	LAYER 4					LAYER 6	
THETA		K			THETA		K
0.289267		0.542723			0.316851		0.856688
0.198239		0.165362			0.256166		0.259525
0.118245		0.083012			0.192722		0.12659
0.093419		0.049659			0.170655		0.076132
0.082385		0.026632			0.145829		0.040156
0.079627		0.01759			0.134795		0.026215
0.063076		0.01209					
0.063076		0.009188					
0.057559		0.007215					
0.054801		0.004974					
0.046526		0.002784					
0.041009		0.001931					
0.041009		0.001411					
0.032734		0.00059					
0.027217		0.000442					
0.0217		0.000198					
0.0217		0.000138					
0.0217		9.89E-05					

APPENDIX D

EXPERIMENTAL DATA: HETEROGENEOUS SOIL PROFILE

SEVILLETA SAND - 6.5 CM STONE LAYER

EXPERIMENT #15 HETROGENEOUS SOIL PROFILE: 6.5 CM STONE LAYER

TENSIOMETER READINGS mbars

MINUTES	T1	T2	T3	T4	T5
1	-33.5	-33	-27	-32	-30
15	-46.5	-43	-36	-38	-35.5
30	-50	-46	-40	-41	-38.5
45	-52.5	-48.5	-43	-44.5	-42
60	-54.5	-51.5	-46	-46	-43
75	-55	-52.5	-47.5	-47.5	-45
90	-57	-53.5	-48.5	-48	-47
120	-59.5	-55.5	-51	-51	-48
155	-61.5	-57	-52	-53	-50
330	-66.5	-62.5	-57.5	-58.5	-56
450	-68.5	-64.5	-59.5	-60.5	-58
560	-70	-67	-60.5	-62	-60
1220	-76.5	-72	-66.5	-68	-66
2030	-80	-76.5	-70.5	-72.5	-70.5
2955	-83	-79	-72	-75	-74

TENSION READINGS cm H2O

MINUTES	T1	T2	T3	T4	T5
1	-34.16	-33.6501	-27.5319	-32.6304	-30.591
15	-47.4161	-43.8471	-36.7092	-38.7486	-36.1994
30	-50.985	-46.9062	-40.788	-41.8077	-39.2585
45	-53.5343	-49.4555	-43.8471	-45.3767	-42.8274
60	-55.5737	-52.5146	-46.9062	-46.9062	-43.8471
75	-56.0835	-53.5343	-48.4358	-48.4358	-45.8865
90	-58.1229	-54.554	-49.4555	-48.9456	-47.9259
120	-60.6722	-56.5934	-52.0047	-52.0047	-48.9456
155	-62.7116	-58.1229	-53.0244	-54.0441	-50.985
330	-67.8101	-63.7313	-58.6328	-59.6525	-57.1032
450	-69.8495	-65.7707	-60.6722	-61.6919	-59.1426
560	-71.379	-68.3199	-61.6919	-63.2214	-61.182
1220	-78.0071	-73.4184	-67.8101	-69.3396	-67.3002
2030	-81.576	-78.0071	-71.8889	-73.9283	-71.8889
2955	-84.6351	-80.5563	-73.4184	-76.4775	-75.4578

	CORRECTED TENSIOMETER READINGS AT CUPS				
MINUTES	T1	T2	T3	T4	T5
1	-20.66	-20.1501	-14.0319	-19.1304	-17.091
15	-33.9161	-30.3471	-23.2092	-25.2486	-22.6994
30	-37.485	-33.4062	-27.288	-28.3077	-25.7585
45	-40.0343	-35.9555	-30.3471	-31.8767	-29.3274
60	-42.0737	-39.0146	-33.4062	-33.4062	-30.3471
75	-42.5835	-40.0343	-34.9358	-34.9358	-32.3865
90	-44.6229	-41.054	-35.9555	-35.4456	-34.4259
120	-47.1722	-43.0934	-38.5047	-38.5047	-35.4456
155	-49.2116	-44.6229	-39.5244	-40.5441	-37.485
330	-54.3101	-50.2313	-45.1328	-46.1525	-43.6032
450	-56.3495	-52.2707	-47.1722	-48.1919	-45.6426
560	-57.879	-54.8199	-48.1919	-49.7214	-47.682
1220	-64.5071	-59.9184	-54.3101	-55.8396	-53.8002
2030	-68.076	-64.5071	-58.3889	-60.4283	-58.3889
2955	-71.1351	-67.0563	-59.9184	-62.9775	-61.9578

	HYDRAULIC HEAD AT TENSIOMETER CUPS H				
MINUTES	T1	T2	T3	T4	T5
1	-31.66	-41.1501	-45.7819	-60.8804	-68.841
15	-44.9161	-51.3471	-54.9592	-66.9986	-74.4494
30	-48.485	-54.4062	-59.038	-70.0577	-77.5085
45	-51.0343	-56.9555	-62.0971	-73.6267	-81.0774
60	-53.0737	-60.0146	-65.1562	-75.1562	-82.0971
75	-53.5835	-61.0343	-66.6858	-76.6858	-84.1365
90	-55.6229	-62.054	-67.7055	-77.1956	-86.1759
120	-58.1722	-64.0934	-70.2547	-80.2547	-87.1956
155	-60.2116	-65.6229	-71.2744	-82.2941	-89.235
330	-65.3101	-71.2313	-76.8828	-87.9025	-95.3532
450	-67.3495	-73.2707	-78.9222	-89.9419	-97.3926
560	-68.879	-75.8199	-79.9419	-91.4714	-99.432
1220	-75.5071	-80.9184	-86.0601	-97.5896	-105.55
2030	-79.076	-85.5071	-90.1389	-102.178	-110.139
2955	-82.1351	-88.0563	-91.6684	-104.728	-113.708

		WATER CONTENT via TDR				
MINUTES	TDR 1	THETA 1	TDR 2	THETA 2	TDR 3	THETA 3
1	0.333	0.218927	0.435	0.359606	0.405	0.31823
15	0.299	0.172034	0.423	0.343056	0.399	0.309955
30	0.279	0.14445	0.398	0.308576	0.396	0.305817
45	0.267	0.127899	0.372	0.272716	0.381	0.285129
60	0.255	0.111349	0.347	0.238236	0.355	0.24927
75	0.247	0.100315	0.331	0.216169	0.344	0.234098
90	0.244	0.096177	0.322	0.203756	0.33	0.214789
120	0.236	0.085144	0.308	0.184447	0.312	0.189964
155	0.231	0.078248	0.296	0.167896	0.301	0.174792
330	0.217	0.058939	0.269	0.130657	0.27	0.132037
450	0.214	0.054801	0.262	0.121003	0.26	0.118245
560	0.21	0.049284	0.256	0.112728	0.255	0.111349
1220	0.201	0.036871	0.24	0.09066	0.234	0.082385
2030	0.197	0.031354	0.232	0.079627	0.227	0.072731
2955	0.196	0.029975	0.228	0.07411	0.221	0.064455

MINUTES	TDR 4	THETA 4	TDR 5	THETA 5
1	0.296	0.167896	0.299	0.172034
15	0.287	0.155483	0.29	0.159621
30	0.281	0.147208	0.283	0.149966
45	0.27	0.132037	0.268	0.129278
60	ND	ND	ND	ND
75	0.257	0.114107	0.258	0.115486
90	0.255	0.111349	0.255	0.111349
120	0.246	0.098936	0.249	0.103073
155	0.242	0.093419	0.244	0.096177
330	0.226	0.071351	0.227	0.072731
450	0.219	0.061697	0.222	0.065835
560	0.218	0.060318	0.217	0.058939
1220	0.207	0.045146	0.204	0.041009
2030	0.201	0.036871	0.198	0.032734
2955	0.193	0.025838	0.193	0.025838

	SLOPE OF THE WETTNESS CURVE dTH/dt				
MINUTES	dTH/dt 1	dTH/dt 2	dTH/dt 3	dTH/dt 4	dTH/dt 5
1	-0.01673	-0.00371	-0.00073	-0.00219	-0.00237
15	-0.00213	-0.00272	-0.00134	-0.00104	-0.00111
30	-0.00111	-0.00203	-0.00135	-0.00071	-0.00075
45	-0.00074	-0.00157	-0.00126	-0.00054	-0.00057
60	-0.00054	-0.00125	-0.00113	-0.00044	-0.00046
75	-0.00043	-0.00101	-0.001	-0.00037	-0.00038
90	-0.00035	-0.00084	-0.00088	-0.00032	-0.00033
120	-0.00025	-0.0006	-0.00069	-0.00024	-0.00025
155	-0.00019	-0.00043	-0.00052	-0.00019	-0.0002
330	-7.4E-05	-0.00014	-0.00017	-8.6E-05	-8.8E-05
450	-5E-05	-8.4E-05	-9.8E-05	-6E-05	-6.1E-05
560	-3.8E-05	-5.8E-05	-6.5E-05	-4.6E-05	-4.6E-05
1220	-1.3E-05	-1.7E-05	-1.3E-05	-1.7E-05	-1.7E-05
2030	-6.6E-06	-8.8E-06	-4.3E-06	-8.2E-06	-8.1E-06
2955	-3.9E-06	-5.6E-06	-1.9E-06	-4.8E-06	-4.7E-06

WATER CONTENT dTH/dt TIMES THE THICKNESS OF THE LAYER					
MINUTES	T1	T2	T3	T4	T5
1	0.334615	0.037113	0.007267	0.02189	0.023724
15	0.042667	0.027181	0.013365	0.010367	0.011093
30	0.022192	0.020302	0.013539	0.007065	0.007499
45	0.014726	0.015688	0.012563	0.005409	0.005708
60	0.010873	0.012457	0.011288	0.004383	0.004604
75	0.008534	0.010115	0.010008	0.003677	0.003848
90	0.00697	0.008366	0.008828	0.003159	0.003295
120	0.005025	0.005986	0.006868	0.002448	0.002541
155	0.003726	0.004294	0.005194	0.001921	0.001984
330	0.00148	0.001385	0.001711	0.000862	0.000879
450	0.000998	0.000836	0.000981	0.0006	0.000608
560	0.000752	0.000584	0.000646	0.000459	0.000464
1220	0.000267	0.000173	0.00013	0.000166	0.000166
2030	0.000133	8.76E-05	4.28E-05	8.17E-05	8.12E-05
2955	7.85E-05	5.61E-05	1.86E-05	4.76E-05	4.71E-05

	SLOPE OF THE HEAD WITH DEPTH CURVE dH/dz				
MINUTES	G1	G2	G3	G4	G5
1	0.949015	0.46318	1.50985	0.79606	0.724642
15	0.643105	0.36121	1.20394	0.745075	0.783677
30	0.59212	0.46318	1.10197	0.745075	0.815878
45	0.59212	0.514165	1.152955	0.745075	0.853446
60	0.69409	0.514165	1	0.69409	0.86418
75	0.745075	0.56515	1	0.745075	0.885647
90	0.643105	0.56515	0.949015	0.89803	0.907115
120	0.59212	0.616135	1	0.69409	0.917848
155	0.541135	0.56515	1.10197	0.69409	0.939316
330	0.59212	0.56515	1.10197	0.745075	1.003718
450	0.59212	0.56515	1.10197	0.745075	1.025185
560	0.69409	0.412195	1.152955	0.79606	1.046653
1220	0.541135	0.514165	1.152955	0.79606	1.111055
2030	0.643105	0.46318	1.20394	0.79606	1.159356
2955	0.59212	0.36121	1.30591	0.89803	1.196924

	FLUX THROUGH EACH LAYER				
MINUTES	Q1	Q2	Q3	Q4	Q5
1	0.334615	0.371728	0.378995	0.400885	0.424609
15	0.042667	0.069848	0.083213	0.09358	0.104673
30	0.022192	0.042493	0.056033	0.063098	0.070598
45	0.014726	0.030414	0.042977	0.048386	0.054094
60	0.010873	0.02333	0.034619	0.039002	0.043606
75	0.008534	0.018648	0.028656	0.032333	0.036181
90	0.00697	0.015337	0.024164	0.027324	0.030619
120	0.005025	0.011011	0.017879	0.020328	0.022869
155	0.003726	0.00802	0.013214	0.015135	0.01712
330	0.00148	0.002865	0.004576	0.005439	0.006317
450	0.000998	0.001834	0.002815	0.003415	0.004022
560	0.000752	0.001336	0.001982	0.002441	0.002904
1220	0.000267	0.00044	0.000569	0.000736	0.000902
2030	0.000133	0.00022	0.000263	0.000345	0.000426
2955	7.85E-05	0.000135	0.000153	0.000201	0.000248

		CONDUCTIVITY AS A FUNCTION OF THETA					
	MINUTES	K1	K2	K3	K4	K5	
	1	0.352592	0.802556	0.251015	0.503586	0.585957	
	15	0.066345	0.193372	0.069117	0.125599	0.133567	
	30	0.037478	0.091742	0.050848	0.084687	0.086529	
	45	0.024871	0.059153	0.037276	0.064941	0.063383	
	60	0.015665	0.045375	0.034619	0.056191	0.050459	
	75	0.011453	0.032997	0.028656	0.043396	0.040853	
	90	0.010838	0.027137	0.025463	0.030426	0.033754	
	120	0.008486	0.017871	0.017879	0.029287	0.024916	
	155	0.006885	0.014191	0.011991	0.021806	0.018226	
	330	0.0025	0.00507	0.004153	0.0073	0.006294	
	450	0.001685	0.003246	0.002555	0.004583	0.003924	
	560	0.001083	0.003241	0.001719	0.003066	0.002775	
	1220	0.000493	0.000855	0.000494	0.000924	0.000811	
	2030	0.000206	0.000475	0.000218	0.000433	0.000367	
	2955	0.000133	0.000372	0.000117	0.000224	0.000207	

	SOIL WATER RETENTION DATA 6.5 CM STONE LAYER						
	FITTED CURVE					LAYER 1	
THETA		TENSION			THETA		TENSION
0.0016		136.8			0.218927		20.65995
0.0033		112.2			0.172034		33.91605
0.0065		91.96			0.14445		37.485
0.013		75.28			0.127899		40.03425
0.0195		66.87			0.111349		42.07365
0.026		61.41			0.100315		42.5835
0.0326		57.44			0.096177		44.6229
0.0391		54.34			0.085144		47.17215
0.0456		51.81			0.078248		49.21155
0.0521		49.68			0.058939		54.31005
0.0586		47.84			0.054801		56.34945
0.0651		46.22			0.049284		57.879
0.0716		44.78			0.036871		64.50705
0.0781		43.48			0.031354		68.076
0.0846		42.28			0.029975		71.1351
0.0912		41.19					
0.0977		40.17				LAYER 2	
0.1042		39.21			THETA		TENSION
0.1107		38.31			0.359606		ND
0.1172		37.46			0.343056		20.1501
0.1237		36.65			0.308576		30.3471
0.1302		35.88			0.272716		33.4062
0.1367		35.13			0.238236		35.95545
0.1432		34.41			0.216169		39.01455
0.1498		33.72			0.203756		40.03425
0.1563		33.04			0.184447		41.05395
0.1628		32.39			0.167896		43.09335
0.1693		31.74			0.130657		44.6229
0.1758		31.11			0.121003		50.23125
0.1823		30.48			0.112728		52.27065
0.1888		29.86			0.09066		54.8199
0.1953		29.25			0.079627		59.9184
0.2018		28.63			ND		64.50705
0.2084		28.02					
0.2149		27.4					
0.2214		26.78					
0.2279		26.14					
0.2344		25.5					
0.2409		24.83					
0.2474		24.15					
0.2539		23.43					
0.2604		22.68					
0.267		21.88					
0.2735		21.01					
0.28		20.05					

0.2865		18.97					
0.293		17.7					
0.2995		16.08					
0.306		13.71					
0.3093		11.72					
	LAYER 3					LAYER 5	
THETA		TENSION			THETA		TENSION
0.143204		14.0319			0.172034		17.091
0.13948		23.2092			0.159621		22.69935
0.137618		27.288			0.149966		25.75845
0.128308		30.3471			0.129278		29.3274
0.112171		33.4062			0.1225		30.3471
0.105344		34.93575			0.115486		32.3865
0.096655		35.95545			0.111349		34.4259
0.085484		38.5047			0.103073		35.4456
0.078656		39.5244			0.096177		37.485
0.059417		45.13275			0.072731		43.6032
0.05321		47.17215			0.065835		45.6426
0.050107		48.19185			0.058939		47.682
0.037073		54.31005			0.041009		53.8002
0.032729		58.38885			0.032734		58.38885
0.029005		59.9184			0.025838		61.9578
	LAYER 4						
THETA		TENSION					
0.167896		19.1304					
0.155483		25.2486					
0.147208		28.3077					
0.132037		31.87665					
0.123		33.4062					
0.114107		34.93575					
0.111349		35.4456					
0.098936		38.5047					
0.093419		40.5441					
0.071351		46.15245					
0.061697		48.19185					
0.060318		49.7214					
0.045146		55.8396					
0.036871		60.42825					
0.025838		62.9775					

	HYDRAULIC CONDUCTIVITY TENSION DATA 6.5 CM STONE LAYER						
	FITTED CURVE					LAYER 1	
TENSION		K			TENSION		K
123.6		9.47E-08			20.65995		0.352592
103.1		7.97E-07			33.91605		0.066345
86.02		6.7E-06			37.485		0.037478
71.64		5.65E-05			40.03425		0.024871
64.29		0.000197			42.07365		0.015665
59.47		0.000477			42.5835		0.011453
55.94		0.00095			44.6229		0.010838
53.17		0.001668			47.17215		0.008486
50.9		0.002687			49.21155		0.006885
48.97		0.004064			54.31005		0.0025
47.31		0.005857			56.34945		0.001685
45.84		0.008127			57.879		0.001083
44.52		0.01093			64.50705		0.000493
43.33		0.01435			68.076		0.000206
42.24		0.01842			71.1351		0.000133
41.23		0.02324					
40.28		0.02886				LAYER 2	
39.4		0.03536			TENSION		K
38.57		0.04281			20.1501		0.802556
37.78		0.0513			30.3471		0.193372
37.03		0.06089			33.4062		0.091742
36.3		0.07168			35.95545		0.059153
35.61		0.08375			39.01455		0.045375
34.94		0.09719			40.03425		0.032997
34.29		0.1121			41.05395		0.027137
33.65		0.1286			43.09335		0.017871
33.03		0.1467			44.6229		0.014191
32.42		0.1667			50.23125		0.00507
31.82		0.1885			52.27065		0.003246
31.23		0.2123			54.8199		0.003241
30.64		0.2383			59.9184		0.000855
30.06		0.2666			64.50705		0.000475
29.47		0.2973					
28.89		0.3307					
28.3		0.3668					
27.7		0.4059					
27.09		0.4482					
26.47		0.4939					
25.83		0.5433					
25.17		0.5967					
24.47		0.6545					
23.74		0.7171					
22.96		0.7849					
22.12		0.8588					
21.18		0.9394					

20.12		1.028					
18.85		1.126					
17.25		1.237					
14.87		1.366					
12.85		1.444					
	LAYER 3					LAYER 5	
TENSION		K			TENSION		K
14.0319		0.251015			17.091		0.585957
23.2092		0.069117			22.69935		0.133567
27.288		0.050848			25.75845		0.086529
30.3471		0.037276			29.3274		0.063383
33.4062		0.034619			30.3471		0.050459
34.93575		0.028656			32.3865		0.040853
35.95545		0.025463			34.4259		0.033754
38.5047		0.017879			35.4456		0.024916
39.5244		0.011991			37.485		0.018226
45.13275		0.004153			43.6032		0.006294
47.17215		0.002555			45.6426		0.003924
48.19185		0.001719			47.682		0.002775
54.31005		0.000494			53.8002		0.000811
58.38885		0.000218			58.38885		0.000367
59.9184		0.000117			61.9578		0.000207
	LAYER 4						
TENSION		K					
19.1304		0.503586					
25.2486		0.125599					
28.3077		0.084687					
31.87665		0.064941					
33.4062		0.056191					
34.93575		0.043396					
35.4456		0.030426					
38.5047		0.029287					
40.5441		0.021806					
46.15245		0.0073					
48.19185		0.004583					
49.7214		0.003066					
55.8396		0.000924					
60.42825		0.000433					
62.9775		0.000224					

	HYDRAULIC CONDUCTIVITY DATA 6.5 CM STONE LAYER						
	FITTED CURVE					LAYER 1	
THETA		K			THETA		K
0.0016		4.58E-08			0.218927		0.352592
0.0033		3.86E-07			0.172034		0.066345
0.0065		3.24E-06			0.14445		0.037478
0.013		2.73E-05			0.127899		0.024871
0.0195		9.52E-05			0.111349		0.015665
0.026		0.000231			0.100315		0.011453
0.0326		0.00046			0.096177		0.010838
0.0391		0.000807			0.085144		0.008486
0.0456		0.001301			0.078248		0.006885
0.0521		0.001968			0.058939		0.0025
0.0586		0.002836			0.054801		0.001685
0.0651		0.003936			0.049284		0.001083
0.0716		0.005297			0.036871		0.000493
0.0781		0.006951			0.031354		0.000206
0.0846		0.008929			0.029975		0.000133
0.0912		0.01127					
0.0977		0.01399				LAYER 2	
0.1042		0.01715			THETA		K
0.1107		0.02077			0.359606		0.802556
0.1172		0.0249			0.343056		0.193372
0.1237		0.02956			0.308576		0.091742
0.1302		0.03482			0.272716		0.059153
0.1367		0.04069			0.238236		0.045375
0.1432		0.04725			0.216169		0.032997
0.1498		0.05452			0.203756		0.027137
0.1563		0.06256			0.184447		0.017871
0.1628		0.07142			0.167896		0.014191
0.1693		0.08116			0.130657		0.00507
0.1758		0.09184			0.121003		0.003246
0.1823		0.1035			0.112728		0.003241
0.1888		0.1163			0.09066		0.000855
0.1953		0.1301			0.079627		0.000475
0.2018		0.1452			0.07411		0.000372
0.2084		0.1616					
0.2149		0.1794					
0.2214		0.1987					
0.2279		0.2195					
0.2344		0.2421					
0.2409		0.2666					
0.2474		0.2931					
0.2539		0.3218					
0.2604		0.353					
0.267		0.3869					
0.2735		0.4239					
0.28		0.4644					

0.2865		0.5091					
0.293		0.559					
0.2995		0.6155					
0.306		0.6824					
0.3093		0.7227					
0.3093		0.78					
	LAYER 3					LAYER 5	
THETA		K			THETA		K
0.143204		0.251015			0.172034		0.585957
0.13948		0.069117			0.159621		0.133567
0.137618		0.050848			0.149966		0.086529
0.128308		0.037276			0.129278		0.063383
0.112171		0.034619			ND		0.050459
0.105344		0.028656			0.115486		0.040853
0.096655		0.025463			0.111349		0.033754
0.085484		0.017879			0.103073		0.024916
0.078656		0.011991			0.096177		0.018226
0.059417		0.004153			0.072731		0.006294
0.05321		0.002555			0.065835		0.003924
0.050107		0.001719			0.058939		0.002775
0.037073		0.000494			0.041009		0.000811
0.032729		0.000218			0.032734		0.000367
0.029005		0.000117			0.025838		0.000207
	LAYER 4						
THETA		K					
0.167896		0.503586					
0.155483		0.125599					
0.147208		0.084687					
0.132037		0.064941					
ND		0.056191					
0.114107		0.043396					
0.111349		0.030426					
0.098936		0.029287					
0.093419		0.021806					
0.071351		0.0073					
0.061697		0.004583					
0.060318		0.003066					
0.045146		0.000924					
0.036871		0.000433					
0.025838		0.000224					

APPENDIX E

EXPERIMENTAL DATA: HETEROGENEOUS SOIL PROFILE

SEVILLETA SAND - 10 CM STONE LAYER

EXPERIMENT #14 HETEROGENEOUS SOIL PROFILE: 10 CM STONE LAYER

TENSIOMETER READINGS mbar

MINUTES	T1	T2	T3	T4	T5
0	-36	-31.5	-28	-33.5	-32
15	-46.5	-40	-37	-38.5	-34.5
30	-49.5	-46.5	-42	-41	-38.5
45	-54.5	-49.5	-45	-45.5	-41
60	-55.5	-51.5	-47	-45	-43.5
80	-58	-53	-51	-50.5	-54.5
105	-60.5	-55.5	-53	-52.5	-48.5
135	-61.5	-58	-55	-54.5	-50
300	-67.5	-63	-61	-57.5	-55.5
360	-69	-64	-62	-62	-57
570	-72.5	-68	-65	-64.5	-61.5
825	-75	-71	-68.5	-68.5	-64
1575	-81	-77	-75	-74	-69.5
3000	-83.5	-78.5	-77	-76	-73
4912	-89.5	-85	-83	-82.5	-79.5

TENSIOMETER READINGS cm H2O

MINUTES	T1	T2	T3	T4	T5
0	-36.7092	-32.1206	-28.5516	-34.16	-32.6304
15	-47.4161	-40.788	-37.7289	-39.2585	-35.1797
30	-50.4752	-47.4161	-42.8274	-41.8077	-39.2585
45	-55.5737	-50.4752	-45.8865	-46.3964	-41.8077
60	-56.5934	-52.5146	-47.9259	-45.8865	-44.357
80	-59.1426	-54.0441	-52.0047	-51.4949	-55.5737
105	-61.6919	-56.5934	-54.0441	-53.5343	-49.4555
135	-62.7116	-59.1426	-56.0835	-55.5737	-50.985
300	-68.8298	-64.2411	-62.2017	-58.6328	-56.5934
360	-70.3593	-65.2608	-63.2214	-63.2214	-58.1229
570	-73.9283	-69.3396	-66.2805	-65.7707	-62.7116
825	-76.4775	-72.3987	-69.8495	-69.8495	-65.2608
1575	-82.5957	-78.5169	-76.4775	-75.4578	-70.8692
3000	-85.145	-80.0465	-78.5169	-77.4972	-74.4381
4912	-91.2632	-86.6745	-84.6351	-84.1253	-81.0662

	CORRECTED TENSIOMETER READINGS AT CUPS				
MINUTES	T1	T2	T3	T4	T5
0	-23.2092	-18.6206	-15.0516	-20.66	-19.1304
15	-33.9161	-27.288	-24.2289	-25.7585	-21.6797
30	-36.9752	-33.9161	-29.3274	-28.3077	-25.7585
45	-42.0737	-36.9752	-32.3865	-32.8964	-28.3077
60	-43.0934	-39.0146	-34.4259	-32.3865	-30.857
80	-45.6426	-40.5441	-38.5047	-37.9949	-42.0737
105	-48.1919	-43.0934	-40.5441	-40.0343	-35.9555
135	-49.2116	-45.6426	-42.5835	-42.0737	-37.485
300	-55.3298	-50.7411	-48.7017	-45.1328	-43.0934
360	-56.8593	-51.7608	-49.7214	-49.7214	-44.6229
570	-60.4283	-55.8396	-52.7805	-52.2707	-49.2116
825	-62.9775	-58.8987	-56.3495	-56.3495	-51.7608
1575	-69.0957	-65.0169	-62.9775	-61.9578	-57.3692
3000	-71.645	-66.5465	-65.0169	-63.9972	-60.9381
4912	-77.7632	-73.1745	-71.1351	-70.6253	-67.5662

	HYDRAULIC HEAD AT TENSIOMETER CUPS cm				
MINUTES	T1	T2	T3	T4	T5
0	-33.7092	-39.8706	-46.5516	-62.16	-70.6304
15	-44.4161	-48.538	-55.7289	-67.2585	-73.1797
30	-47.4752	-55.1661	-60.8274	-69.8077	-77.2585
45	-52.5737	-58.2252	-63.8865	-74.3964	-79.8077
60	-53.5934	-60.2646	-65.9259	-73.8865	-82.357
80	-56.1426	-61.7941	-70.0047	-79.4949	-93.5737
105	-58.6919	-64.3434	-72.0441	-81.5343	-87.4555
135	-59.7116	-66.8926	-74.0835	-83.5737	-88.985
300	-65.8298	-71.9911	-80.2017	-86.6328	-94.5934
360	-67.3593	-73.0108	-81.2214	-91.2214	-96.1229
570	-70.9283	-77.0896	-84.2805	-93.7707	-100.712
825	-73.4775	-80.1487	-87.8495	-97.8495	-103.261
1575	-79.5957	-86.2669	-94.4775	-103.458	-108.869
3000	-82.145	-87.7965	-96.5169	-105.497	-112.438
4912	-88.2632	-94.4245	-102.635	-112.125	-119.066

WATER CONTENT via TDR

MINUTES	TDR 1	THETA 1	TDR 2	THETA 2	TDR 3	THETA 3
0	0.298	0.170655	0.419	0.337539	0.369	0.268578
15	0.269	0.130657	0.406	0.319609	0.363	0.260303
30	0.256	0.112728	0.381	0.285129	0.357	0.252028
45	0.245	0.097556	0.352	0.245132	0.342	0.23134
60	0.24	0.09066	0.333	0.218927	0.326	0.209272
80	0.236	0.085144	0.312	0.189964	0.311	0.188584
105	0.23	0.076868	0.298	0.170655	0.293	0.163759
135	0.224	0.068593	0.287	0.155483	0.279	0.14445
300	0.212	0.052043	0.26	0.118245	0.249	0.103073
360	0.207	0.045146	0.252	0.107211	0.242	0.093419
570	0.202	0.03825	0.242	0.093419	0.231	0.078248
825	0.197	0.031354	0.233	0.081006	0.222	0.065835
1575	0.191	0.023079	0.223	0.067214	0.21	0.049284
3000	0.184	0.013425	0.198	0.032734	0.187	0.017562
4912	0.182	0.010666	0.196	0.029975	0.185	0.014804

MINUTES	TDR 4	THETA 4	TDR 5	THETA 5
0	0.285	0.152725	0.3	0.173413
15	0.278	0.14307	0.293	0.163759
30	0.272	0.134795	0.284	0.151346
45	0.269	0.130657	0.277	0.141691
60	0.263	0.122382	0.272	0.134795
80	0.259	0.116865	0.266	0.12652
105	0.251	0.105832	0.259	0.116865
135	0.249	0.103073	0.253	0.10859
300	0.229	0.075489	0.233	0.081006
360	0.224	0.068593	0.227	0.072731
570	0.216	0.057559	0.218	0.060318
825	0.208	0.046526	0.211	0.050663
1575	0.197	0.031354	0.204	0.041009
3000	0.189	0.020321	0.192	0.024458
4912	0.187	0.017562	0.191	0.023079

	SLOPE OF THE WETTNESS CURVE dTH/dt				
MINUTES	T1	T2	T3	T4	T5
0	1.61E-07	-0.00694	-0.00154	8.916337	-0.0022
15	-0.00176	-0.00292	-0.00138	-0.00056	-0.00105
30	-0.00094	-0.00185	-0.00122	-0.00045	-0.00072
45	-0.00063	-0.00135	-0.00109	-0.00038	-0.00056
60	-0.00047	-0.00105	-0.00097	-0.00033	-0.00045
80	-0.00034	-0.0008	-0.00083	-0.00029	-0.00036
105	-0.00025	-0.00061	-0.00068	-0.00024	-0.00029
135	-0.00019	-0.00047	-0.00054	-0.00021	-0.00023
300	-7.2E-05	-0.00018	-0.00017	-0.00011	-0.0001
360	-5.7E-05	-0.00015	-0.00012	-8.9E-05	-8.3E-05
570	-3.2E-05	-7.9E-05	-4.9E-05	-5.4E-05	-4.8E-05
825	-1.9E-05	-4.7E-05	-3.3E-05	-3.4E-05	-3E-05
1575	-7.9E-06	-1.9E-05	-2.2E-05	-1.4E-05	-1.3E-05
3000	-3.1E-06	-7.1E-06	-1.1E-05	-4.9E-06	-5.1E-06
4912	-1.5E-06	-3.3E-06	-4.6E-06	-2.2E-06	-2.5E-06

	WATER CONTENT dTH/dt TIMES THE THICKNESS OF THE LAYER				
MINUTES	T1	T2	T3	T4	T5
0	-3.2E-06	0.069359	0.006946	-89.1634	0.021963
15	0.035241	0.029189	0.006211	0.005619	0.010519
30	0.018882	0.018533	0.005512	0.00449	0.007219
45	0.012627	0.013498	0.004894	0.00381	0.005555
60	0.009354	0.010524	0.004347	0.003333	0.00452
80	0.006852	0.008042	0.003716	0.002867	0.003612
105	0.005057	0.006125	0.00306	0.002442	0.002873
135	0.003789	0.004689	0.00243	0.002069	0.002291
300	0.001443	0.001833	0.000755	0.001071	0.001017
360	0.001146	0.001454	0.000527	0.000894	0.000828
570	0.000632	0.000791	0.000222	0.000538	0.00048
825	0.000386	0.000474	0.000149	0.000338	0.000301
1575	0.000157	0.000187	9.93E-05	0.000136	0.000127
3000	6.2E-05	7.11E-05	5.06E-05	4.93E-05	5.07E-05
4912	2.96E-05	3.35E-05	2.05E-05	2.15E-05	2.45E-05

	SLOPE OF THE HEAD WITH DEPTH CURVE dH/dt				
MINUTES	G1	G2	G3	G4	G5
0	0.616135	0.668105	1.560835	0.847045	0.743478
15	0.412195	0.71909	1.152955	0.59212	0.770312
30	0.76909	0.566135	0.89803	0.745075	0.813247
45	0.56515	0.566135	1.050985	0.541135	0.840081
60	0.66712	0.566135	0.79606	0.847045	0.866915
80	0.56515	0.82106	0.949015	1.40788	0.984986
105	0.56515	0.770075	0.949015	0.59212	0.920584
135	0.718105	0.71909	0.949015	0.541135	0.936684
300	0.616135	0.82106	0.643105	0.79606	0.995719
360	0.56515	0.82106	1	0.49015	1.01182
570	0.616135	0.71909	0.949015	0.69409	1.060122
825	0.66712	0.770075	1	0.541135	1.086956
1575	0.66712	0.82106	0.89803	0.541135	1.145991
3000	0.56515	0.872045	0.89803	0.69409	1.183559
4912	0.616135	0.82106	0.949015	0.69409	1.253328

	FLUX THROUGH EACH LAYER				
MINUTES	Q1	Q2	Q3	Q4	Q5
0	-3.2E-06	0.069356	0.076302	-89.0871	-89.0651
15	0.035241	0.06443	0.070641	0.07626	0.086778
30	0.018882	0.037415	0.042927	0.047417	0.054636
45	0.012627	0.026125	0.031019	0.034829	0.040384
60	0.009354	0.019878	0.024225	0.027559	0.032078
80	0.006852	0.014895	0.018611	0.021478	0.02509
105	0.005057	0.011182	0.014241	0.016683	0.019556
135	0.003789	0.008478	0.010908	0.012977	0.015268
300	0.001443	0.003276	0.004032	0.005103	0.006119
360	0.001146	0.0026	0.003127	0.004021	0.004849
570	0.000632	0.001423	0.001645	0.002183	0.002663
825	0.000386	0.00086	0.001009	0.001348	0.001649
1575	0.000157	0.000344	0.000443	0.000579	0.000706
3000	6.2E-05	0.000133	0.000184	0.000233	0.000284
4912	2.96E-05	6.31E-05	8.36E-05	0.000105	0.00013

	CONDUCTIVITY AS A FUNCTION OF THETA					
MINUTES	K1	K2	K3	K4	K5	
0	-5.2E-06	0.10381	0.048886	-105.174	-119.795	
15	0.085496	0.089599	0.061269	0.128791	0.112654	
30	0.024551	0.066088	0.047801	0.06364	0.067182	
45	0.022343	0.046146	0.029514	0.064363	0.048072	
60	0.014021	0.035112	0.030431	0.032535	0.037003	
80	0.012125	0.018141	0.019611	0.015256	0.025472	
105	0.008948	0.01452	0.015006	0.028175	0.021244	
135	0.005276	0.011789	0.011494	0.023981	0.0163	
300	0.002342	0.00399	0.006269	0.00641	0.006146	
360	0.002029	0.003167	0.003127	0.008203	0.004792	
570	0.001026	0.001979	0.001733	0.003145	0.002512	
825	0.000578	0.001117	0.001009	0.00249	0.001517	
1575	0.000236	0.000419	0.000494	0.001071	0.000616	
3000	0.00011	0.000153	0.000205	0.000336	0.00024	
4912	4.81E-05	7.69E-05	8.81E-05	0.000151	0.000103	

	SOIL WATER RETENTION DATA 10 CM STONE LAYER						
	FITTED CURVE					LAYER 1	
THETA		TENSION			THETA		TENSION
0.0016		136.8			0.170655		23.2092
0.0033		112.2			0.130657		33.91605
0.0065		91.96			0.112728		36.97515
0.013		75.28			0.097556		42.07365
0.0195		66.87			0.09066		43.09335
0.026		61.41			0.085144		45.6426
0.0326		57.44			0.076868		48.19185
0.0391		54.34			0.068593		49.21155
0.0456		51.81			0.052043		55.32975
0.0521		49.68			0.045146		56.8593
0.0586		47.84			0.03825		60.42825
0.0651		46.22			0.031354		62.9775
0.0716		44.78			0.023079		69.0957
0.0781		43.48			0.013425		71.64495
0.0846		42.28			0.010666		77.76315
0.0912		41.19					
0.0977		40.17				LAYER 2	
0.1042		39.21			THETA		TENSION
0.1107		38.31			0.337539		18.62055
0.1172		37.46			0.319609		27.288
0.1237		36.65			0.285129		33.91605
0.1302		35.88			0.245132		36.97515
0.1367		35.13			0.218927		39.01455
0.1432		34.41			0.189964		40.5441
0.1498		33.72			0.170655		43.09335
0.1563		33.04			0.155483		45.6426
0.1628		32.39			0.118245		50.7411
0.1693		31.74			0.107211		51.7608
0.1758		31.11			0.093419		55.8396
0.1823		30.48			0.081006		58.8987
0.1888		29.86			0.067214		65.0169
0.1953		29.25			0.032734		66.54645
0.2018		28.63			0.029975		73.1745
0.2084		28.02					
0.2149		27.4					
0.2214		26.78					
0.2279		26.14					
0.2344		25.5					
0.2409		24.83					
0.2474		24.15					
0.2539		23.43					
0.2604		22.68					
0.267		21.88					
0.2735		21.01					
0.28		20.05					

0.2865		18.97					
0.293		17.7					
0.2995		16.08					
0.306		13.71					
0.3093		11.72					
	LAYER 3					LAYER 5	
THETA		TENSION			THETA		TENSION
0.12086		15.0516			0.173413		19.1304
0.117136		24.2289			0.163759		21.67965
0.113413		29.3274			0.151346		25.75845
0.104103		32.3865			0.141691		28.3077
0.094173		34.4259			0.134795		30.85695
0.084863		38.5047			0.12652		42.07365
0.073691		40.5441			0.116865		35.95545
0.065002		42.5835			0.10859		37.485
0.046383		48.7017			0.081006		43.09335
0.042038		49.7214			0.072731		44.6229
0.035211		52.7805			0.060318		49.21155
0.029626		56.34945			0.050663		51.7608
0.022178		62.9775			0.041009		57.36915
0.007903		65.0169			0.024458		60.9381
0.006662		71.1351			0.023079		67.56615
	LAYER 4						
THETA		TENSION					
0.152725		20.65995					
0.14307		25.75845					
0.134795		28.3077					
0.130657		32.89635					
0.122382		32.3865					
0.116865		37.99485					
0.105832		40.03425					
0.103073		42.07365					
0.075489		45.13275					
0.068593		49.7214					
0.057559		52.27065					
0.046526		56.34945					
0.031354		61.9578					
0.020321		63.9972					
0.017562		70.62525					

	HYDRAULIC CONDUCTIVITY TENSION DATA 10 CM STONE LAYER						
	FITTED CURVE					LAYER 1	
TENSION		K			TENSION		K
123.6		9.47E-08			23.2092		ND
103.1		7.97E-07			33.91605		0.085496
86.02		6.7E-06			36.97515		0.024551
71.64		5.65E-05			42.07365		0.022343
64.29		0.000197			43.09335		0.014021
59.47		0.000477			45.6426		0.012125
55.94		0.00095			48.19185		0.008948
53.17		0.001668			49.21155		0.005276
50.9		0.002687			55.32975		0.002342
48.97		0.004064			56.8593		0.002029
47.31		0.005857			60.42825		0.001026
45.84		0.008127			62.9775		0.000578
44.52		0.01093			69.0957		0.000236
43.33		0.01435			71.64495		0.00011
42.24		0.01842			77.76315		4.81E-05
41.23		0.02324					
40.28		0.02886				LAYER 2	
39.4		0.03536			TENSION		K
38.57		0.04281			18.62055		0.10381
37.78		0.0513			27.288		0.089599
37.03		0.06089			33.91605		0.066088
36.3		0.07168			36.97515		0.046146
35.61		0.08375			39.01455		0.035112
34.94		0.09719			40.5441		0.018141
34.29		0.1121			43.09335		0.01452
33.65		0.1286			45.6426		0.011789
33.03		0.1467			50.7411		0.00399
32.42		0.1667			51.7608		0.003167
31.82		0.1885			55.8396		0.001979
31.23		0.2123			58.8987		0.001117
30.64		0.2383			65.0169		0.000419
30.06		0.2666			66.54645		0.000153
29.47		0.2973			73.1745		7.69E-05
28.89		0.3307					
28.3		0.3668					
27.7		0.4059					
27.09		0.4482					
26.47		0.4939					
25.83		0.5433					
25.17		0.5967					
24.47		0.6545					
23.74		0.7171					
22.96		0.7849					
22.12		0.8588					
21.18		0.9394					

20.12		1.028					
18.85		1.126					
17.25		1.237					
14.87		1.366					
12.85		1.444					
	LAYER 3					LAYER 5	
TENSION		K			TENSION		K
15.0516		0.048886			19.1304		ND
24.2289		0.061269			21.67965		0.112654
29.3274		0.047801			25.75845		0.067182
32.3865		0.029514			28.3077		0.048072
34.4259		0.030431			30.85695		0.037003
38.5047		0.019611			33		0.025472
40.5441		0.015006			35.95545		0.021244
42.5835		0.011494			37.485		0.0163
48.7017		0.006269			43.09335		0.006146
49.7214		0.003127			44.6229		0.004792
52.7805		0.001733			49.21155		0.002512
56.34945		0.001009			51.7608		0.001517
62.9775		0.000494			57.36915		0.000616
65.0169		0.000205			60.9381		0.00024
71.1351		8.81E-05			67.56615		0.000103
	LAYER 4						
TENSION		K					
20.65995		0.128791					
25.75845		0.06364					
28.3077		0.064363					
32.89635		0.032535					
32.3865		0.015256					
37.99485		0.028175					
40.03425		0.023981					
42.07365		0.00641					
45.13275		0.008203					
49.7214		0.003145					
52.27065		0.00249					
56.34945		0.001071					
61.9578		0.000336					
63.9972		0.000151					
70.62525		ND					

	HYDRAULIC CONDUCTIVITY DATA 10 CM STONE LAYER						
	FITTED CURVE					LAYER 1	
THETA		K			THETA		K
0.0016		4.58E-08			0.170655		ND
0.0033		3.86E-07			0.130657		0.085496
0.0065		3.24E-06			0.112728		0.024551
0.013		2.73E-05			0.097556		0.022343
0.0195		9.52E-05			0.09066		0.014021
0.026		0.000231			0.085144		0.012125
0.0326		0.00046			0.076868		0.008948
0.0391		0.000807			0.068593		0.005276
0.0456		0.001301			0.052043		0.002342
0.0521		0.001968			0.045146		0.002029
0.0586		0.002836			0.03825		0.001026
0.0651		0.003936			0.031354		0.000578
0.0716		0.005297			0.023079		0.000236
0.0781		0.006951			0.013425		0.00011
0.0846		0.008929			0.010666		4.81E-05
0.0912		0.01127					
0.0977		0.01399				LAYER 2	
0.1042		0.01715			THETA		K
0.1107		0.02077			0.337539		0.10381
0.1172		0.0249			0.319609		0.089599
0.1237		0.02956			0.285129		0.066088
0.1302		0.03482			0.245132		0.046146
0.1367		0.04069			0.218927		0.035112
0.1432		0.04725			0.189964		0.018141
0.1498		0.05452			0.170655		0.01452
0.1563		0.06256			0.155483		0.011789
0.1628		0.07142			0.118245		0.00399
0.1693		0.08116			0.107211		0.003167
0.1758		0.09184			0.093419		0.001979
0.1823		0.1035			0.081006		0.001117
0.1888		0.1163			0.067214		0.000419
0.1953		0.1301			0.032734		0.000153
0.2018		0.1452			0.029975		7.69E-05
0.2084		0.1616					
0.2149		0.1794					
0.2214		0.1987					
0.2279		0.2195					
0.2344		0.2421					
0.2409		0.2666					
0.2474		0.2931					
0.2539		0.3218					
0.2604		0.353					
0.267		0.3869					
0.2735		0.4239					
0.28		0.4644					

0.2865		0.5091					
0.293		0.559					
0.2995		0.6155					
0.306		0.6824					
0.3093		0.7227					
0.3093		0.78					
	LAYER 3					LAYER 5	
THETA		K			THETA		K
0.12086		0.048886			0.173413		ND
0.117136		0.061269			0.163759		0.112654
0.113413		0.047801			0.151346		0.067182
0.104103		0.029514			0.141691		0.048072
0.094173		0.030431			0.134795		0.037003
0.084863		0.019611			0.12652		0.025472
0.073691		0.015006			0.116865		0.021244
0.065002		0.011494			0.10859		0.0163
0.046383		0.006269			0.081006		0.006146
0.042038		0.003127			0.072731		0.004792
0.035211		0.001733			0.060318		0.002512
0.029626		0.001009			0.050663		0.001517
0.022178		0.000494			0.041009		0.000616
0.007903		0.000205			0.024458		0.00024
0.006662		8.81E-05			0.023079		0.000103
	LAYER 4						
THETA		K					
0.152725		ND					
0.14307		0.128791					
0.134795		0.06364					
0.130657		0.064363					
0.122382		0.032535					
0.116865		0.015256					
0.105832		0.028175					
0.103073		0.023981					
0.075489		0.00641					
0.068593		0.008203					
0.057559		0.003145					
0.046526		0.00249					
0.031354		0.001071					
0.020321		0.000336					
0.017562		0.000151					

APPENDIX F

EXPERIMENTAL DATA: HETEROGENEOUS PROFILE

SEVILLETA SAND - 16 CM STONE LAYER

	EXPERIMENT #13 HETEROGENEOUS SOIL PROFILE: 16CM STONE LAYER						
	TENSIOMETER READINGS : via PRESSURE TRANSDUCER cm H2O						
PTD 1	PTD 2	PTD 3	PTD 4	PTD 5	PTD 6	PTD 7	PTD 8
-25.3293	-20.79	-22.1124	-30.4592	-12.5986	-26.0852	-29.8937	-21.5552
-30.8874	-24.7	-24.6963	-31.4272	-36.0399	-28.3236	-31.2545	-19.7144
-48.6202	-40.84	-42.2193	-35.2024	-28.5979	-40.407	-39.8404	-27.672
-51.9927	-46.46	-48.7731	-37.9516	-46.0283	-45.1842	-44.0109	-30.4381
-54.6729	-48.94	-48.5355	-41.0879	-49.7197	-48.5854	-47.3199	-33.6036
-56.374	-51.79	-53.8815	-43.595	-51.8122	-51.0563	-49.6206	-35.5711
-58.0454	-53.74	-56.4951	-45.802	-52.6314	-53.0428	-51.0793	-36.5646
-59.2915	-55	-57.1485	-48.3576	-54.3882	-54.2928	-52.6261	-37.4704
-60.3695	-55.59	-54.6339	-49.5482	-55.4344	-55.1261	-54.3491	-40.2658
-61.3486	-56.55	-54.4359	-50.6033	-56.9643	-55.4749	-55.4456	-42.6229
-65.1167	-60.26	-61.5144	-53.0717	-60.6655	-59.1959	-58.8232	-50.483
-68.1035	-63.57	-64.722	-60.6899	-63.439	-61.7638	-62.7392	-53.5804
-73.6419	-68.9	-70.167	-68.7146	-68.9366	-67.1514	-68.388	-66.0768
-87.6857	-81.1	-82.245	-82.8474	-81.965	-80.5236	-81.6045	-79.0602
-89.2681	-83.1	-84.225	-81.3954	-84.1364	-82.5585	-83.6604	-79.5472
	AVERAGED TENSION OF P.T.D. AND PROPER STATION PLACEMENT OF P.T.D.						
	RUNTIME	T1	T2	T3	T4	T5	
	1	-25.3293	-21.4512	-19.3419	-25.7245	-30.4592	
	15	-30.8874	-24.6982	-32.1818	-25.4845	-31.4272	
	30	-48.6202	-41.5297	-34.5025	-33.7562	-35.2024	
	45	-51.9927	-47.6166	-45.6063	-37.2245	-37.9516	
	60	-54.6729	-48.7378	-49.1526	-40.4618	-41.0879	
	75	-56.374	-52.8358	-51.4343	-42.5959	-43.595	
	90	-58.0454	-55.1176	-52.8371	-43.822	-45.802	
	105	-59.2915	-56.0743	-54.3405	-45.0483	-48.3576	
	120	-60.3695	-55.112	-55.2803	-47.3075	-49.5482	
	135	-61.3486	-55.493	-56.2196	-49.0343	-50.6033	
	225	-65.1167	-60.8872	-59.9307	-54.6531	-53.0717	
	330	-68.1035	-64.146	-62.6014	-58.1598	-60.6899	
	705	-73.6419	-69.5335	-68.044	-67.2324	-68.7146	
	4275	-87.6857	-81.6725	-81.2443	-80.3324	-82.8474	
	7200	-89.2681	-83.6625	-83.3475	-81.6038	-81.3954	

CORRECTED TENSIOMETER READINGS AT CUPS cm						
RUNTIME	T1	T2	T3	T4	T5	
1	-11.8293	-7.9512	-5.8419	-12.2245	-16.9592	
15	-17.3874	-11.1982	-18.6818	-11.9845	-17.9272	
30	-35.1202	-28.0297	-21.0025	-20.2562	-21.7024	
45	-38.4927	-34.1166	-32.1063	-23.7245	-24.4516	
60	-41.1729	-35.2378	-35.6526	-26.9618	-27.5879	
75	-42.874	-39.3358	-37.9343	-29.0959	-30.095	
90	-44.5454	-41.6176	-39.3371	-30.322	-32.302	
105	-45.7915	-42.5743	-40.8405	-31.5483	-34.8576	
120	-46.8695	-41.612	-41.7803	-33.8075	-36.0482	
135	-47.8486	-41.993	-42.7196	-35.5343	-37.1033	
225	-51.6167	-47.3872	-46.4307	-41.1531	-39.5717	
330	-54.6035	-50.646	-49.1014	-44.6598	-47.1899	
705	-60.1419	-56.0335	-54.544	-53.7324	-55.2146	
4275	-74.1857	-68.1725	-67.7443	-66.8324	-69.3474	
7200	-75.7681	-70.1625	-69.8475	-68.1038	-67.8954	

	HTDRAULIC HEAD AT TENSIOMETER CUPS cm H2O						
PTD 1	PTD 2	PTD 3	PTD 4	PTD 5	PTD 6	PTD 7	PTD 8
-30.8293	-36.29	-37.6124	-76.9592	-38.0986	-52.5852	-65.3937	-57.5552
-36.3874	-40.2	-40.1963	-77.9272	-61.5399	-54.8236	-66.7545	-55.7144
-54.1202	-56.34	-57.7193	-81.7024	-54.0979	-66.907	-75.3404	-63.672
-57.4927	-61.96	-64.2731	-84.4516	-71.5283	-71.6842	-79.5109	-66.4381
-60.1729	-64.44	-64.0355	-87.5879	-75.2197	-75.0854	-82.8199	-69.6036
-61.874	-67.29	-69.3815	-90.095	-77.3122	-77.5563	-85.1206	-71.5711
-63.5454	-69.24	-71.9951	-92.302	-78.1314	-79.5428	-86.5793	-72.5646
-64.7915	-70.5	-72.6485	-94.8576	-79.8882	-80.7928	-88.1261	-73.4704
-65.8695	-71.09	-70.1339	-96.0482	-80.9344	-81.6261	-89.8491	-76.2658
-66.8486	-72.05	-69.9359	-97.1033	-82.4643	-81.9749	-90.9456	-78.6229
-70.6167	-75.76	-77.0144	-99.5717	-86.1655	-85.6959	-94.3232	-86.483
-73.6035	-79.07	-80.222	-107.19	-88.939	-88.2638	-98.2392	-89.5804
-79.1419	-84.4	-85.667	-115.215	-94.4366	-93.6514	-103.888	-102.077
-93.1857	-96.6	-97.745	-129.347	-107.465	-107.024	-117.105	-115.06
-94.7681	-98.6	-99.725	-127.895	-109.636	-109.059	-119.16	-115.547

	AVERAGED HEAD AND PROPER STATION PLACEMENT (-cm)					
	RUNTIME	STAT 1	STAT2	STAT3	STAT4	STAT5
	1	30.8293	36.9512	52.5852	65.3937	76.9592
	15	36.3874	40.19815	54.8236	66.7545	77.9272
	30	54.1202	57.02965	66.907	75.3404	81.7024
	45	57.4927	63.11655	71.6842	79.5109	84.4516
	60	60.1729	64.23775	75.0854	82.8199	87.5879
	75	61.874	68.33575	77.5563	85.1206	90.095
	90	63.5454	70.61755	79.5428	86.5793	92.302
	105	64.7915	71.57425	80.7928	88.1261	94.8576
	120	65.8695	70.61195	81.6261	89.8491	96.0482
	135	66.8486	70.99295	81.9749	90.9456	97.1033
	225	70.6167	76.3872	85.6959	94.3232	99.5717
	330	73.6035	79.646	88.2638	98.2392	107.1899
	705	79.1419	85.0335	93.6514	103.888	115.2146
	4275	93.1857	97.1725	107.0236	117.1045	129.3474
	7200	94.7681	99.1625	109.0585	119.1604	127.8954

		WATER CONTENT via TDR				
RUNTIME	TDR 1	THETA 1	TDR 2	THETA 2	TDR 3	THETA 3
1	0.407	0.320988	0.415	0.332022	0.393	0.30168
15	0.405	0.31823	0.412	0.327885	0.389	0.296163
30	0.361	0.257545	0.392	0.3003	0.382	0.286508
45	0.335	0.221685	0.376	0.278233	0.373	0.274095
60	0.317	0.19686	0.353	0.246511	0.36	0.256166
75	0.306	0.181688	0.339	0.227202	0.346	0.236857
90	0.297	0.169275	0.327	0.210652	0.336	0.223065
105	0.292	0.162379	0.32	0.200997	0.329	0.21341
120	0.284	0.151346	0.312	0.189964	0.319	0.199618
135	0.282	0.148587	0.308	0.184447	0.315	0.194101
225	0.264	0.123761	0.287	0.155483	0.291	0.161
330	0.254	0.109969	0.274	0.137554	0.272	0.134795
705	0.238	0.087902	0.253	0.10859	0.256	0.112728
4275	0.218	0.060318	0.23	0.076868	0.229	0.075489
7200	0.213	0.053422	0.223	0.067214	0.224	0.068593

	WATER CONTENT via TDR			
RUNTIME	TDR 4	THETA 4	TDR 5	THETA 5
1	0.295	0.166517	0.298	0.170655
15	0.279	0.14445	0.294	0.165138
30	0.273	0.136174	0.284	0.151346
45	0.268	0.129278	0.277	0.141691
60	0.264	0.123761	0.27	0.132037
75	0.261	0.119624	0.266	0.12652
90	0.257	0.114107	0.258	0.115486
105	0.255	0.111349	0.255	0.111349
120	0.25	0.104453	0.251	0.105832
135	0.251	0.105832	0.249	0.103073
225	0.242	0.093419	0.238	0.087902
330	0.235	0.083764	0.23	0.076868
705	0.222	0.065835	0.22	0.063076
4275	0.2	0.035492	0.202	0.03825
7200	0.195	0.028596	0.196	0.029975

	SLOPE OF THE WETTNESS CURVE dTH/dt				
RUNTIME	STAT 1	STAT 2	STAT 3	STAT 4	STAT 5
1	Error	8.71E+15	-0.00096	-0.00524	3.40E-07
15	-0.00652	-0.01024	-0.00128	-0.00098	-0.00158
30	-0.00287	-0.00166	-0.00121	-0.00059	-0.00089
45	-0.00172	-0.00187	-0.00109	-0.00043	-0.00061
60	-0.00118	-0.00149	-0.00097	-0.00034	-0.00047
75	-0.00088	-0.00115	-0.00086	-0.00028	-0.00037
90	-0.00068	-0.00091	-0.00076	-0.00024	-0.00031
105	-0.00056	-0.00073	-0.00067	-0.00021	-0.00027
120	-0.00046	-0.0006	-0.0006	-0.00019	-0.00023
135	-0.00039	-0.0005	-0.00054	-0.00017	-0.0002
225	-0.00019	-0.00022	-0.0003	-0.0001	-0.00012
330	-0.00011	-0.00012	-0.00017	-6.92E-05	-7.69E-05
705	-3.55E-05	-3.70E-05	-4.64E-05	-3.03E-05	-3.18E-05
4275	-1.89E-06	-3.90E-06	-1.20E-06	-3.33E-06	-3.28E-06
7200	-7.59E-07	-2.30E-06	-3.97E-07	-1.66E-06	-1.63E-06

WATER CONTENT dTH/dt TIMES THE THICKNESS OF THE LAYER					
RUNTIME	STAT 1	STAT 2	STAT 3	STAT 4	STAT 5
1	0	-5.6E+16	0.004329	0.052422	-3.4E-06
15	0.130409	0.065823	0.005781	0.009812	0.015815
30	0.057447	0.010679	0.005449	0.005916	0.008881
45	0.034339	0.011997	0.004908	0.004309	0.006134
60	0.023576	0.009559	0.004359	0.003405	0.00466
75	0.017518	0.007405	0.003858	0.002819	0.003741
90	0.0137	0.005825	0.003415	0.002406	0.003114
105	0.011106	0.004682	0.003031	0.002098	0.00266
120	0.009245	0.003843	0.002699	0.001859	0.002315
135	0.007855	0.003213	0.002412	0.001667	0.002046
225	0.003828	0.001431	0.001333	0.001021	0.001179
330	0.002203	0.000772	0.000768	0.000692	0.000769
705	0.00071	0.000238	0.000209	0.000303	0.000318
4275	3.78E-05	2.5E-05	5.42E-06	3.33E-05	3.28E-05
7200	1.52E-05	1.48E-05	1.79E-06	1.66E-05	1.63E-05

	SLOPE OF THE HEAD WITH DEPTH CURVE dH/dz				
RUNTIME	G1	G2	G3	G4	G5
1	0.61219	1.5634	1.28085	1.15655	0.810097
15	0.381075	1.462545	1.19309	1.11727	0.820286
30	0.290945	0.987735	0.84334	0.6362	0.860025
45	0.562385	0.856765	0.78267	0.49407	0.888964
60	0.406485	1.084765	0.77345	0.4768	0.921978
75	0.646175	0.922055	0.75643	0.49744	0.948368
90	0.707215	0.892525	0.70365	0.57227	0.9716
105	0.678275	0.921855	0.73333	0.67315	0.998501
120	0.474245	1.101415	0.8223	0.61991	1.011034
135	0.414435	1.098195	0.89707	0.61577	1.02214
225	0.57705	0.93087	0.86273	0.52485	1.048123
330	0.60425	0.86178	0.99754	0.89507	1.128315
705	0.58916	0.86179	1.02366	1.13266	1.212785
4275	0.39868	0.98511	1.00809	1.22429	1.361552
7200	0.43944	0.9896	1.01019	0.8735	1.346267

	FLUX THROUGH EACH LAYER				
RUNTIME	Q1	Q2	Q3	Q4	Q5
1	0	-5.6E+16	-5.6E+16	-5.6E+16	-5.6E+16
15	0.130409	0.196232	0.202013	0.211825	0.22764
30	0.057447	0.068126	0.073575	0.079491	0.088372
45	0.034339	0.046336	0.051244	0.055553	0.061687
60	0.023576	0.033135	0.037494	0.040899	0.045559
75	0.017518	0.024922	0.02878	0.031599	0.03534
90	0.0137	0.019524	0.022939	0.025346	0.02846
105	0.011106	0.015788	0.018819	0.020916	0.023576
120	0.009245	0.013088	0.015787	0.017646	0.019961
135	0.007855	0.011068	0.01348	0.015148	0.017194
225	0.003828	0.005259	0.006592	0.007613	0.008792
330	0.002203	0.002975	0.003743	0.004435	0.005204
705	0.00071	0.000947	0.001156	0.001459	0.001777
4275	3.78E-05	6.28E-05	6.82E-05	0.000101	0.000134
7200	1.52E-05	2.99E-05	3.17E-05	4.84E-05	6.47E-05

	CONDUCTIVITY AS A FUNCTION OF THETA				
RUNTIME	K1	K2	K3	K4	K5
1	0	-3.6E+16	-4.4E+16	-4.8E+16	-6.9E+16
15	0.342214	0.134171	0.169319	0.189592	0.277513
30	0.197451	0.068972	0.087243	0.124947	0.102755
45	0.06106	0.054082	0.065473	0.112439	0.069392
60	0.058	0.030545	0.048476	0.085779	0.049415
75	0.02711	0.027029	0.038047	0.063524	0.037264
90	0.019372	0.021876	0.032601	0.044289	0.029291
105	0.016373	0.017126	0.025662	0.031073	0.023611
120	0.019494	0.011883	0.019199	0.028465	0.019743
135	0.018954	0.010079	0.015027	0.0246	0.016822
225	0.006634	0.00565	0.007641	0.014504	0.008388
330	0.003646	0.003453	0.003753	0.004955	0.004612
705	0.001204	0.001099	0.001129	0.001288	0.001465
4275	9.48E-05	6.38E-05	6.77E-05	8.29E-05	9.86E-05
7200	3.45E-05	3.03E-05	3.14E-05	5.54E-05	4.81E-05

	SOIL WATER RETENTION DATA 16 CM STONE LAYER						
	FITTED CURVE					LAYER 1	
THETA		TENSION			THETA		TENSION
0.0016		136.8			0.320988		11.8293
0.0033		112.2			0.31823		17.3874
0.0065		91.96			0.257545		35.1202
0.013		75.28			0.221685		38.4927
0.0195		66.87			0.19686		41.1729
0.026		61.41			0.181688		42.874
0.0326		57.44			0.169275		44.5454
0.0391		54.34			0.162379		45.7915
0.0456		51.81			0.151346		46.8695
0.0521		49.68			0.148587		47.8486
0.0586		47.84			0.123761		51.6167
0.0651		46.22			0.109969		54.6035
0.0716		44.78			0.087902		60.1419
0.0781		43.48			0.060318		74.1857
0.0846		42.28			0.053422		75.7681
0.0912		41.19					
0.0977		40.17				LAYER 2	
0.1042		39.21			THETA		TENSION
0.1107		38.31			0.14941		7.9512
0.1172		37.46			0.147548		11.19815
0.1237		36.65			0.135135		28.02965
0.1302		35.88			0.125205		34.11655
0.1367		35.13			0.11093		35.23775
0.1432		34.41			0.102241		39.33575
0.1498		33.72			0.094793		41.61755
0.1563		33.04			0.090449		42.57425
0.1628		32.39			0.085484		41.61195
0.1693		31.74			0.083001		41.99295
0.1758		31.11			0.069967		47.3872
0.1823		30.48			0.061899		50.646
0.1888		29.86			0.048866		56.0335
0.1953		29.25			0.034591		68.1725
0.2018		28.63			0.030246		70.1625
0.2084		28.02					
0.2149		27.4					
0.2214		26.78					
0.2279		26.14					
0.2344		25.5					
0.2409		24.83					
0.2474		24.15					
0.2539		23.43					
0.2604		22.68					
0.267		21.88					
0.2735		21.01					
0.28		20.05					

0.2865		18.97					
0.293		17.7					
0.2995		16.08					
0.306		13.71					
0.3093		11.72					
	LAYER 3					LAYER 5	
THETA		TENSION			THETA		TENSION
0.135756		5.8419			0.141691		24.4516
0.133273		18.68175			0.132037		27.5879
0.128929		21.00245			0.12652		30.095
0.123343		32.10625			0.115486		32.302
0.115275		35.65255			0.111349		34.8576
0.106585		37.93425			0.105832		36.0482
0.100379		39.3371			0.103073		37.1033
0.096035		40.8405			0.087902		39.5717
0.089828		41.78025			0.076868		47.1899
0.087346		42.7196			0.063076		55.2146
0.07245		46.4307			0.03825		69.3474
0.060658		49.1014			0.029975		67.8954
0.050727		54.544					
0.03397		67.7443					
0.030867		69.84745					
	LAYER 4						
THETA		TENSION					
0.166517		12.22445					
0.14445		11.98445					
0.136174		20.2562					
0.129278		23.7245					
0.123761		26.96175					
0.119624		29.09585					
0.114107		30.32195					
0.111349		31.54825					
0.104453		33.80745					
0.105832		35.53425					
0.093419		41.1531					
0.083764		44.6598					
0.065835		53.7324					
0.035492		66.83235					
0.028596		68.1038					

	HYDRAULIC CONDUCTIVITY TENSION DATA 16 CM STONE LAYER						
	FITTED CURVE					LAYER 1	
TENSION	K				TENSION		K
123.6	9.47E-08				11.8293		ND
103.1	7.97E-07				17.3874		0.342214
86.02	6.7E-06				35.1202		0.197451
71.64	5.65E-05				38.4927		0.06106
64.29	0.000197				41.1729		0.058
59.47	0.000477				42.874		0.02711
55.94	0.00095				44.5454		0.019372
53.17	0.001668				45.7915		0.016373
50.9	0.002687				46.8695		0.019494
48.97	0.004064				47.8486		0.018954
47.31	0.005857				51.6167		0.006634
45.84	0.008127				54.6035		0.003646
44.52	0.01093				60.1419		0.001204
43.33	0.01435				74.1857		9.48E-05
42.24	0.01842				75.7681		3.45E-05
41.23	0.02324						
40.28	0.02886					LAYER 2	
39.4	0.03536				TENSION		K
38.57	0.04281				7.9512		ND
37.78	0.0513				11.19815		0.134171
37.03	0.06089				28.02965		0.068972
36.3	0.07168				34.11655		0.054082
35.61	0.08375				35.23775		0.030545
34.94	0.09719				39.33575		0.027029
34.29	0.1121				41.61755		0.021876
33.65	0.1286				42.57425		0.017126
33.03	0.1467				41.61195		0.011883
32.42	0.1667				41.99295		0.010079
31.82	0.1885				47.3872		0.00565
31.23	0.2123				50.646		0.003453
30.64	0.2383				56.0335		0.001099
30.06	0.2666				68.1725		6.38E-05
29.47	0.2973				70.1625		3.03E-05
28.89	0.3307						
28.3	0.3668						
27.7	0.4059						
27.09	0.4482						
26.47	0.4939						
25.83	0.5433						
25.17	0.5967						
24.47	0.6545						
23.74	0.7171						
22.96	0.7849						
22.12	0.8588						
21.18	0.9394						

20.12	1.028						
18.85	1.126						
17.25	1.237						
14.87	1.366						
12.85	1.444						
	LAYER 3					LAYER 5	
TENSION		K			TENSION		K
5.8419		ND			ND		0.277513
18.68175		0.169319			ND		0.102755
21.00245		0.087243			24.4516		0.069392
32.10625		0.065473			27.5879		0.049415
35.65255		0.048476			30.095		0.037264
37.93425		0.038047			32.302		0.029291
39.3371		0.032601			34.8576		0.023611
40.8405		0.025662			36.0482		0.019743
41.78025		0.019199			37.1033		0.016822
42.7196		0.015027			39.5717		0.008388
46.4307		0.007641			47.1899		0.004612
49.1014		0.003753			55.2146		0.001465
54.544		0.001129			69.3474		9.86E-05
67.7443		6.77E-05			67.8954		4.81E-05
69.84745		3.14E-05					
	LAYER 4						
TENSION		K					
12.22445		ND					
11.98445		0.189592					
20.2562		0.124947					
23.7245		0.112439					
26.96175		0.085779					
29.09585		0.063524					
30.32195		0.044289					
31.54825		0.031073					
33.80745		0.028465					
35.53425		0.0246					
41.1531		0.014504					
44.6598		0.004955					
53.7324		0.001288					
66.83235		8.29E-05					
68.1038		5.54E-05					

	HYDRAULIC CONDUCTIVITY DATA 16 CM STONE LAYER						
	FITTED CURVE					LAYER 1	
THETA		K			THETA		K
0.0016		4.58E-08			0.320988		ND
0.0033		3.86E-07			0.31823		0.342214
0.0065		3.24E-06			0.257545		0.197451
0.013		2.73E-05			0.221685		0.06106
0.0195		9.52E-05			0.19686		0.058
0.026		0.000231			0.181688		0.02711
0.0326		0.00046			0.169275		0.019372
0.0391		0.000807			0.162379		0.016373
0.0456		0.001301			0.151346		0.019494
0.0521		0.001968			0.148587		0.018954
0.0586		0.002836			0.123761		0.006634
0.0651		0.003936			0.109969		0.003646
0.0716		0.005297			0.087902		0.001204
0.0781		0.006951			0.060318		9.48E-05
0.0846		0.008929			0.053422		3.45E-05
0.0912		0.01127					
0.0977		0.01399				LAYER 2	
0.1042		0.01715			THETA		K
0.1107		0.02077			0.147548		0.134171
0.1172		0.0249			0.135135		0.068972
0.1237		0.02956			0.125205		0.054082
0.1302		0.03482			0.11093		0.030545
0.1367		0.04069			0.102241		0.027029
0.1432		0.04725			0.094793		0.021876
0.1498		0.05452			0.090449		0.017126
0.1563		0.06256			0.085484		0.011883
0.1628		0.07142			0.083001		0.010079
0.1693		0.08116			0.069967		0.00565
0.1758		0.09184			0.061899		0.003453
0.1823		0.1035			0.048866		0.001099
0.1888		0.1163			0.034591		6.38E-05
0.1953		0.1301			0.030246		3.03E-05
0.2018		0.1452					
0.2084		0.1616					
0.2149		0.1794					
0.2214		0.1987					
0.2279		0.2195					
0.2344		0.2421					
0.2409		0.2666					
0.2474		0.2931					
0.2539		0.3218					
0.2604		0.353					
0.267		0.3869					
0.2735		0.4239					
0.28		0.4644					

0.2865		0.5091					
0.293		0.559					
0.2995		0.6155					
0.306		0.6824					
0.3093		0.7227					
0.3093		0.78					
	LAYER 3					LAYER 5	
THETA		K			THETA		K
0.133273		0.169319			0.170655		ND
0.128929		0.087243			0.165138		0.277513
0.123343		0.065473			0.151346		0.102755
0.115275		0.048476			0.141691		0.069392
0.106585		0.038047			0.132037		0.049415
0.100379		0.032601			0.12652		0.037264
0.096035		0.025662			0.115486		0.029291
0.089828		0.019199			0.111349		0.023611
0.087346		0.015027			0.105832		0.019743
0.07245		0.007641			0.103073		0.016822
0.060658		0.003753			0.087902		0.008388
0.050727		0.001129			0.076868		0.004612
0.03397		6.77E-05			0.063076		0.001465
0.030867		3.14E-05			0.03825		9.86E-05
					0.029975		4.81E-05
	LAYER 4						
THETA		K					
0.166517		ND					
0.14445		0.189592					
0.136174		0.124947					
0.129278		0.112439					
0.123761		0.085779					
0.119624		0.063524					
0.114107		0.044289					
0.111349		0.031073					
0.104453		0.028465					
0.105832		0.0246					
0.093419		0.014504					
0.083764		0.004955					
0.065835		0.001288					
0.035492		8.29E-05					
0.028596		5.54E-05					